THE EFFECTS
OF
HYDRO POWER PLANTS' GOVERNOR SETTINGS
ON THE
TURKISH POWER SYSTEM FREQUENCY

A THESIS SUBMITTED TO
THE GRADUATE SCHOOL OF NATURAL AND APPLIED SCIENCES
OF
MIDDLE EAST TECHNICAL UNIVERSITY

BY

MAHMUT ERKUT CEBECİ

IN PARTIAL FULFILLMENT OF THE REQUIREMENTS
FOR
THE DEGREE OF MASTER OF SCIENCE
IN
ELECTRICAL AND ELECTRONICS ENGINEERING

FEBRUARY 2008

Approval of thesis:

"THE EFFECTS OF HYDRO POWER PLANTS' GOVERNOR SETTINGS ON THE TURKISH POWER SYSTEM FREQUENCY"

submitted by **MAHMUT ERKUT CEBECİ** in partial fulfillment of the requirements for the degree of **Master of Science in Electrical – Electronics Engineering Department, Middle East Technical University** by,

Prof. Dr. Canan Özgen ____________________
Dean, Graduate School of **Natural and Applied Sciences**

Prof. Dr. İsmet Erkmen ____________________
Head of Department, **Electrical and Electronics Engineering**

Prof. Dr. Arif Ertaş ____________________
Supervisor, **Electrical and Electronics Engineering, METU**

Examining Committee Members

Prof. Dr. Nevzat Özay(*) ____________________
Electrical and Electronics Engineering, METU

Prof. Dr. Arif Ertaş(**) ____________________
Electrical and Electronics Engineering, METU

Prof. Dr. İsmet Erkmen ____________________
Electrical and Electronics Engineering, METU

Assist. Prof. Dr. Ahmet Hava ____________________
Electrical and Electronics Engineering, METU

Ms. Osman Bülent Tör ____________________
Tübitak – UZAY

Date: **08.02.2008**

(*) Head of examining committee
(**) Supervisor

I hereby declare that all information in this document has been obtained and presented in accordance with academic rules and ethical conduct. I also declare that, as required by these rules and conduct, I have fully cited and referenced all material and results that are not original to this work.

Name, Last name: Mahmut Erkut Cebeci

Signature: ____________________

ABSTRACT

THE EFFECTS
OF
HYDRO POWER PLANTS' GOVERNOR SETTINGS
ON THE
TURKISH POWER SYSTEM FREQUENCY

Cebeci, Mahmut Erkut
MS, Department of Electrical and Electronics Engineering
Supervisor: Prof. Dr. Arif Ertaş

February 2008, 124 Pages

This thesis proposes a method and develops a mathematical model for determining the effects of hydro power plants' governor settings on the Turkish power system frequency.

The Turkish power system suffers from frequency oscillations with 20 – 30 seconds period. Besides various negative effects on power plants and customers, these frequency oscillations are one of the most important obstacles before the interconnection of the Turkish power system with the UCTE (Union for the Co-ordination of Transmission of Electricity) network.

Taking observations of the system operators and statistical studies as an initial point, the effects of hydro power plants' governor settings on the Turkish power system frequency are investigated.

In order to perform system wide simulations, initially mathematical models for two major hydro power plants and their stability margins are determined. Utilizing this information a representative power system model is developed. After validation studies, the effects of hydro power plants' governor settings on the Turkish power system frequency are investigated. Further computer simulations are performed to determine possible effects of changing settings and structure of HPP governors to system frequency stability.

Finally, further factors that may have negative effects on frequency oscillations are discussed. The results of study are presented throughout the thesis and summarized in the "Conclusion and Future Work" chapter.

Keywords – frequency stability, speed governor, transient droop reduction.

ÖZ

HİDRO ELEKTRİK SANTRALLERİN HIZ REGÜLATÖR AYARLARININ
TÜRKİYE ELEKTRİK SİSTEMİ
FREKANSINA ETKİLERİ

Cebeci, Mahmut Erkut
Yüksek Lisans, Elektrik – Elektronik Mühendisliği Bölümü
Tez Yöneticisi: Prof. Dr. Arif Ertaş

Şubat 2008, 124 Sayfa

Bu tez, hidro elektrik santrallerin hız regülatör ayarlarının Türkiye elektrik sistemi frekansına etkilerini tespit etmek için, bir metot önerisi ve model uygulaması içermektedir.

Türkiye elektrik sisteminde periyodu 20 – 30 saniye olan frekans salınımları mevcuttur. Santraller ve tüketiciler üzerindeki olumsuz etkilerinin yanı sıra, bu salınımlar Türkiye elektrik sisteminin UCTE (Union for the Co-ordination of Transmission of Electricity) sistemi ile birleşmesi önündeki en büyük engellerden biridir.

Sistem operatörlerinin gözlemlerini ve istatistiki çalışmaları bir başlangıç noktası kabul ederek, hidro elektrik santrallerin hız regülatör ayarlarının Türkiye elektrik sistemi frekans kararlılığına etkilerini incelenmiştir.

Tüm sistemi kapsayan simülasyon çalışmaları yapabilmek için öncelikle iki önemli hidro elektrik santralinin matematiksel modelleri ve karalılık aralıkları belirlenmiştir. Bu bilgiler kullanılarak temsili bir elektrik sistemi modeli hazırlanmıştır. Modelin doğrulanmasından sonra hidro elektrik santrallerin hız

regülatör ayarlarının Türkiye elektrik sistemi frekansına etkilerini incelenmiştir. Bunun yanında hidro elektrik santral hız regülâtörlerinde yapılacak ayar değişiklileri ya da yapısal değişikliklerin sistem frekansına etkilerini belirlemek için bilgisayar simülasyonları yapılmıştır.

Son olarak frekans salınımları üzerinde olumsuz etkileri olabilecek diğer etkenler tartışılmıştır. Sonuçlar tez boyunca sunulmuş ve sonuç kısmında özetlenmiştir.

Anahtar kelimeler – frekans kararlılığı, hız regülatörü, geçici hız düşümü.

To My Parents

My Sister

and My Beloved Fiancée

ACKNOWLEDGMENTS

I would like to thank, first of all, to my supervisor, Prof. Dr. Arif Ertaş, for his guidance, support and trust in me and my studies.

I also would like to thank the members of Hardware Development and Power Systems Group of Tübitak – UZAY starting with the group coordinator Abdullah Nadar. Especially I owe my deepest gratitude to Osman Bülent Tör and Ulaş Karaağaç, who encouraged and advised me throughout the M.S. study. I also thank to my colleagues Oğuz Yılmaz, Müfit Altın and Mevlüt Akdeniz for their support and intimate friendship. Finally I would like to thank all members of group for creating an excellent working and warm friendship environment.

I also would like to thank Osman Bülent Tör for the facilities provided to me by "National Power Quality Project (105G129)" which is being conducted in Tübitak – UZAY.

TABLE OF CONTENTS

LIST OF TABLES

LIST OF FIGURES

C H A P T E R 1

INTRODUCTION

Electrical power systems (also referred as grid or network) may be broadly defined as the group of equipments that generates electrical power by means of various sources and transfers this power to customers. Although the first complete electric power system is built as a DC system at the early 1880s, the DC systems are superseded by AC systems at the beginning of 1900's. Almost all of the power systems that are in operation today are AC systems with a variety of two basic quantities; voltage level and frequency.

The satisfactory operation of a power system is largely dependent on steadiness of these two quantities. Voltage level and frequency should remain in a narrow tolerance band for satisfactory operation of customer devices. However, like most systems, power systems are subject to changes in operating conditions which may be severe in nature, like faults in various locations or loss of a major generator and/or load. This change in operating conditions should be responded to accordingly in order to keep the voltage magnitude and frequency in an acceptable band and keep the customer supplied with adequate waveform.

In order to keep voltage level and frequency in a tolerance band, controlling devices are utilized in generating units. Since voltage level throughout the power system mainly depends on the reactive power demand and flow, controller devices respond to voltage level changes by modifying the generator terminal voltages which change the reactive power outputs of the units. The voltage stability is not in the scope of this study.

The second quantity, frequency, depends on the balance between generated and dissipated power. An unbalance between these two powers results in a change of kinetic energy stored in rotating parts of generators which changes the rotation speed and hence changes the frequency of the network. After any disturbance, unit controllers reestablish the balance between these two powers, and bring frequency back to the rated value. This overall process is termed as “Load/Frequency Control”.

The load/frequency control is performed in three steps. The first step is referred as the “Primary Control (or Regulation)”. The primary control is performed by controllers termed as “Speed Governor” installed in power plants. The primary control is used in order to reestablish the power balance utilizing the spinning reserve of already operating power plants. It has no interest in bringing frequency back to rated value, but to keep the frequency constant with an acceptable deviation from its rated value. The second step is the “Secondary Control”, which brings frequency back to its rated value (50 Hz in Turkey) by changing generating unit outputs. It utilizes remaining reserve of operating power plants, or takes into service units when necessary. With the additional reserve from secondary control, the generating units that have already provided primary reserve are relieved, and essentially, the system will be ready for the next possible disturbance. Finally Tertiary control redistributes reserve by committing generator units considering other factors including the operational costs of plants, environmental concerns, etc.

The load/frequency control philosophy described above is also being applied in the Turkish power system. However the power system suffers from sustained frequency oscillations with 20 – 30 seconds period [5]. These oscillations have negative effects on plants that are contributing to primary control. Since oscillations are sustained, all generating units are constantly changing their power generation by changing the position of regulating valves. This continuous movement of regulating valves not only wears equipment out but also constantly changes pressure on pipes that carry water or steam going into turbines. The failure chance on these pipes increases due to constant variation and shocks of pressure. Hence maintenance and repair costs of plants increase drastically.

Further, these oscillations are an obstacle before the connection of the Turkish power system with the Union for the Co-ordination of Transmission of Electricity (UCTE). UCTE is the interconnected power system of almost all European countries, serving for approximately 450 million people. The interconnection, if realized, will result in improved system security and economy of operation. System security will improve by emergency assistance of both systems to each other. Further, the reserve spared for instances in interconnected system will be less than the sum of reserves spared by individual systems before interconnection. This reduced system reserve may be distributed by the most economical way. Moreover, the most economical units may be utilized which reduce the generation costs for both systems.

Previously a trail operation was performed between Turkish power system and UCTE. After the interconnection, the frequency of the overall system remained stable, however the power flow on interconnection lines begun to oscillate with peak to peak magnitude of approximately 200 MW and period of 20 – 30 seconds as the frequency oscillations of Turkish power system. This phenomenon can be explained as follows: Frequency oscillations are due to the continuous change in power output of generators. The amount of power output change that results in frequency oscillations in Turkish power system has a negligible effect on frequency of UCTE system due to the fact that the inertia of UCTE network is much larger than the inertia of Turkish power system. However the changes in power output of the generator affect the load flow resulting in sustained power oscillations on interconnection lines. Hence it was concluded that the interconnection of two networks is not sustainable before the elimination of frequency oscillation in Turkish power system.

The interconnection of Turkish power system with UCTE is an on going project and as stated above one of the major problems to be solved before interconnection is the frequency oscillation in Turkish power system. During discussions with

National Load Dispatch Center (NLDC) representatives on frequency oscillations, the frequency measurements are investigated for different operating conditions. Together with previous statistical studies of NLDC, frequency measurements indicate that the oscillations increase as the Hydro Power Plant (HPP) contribution to primary frequency control increase. Although this observation by itself is not enough to state that oscillations are due to HPPs, it gives an initial approach to studies for determining the possible reasons behind the problem. This is the main motivation of this thesis study which focuses on the effects of hydro power plants' governor settings on the Turkish power system frequency.

In Turkish power system the HPPs generate approximately 30 % of overall generation, however more than 75 % of the spinning reserve is supplied by HPPs due to the ±2.5 % reserve agreements of combined cycle power plants and insufficient coal quality or controller structure of thermal power plants. Hence the primary regulation characteristic of HPPs has an important role on primary regulation characteristic of Turkish power system. In UCTE network the amount of HPP generation is around 5% of overall generation. Hence the system characteristic is based on other types of plants and any possible negative effects of HPPs governor settings on system frequency that this thesis focus on cannot be observed in UCTE system.

In the study, in order to observe the effects of HPPs on frequency oscillations, first a representative power system model is determined. Given the close linkage between the plant capacity and its effect on frequency regulation, it is not necessary to model every plant's controllers in the system for simulation studies. Hence a priority list which includes the most important power plants based on their rating is prepared in a way such that, the overall response of these plants in the priority list represent the overall response of the power system satisfactorily.

There are three different groups of plants in Turkish power system based on the source of energy; Natural Gas Combined Cycle Power Plants (NGCCPPs), Thermal Power Plants (TPPs), and HPPs. Their installed capacity ratio is almost equal (i.e., ≈30%). The NGCCPPs usually consist of three generators; two gas turbines that burn the natural gas, and one steam turbine that run on the steam generated by high temperature exhaust gases of single or both gas turbines. The TPPs consist of boilers that burn coal or other fuel to generate high pressure steam before steam turbine. Finally the HPPs use the kinetic energy of water as a source for generation. The most important power plants from each group are selected for the priority list as discussed in the following chapter.

Given that the study focuses on HPPs, the hydro plant unit controller models are prepared in detail covering the dynamics and friction of penstock and detailed actual controller models which are determined by site visits and field tests. The control philosophy is resolved for each HPP in the priority list via manufacturer documentation[1]. In addition, controller structure and settings of two major HPPs, Atatürk and Birecik, are investigated on site by field tests as described in Chapter 4. On the other hand, no field tests are performed on any TPPs[2] or NGCCPPs[3] to validate unit controller. The documentations of major TPPs and NGCCPPs provided by TEİAŞ are utilized to model their unit controllers. After determining the unit controller models of individual plants in the priority list, the system model is built by combining them.

MATLAB/SIMULINK [18] and Power System Simulator for Engineering (PSS/E) [19], are utilized for modeling and simulation studies performed in this thesis. The controller models developed by MATLAB software are validated by PSS/E simulations when necessary.

The initial simulation studies are performed to validate the individual plant models of Atatürk and Birecik HPP. After determining the plant models, the stability limits of controller settings are determined for both plants. Acquired results are

---

1) HPPs in priority list: Altınkaya, Atatürk, Berke, Birecik, Hasanuğurlu, Karakaya, Keban, Oymapınar
2) TPPs in priority list: Ambalı (Fueloil), Çayırhan, Elbistan (A and B), İskenderun, Kemerköy, Seyitömer, Soma, Yatağan
3) NGCCPP in priority list: Adapazarı, Aliağa, Ambarlı, Bursa, Gebze, Hamitabat, Temelli, Unimar

used to show the effect of controller setting change on stability and response time of individual units. Further the effects of structural change (addition of derivative of frequency deviation as an input) on stability limits are determined.

The representative power system model is determined by individual plant models and validated by comparison of measurements of three different generation loss events. The chosen events represent three different loading conditions of the power system. After validating the model, following studies are performed in order to determine the effects of HPP controllers on power system frequency;

- Increasing and decreasing the contribution of HPP to primary frequency control
- Changing the “Speed Droop” setting of HPP controllers (“Speed Droop” term is defined further in the chapters)
- Changing the settings of Proportional Integral (PI) controller
- Changing the structure of controller by addition of an input (derivative of frequency deviation)

After studying the effects of hydro power plants’ governor settings on the Turkish power system frequency, further factors that may have negative effects on damping of frequency oscillations are introduced as future studies. Sample simulation studies are performed in order to have an idea about possible effects of these factors.

In conclusion, mathematical models for two major power plants and their stability margins are determined. Acquired information is utilized for determining a representative power system model. Using the validated model, the effects of HPP speed governors on system frequency are studied. Further, possible effects of changing settings and structure of HPP governors to system frequency are investigated. Finally, further factors that may have negative effects on frequency oscillations are discussed. The results of study are presented throughout the thesis and summarized in the “Conclusion and Future Work” chapter.

C H A P T E R 2

GENERAL BACKGROUND

Power System Stability

Power system stability may be broadly defined as the property of a power system that enables it to remain in a state of operating equilibrium under normal operating conditions and to regain an acceptable state of operating equilibrium after being subjected to a physical disturbance, with most system variables bounded so that practically the entire system remains intact [1].

The definition applies to an interconnected power system as a whole. Often, however, the stability of a particular generator or group of generators is also of interest. A remote generator may lose stability (synchronism) without cascading instability of the main system. Similarly, stability of particular loads or load areas may be of interest; motors may lose stability (run down and stall) without cascading instability of the main system.

The power system is a highly nonlinear system that operates in a constantly changing environment; loads, generator outputs and key operating parameters change continually. When subjected to a disturbance, the stability of the system depends on the initial operating conditions as well as the nature of the disturbance.

Stability of a power system is thus a property of the system around an equilibrium set, i.e., the initial operating condition. In an equilibrium set, the various opposing forces that exist in the system are equal instantaneously (as in the case of equilibrium points) or over a cycle (as in the case of slow cyclical variations due to continuous small fluctuations in loads or aperiodic attractors).

Power systems are subjected to a wide range of disturbances, small and large. Small disturbances in the form of load changes occur continually; the system must be able to adjust to the changing conditions and operate satisfactorily. It must also be able to survive numerous disturbances of a severe nature, such as a short circuit on a transmission line or loss of a large generator. A large disturbance may lead to structural changes due to the isolation of the faulted elements.

At an equilibrium set, a power system may be stable for a given (large) physical disturbance, and unstable for another. It is impractical and uneconomical to design power systems to be stable for every possible disturbance. The design contingencies are selected on the basis they have a reasonably high probability of occurrence. Hence, large-disturbance stability always refers to a specified disturbance scenario. A stable equilibrium set thus has a finite region of attraction; the larger the region, the more robust the system with respect to large disturbances. The region of attraction changes with the operating condition of the power system.

The response of the power system to a disturbance may involve much of the equipment. For instance, a fault on a critical element followed by its isolation by protective relays will cause variations in power flows, network bus voltages, and machine rotor speeds; the voltage variations will actuate both generator and transmission network voltage regulators; the generator speed variations will actuate prime mover governors; and the voltage and frequency variations will affect the system loads to varying degrees depending on their individual characteristics. Further, devices used to protect individual equipment may respond to variations in system variables and cause tripping of the equipment, thereby weakening the system and possibly leading to system instability.

If following a disturbance the power system is stable, it will reach a new equilibrium state with the system integrity preserved i.e., with practically all generators and loads connected through a single contiguous transmission system. Some generators and loads may be disconnected by the isolation of faulted elements or intentional tripping to preserve the continuity of operation of bulk of the system. Interconnected systems, for certain severe disturbances, may also be intentionally split into two or more "islands" to preserve as much of the generation and load as possible. The actions of automatic controls and possibly human operators will eventually restore the system to normal state. On the other hand, if the system is unstable, it will result in a run-away or run-down situation; for example, a progressive increase in angular separation of generator rotors, or a progressive decrease in bus voltages. An unstable system condition could lead to cascading outages and a shutdown of a major portion of the power system.

Power systems are continually experiencing fluctuations of small magnitudes. However, for assessing stability when subjected to a specified disturbance, it is usually valid to assume that the system is initially in a true steady-state operating condition.

Classification of Power System Stability

A typical modern power system is a high-order multivariable process whose dynamic response is influenced by a wide array of devices with different characteristics and response rates. Stability is a condition of equilibrium between opposing forces. Depending on the network topology, system operating condition and the form of disturbance, different sets of opposing forces may experience sustained imbalance leading to different forms of instability [1].

Power system stability is essentially a single problem; however, the various forms of instabilities that a power system may undergo cannot be properly understood and effectively dealt with by treating it as such. Because of high dimensionality and complexity of stability problems, it helps to make simplifying assumptions to analyze specific types of problems using an appropriate degree of detail of system representation and appropriate analytical techniques. Analysis of stability, including identifying key factors that contribute to instability and devising methods of improving stable operation, is greatly facilitated by classification of stability into appropriate categories. Classification, therefore, is essential for meaningful practical analysis and resolution of power system stability problems.

The classification of power system stability proposed here is based on the following considerations:

- The physical nature of the resulting mode of instability as indicated by the main system variable in which instability can be observed.
- The size of the disturbance considered which influences the method of calculation and prediction of stability.
- The devices, processes, and the time span that must be taken into consideration in order to assess stability.

Fig. 2-1 gives the overall picture of the power system stability problem, identifying its categories and subcategories.

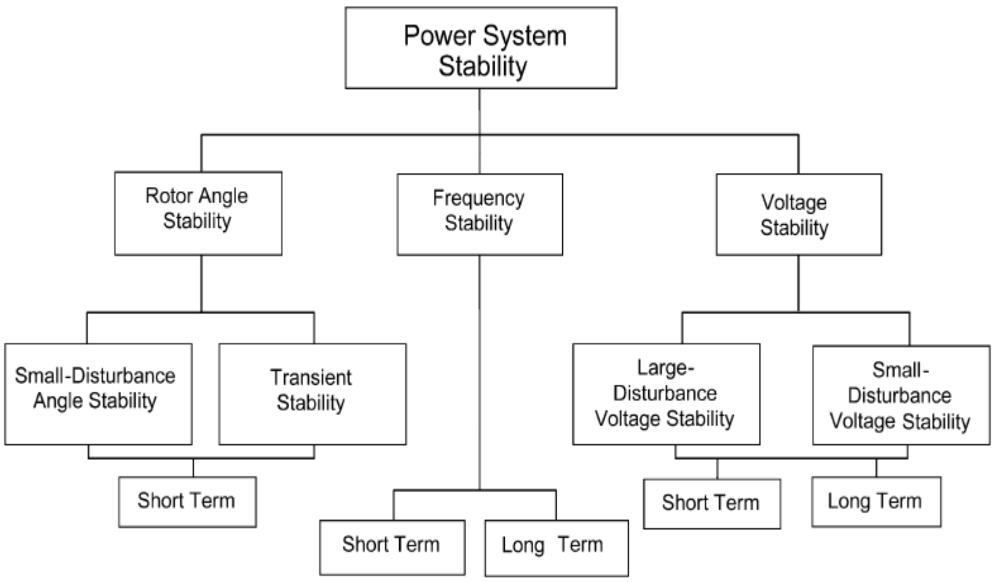

Fig. 2-1. Classification of power system stability

This work mainly focuses on Frequency stability which refers to the ability of a power system to maintain steady frequency following a severe system upset resulting in a significant imbalance between generation and load. It depends on the ability to maintain/restore equilibrium between system generation and load, with minimum unintentional loss of load. Instability that may result occurs in the form of sustained frequency swings leading to tripping of generating units and/or loads [1].

Severe system upsets generally result in large excursions of frequency, power flows, voltage, and other system variables, thereby invoking the actions of processes, controls, and protections that are not modeled in conventional transient stability or voltage stability studies. These processes may be very slow, such as boiler dynamics, or only triggered for extreme system conditions, such as volts/Hertz protection tripping generators. In large interconnected power systems, this type of situation is most commonly associated with conditions following splitting of systems into islands. Stability in this case is a question of whether or not each island will reach a state of operating equilibrium with minimal unintentional loss of load. It is determined by the overall response of the island as evidenced by its mean frequency, rather than relative motion of machines. Generally, frequency stability problems are associated with inadequacies in equipment responses, poor coordination of control and protection equipment, or insufficient generation reserve. In isolated island systems, frequency stability could be of concern for any disturbance causing a relatively significant loss of load or generation.

During frequency excursions, the characteristic times of the processes and devices that are activated will range from fraction of seconds, corresponding to the response of devices such as under-frequency load shedding and generator controls and protections, to several minutes, corresponding to the response of devices such as prime mover energy supply systems and load voltage regulators. Therefore, as identified in Fig. 2-1, frequency stability may be a short-term phenomenon or a long-term phenomenon. An example of short-term frequency instability is the formation of an under-generated island with insufficient under-frequency load shedding such that frequency decays rapidly causing blackout of the island within a few seconds. On the other hand, more complex situations in which frequency instability is caused by steam turbine over-speed controls or boiler/reactor protection and controls are longer-term phenomena with the time frame of interest ranging from tens of seconds to several minutes.

Power System Control

The function of an electric power system is to convert energy from one of the naturally available forms to the electrical form and to transport it to the points of consumption. Energy is seldom consumed in electrical form but is rather converted to other forms such as heat, light and mechanical energy. The advantage of the electrical form of energy is that it can be transported and controlled with relative ease and with higher degree of efficiency and reliability. A properly designed and operated power system should, therefore, meet the following fundamental requirements:

1. The system must be able to meet the continually changing load demand for active and reactive power. Unlike other types of energy, electricity cannot be conveniently stored in sufficient quantities. Therefore, adequate "spinning" reserve of active and reactive power should be maintained and approximately controlled at all times.
2. The system should supply energy at minimum cost and with minimum ecological impact.
3. The "quality" of power supply must meet certain minimum standards with regard to the following factors:
   - 3.1. Constancy of frequency
   - 3.2. Constancy of voltage
   - 3.3. Level of reliability

Several levels of controls involving a complex array of devices are used to meet the above requirements. These are depicted in Fig. 2-2 which identifies the various subsystems of a power system and the associated controls. In this overall structure, these are controllers operating directly on individual system elements. In a generating unit these consist of prime mover controls and excitation controls. The prime mover controls are concerned with speed regulation and control of energy supply system variables such as boiler pressures, temperatures and flows. The function of the excitation control is to regulate generator voltage and reactive power output. The desired active power outputs of the individual generating units are determined by the system generation control [2].

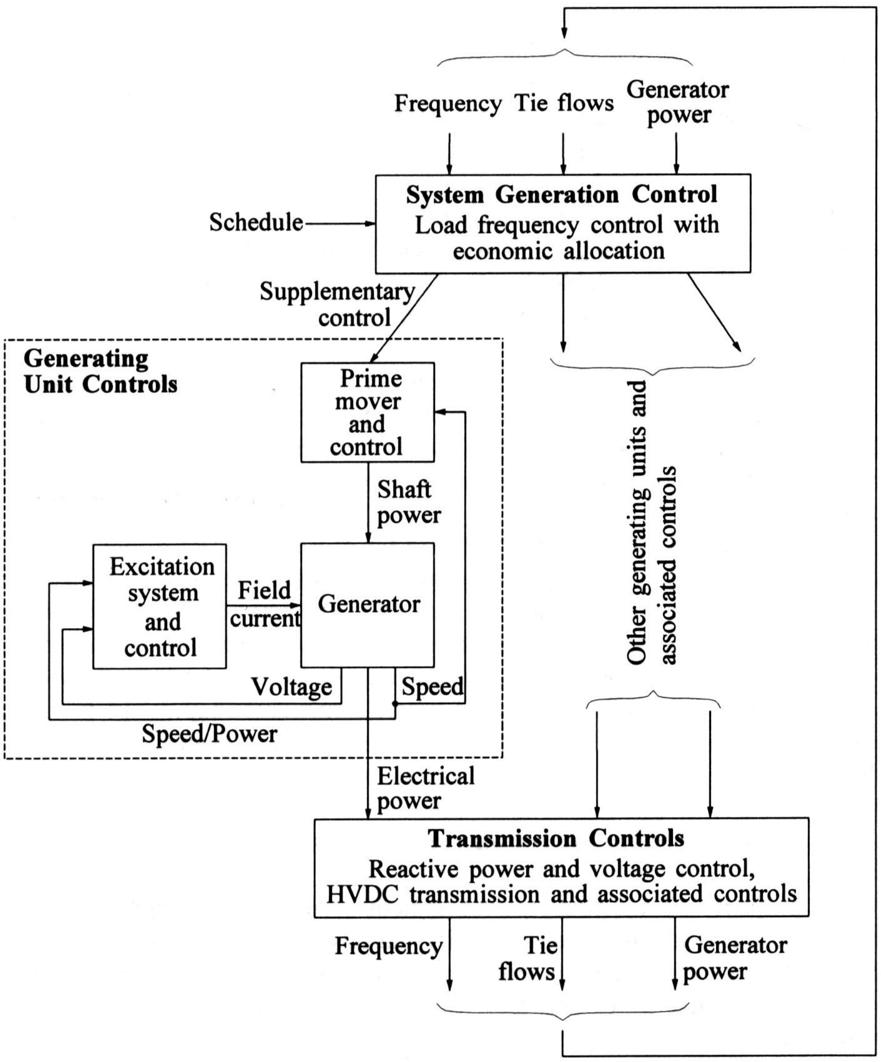

Fig. 2-2. Subsystem of a power system and associated controls

Frequency Control

In any electric system, the active power has to be generated at the same time as it is consumed. Power generated must be maintained in constant equilibrium with power consumed / demanded, otherwise a power deviation occurs. Disturbances in this balance, causing a deviation of the system frequency from its set-point values, will be offset initially by the kinetic energy of the rotating generating sets and motors connected. There is only very limited possibility of storing electric energy as such. It has to be stored as a reservoir (coal, oil, water) for large power systems, and as chemical energy (battery packs) for small systems. This is insufficient for controlling the power equilibrium in real-time, so that the production system must have sufficient flexibility in changing its generation level. It must be able instantly to handle both changes in demand and outages in generation and transmission, which preferably should not become noticeable to network users.

The electric frequency in the network is a measure for the rotation speed of the synchronized generators. By increase in the total demand the system frequency (speed of generators) will decrease, and by decrease in the demand the system frequency will increase. Regulating units will then perform automatic primary control action via load/frequency control (speed governor) and the balance between demand and generation will be re-established. The frequency deviation is influenced by both the total inertia in the system, and the speed of prime mover. Under undisturbed conditions, the system frequency must be maintained within strict limits in order to ensure the full and rapid deployment of control facilities in response to a disturbance [3]. The demand and generation equilibrium is satisfied by the control philosophy depicted in Fig. 2-3.

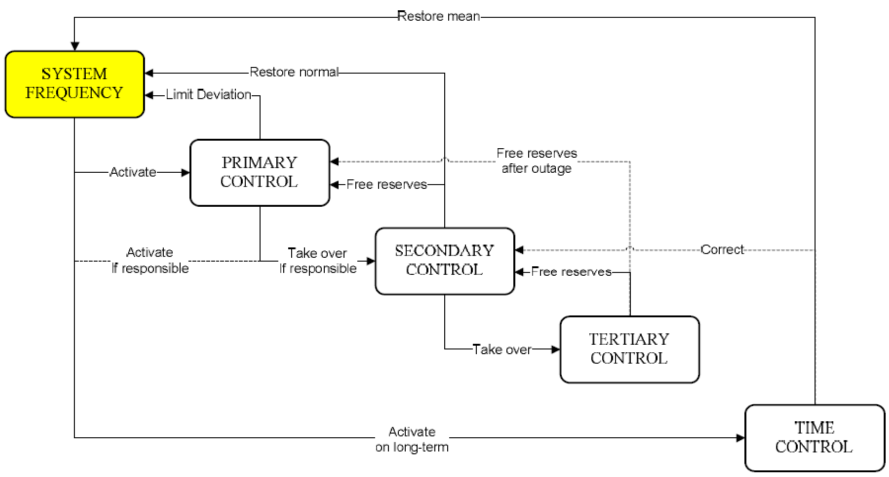

Fig. 2-3. Control philosophy

2.3.1.1. Primary Control

The frequency of a system is dependent on active power balance. As frequency is a common factor throughout the system, a change in active power demand at one point is reflected throughout the system by a change in frequency. Since there are many generators supplying power into the system, some means must be provided to allocate change in demand to the generators. A speed governor on each generating unit provides the primary speed control function by comparing the measured rotor speed with reference speed and responding to difference as depicted in Fig. 2-4 [2]. There are mainly two types of governors; isochronous governor and governors with speed-droop characteristic as described next.

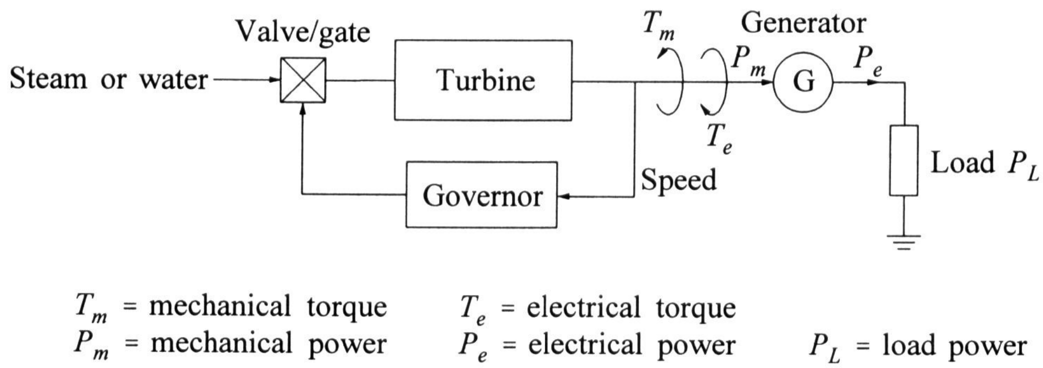

Fig. 2-4. Generator supplying isolated load

2.3.1.1.1. Isochronous Governor

An isochronous governor adjusts the turbine valve/gate to bring the frequency back to the nominal or scheduled value. Fig. 2-5 shows the schematic of such a speed governor system. The measured rotor speed w_r is compared with reference speed w_o. The error signal (equal to speed deviation) is amplified and integrated to produce a control signal ΔY which actuates the main system supply valves/gates. Due to the reset action of this integral controller, ΔY will reach a new steady state only when the speed error Δw_r is zero.

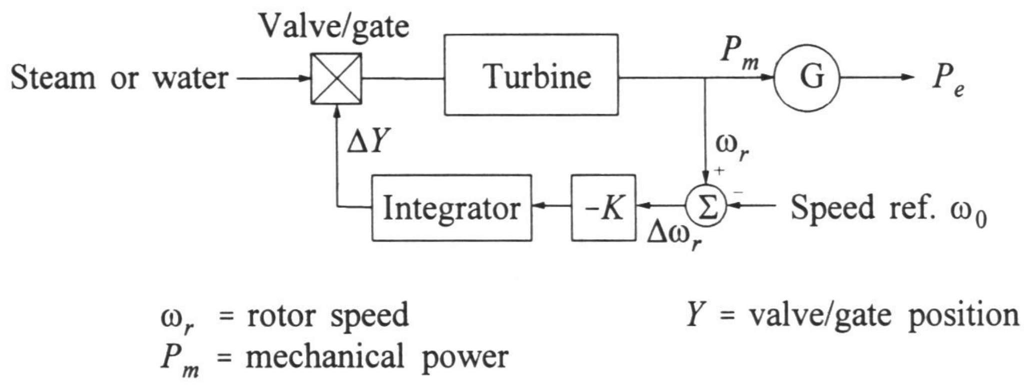

Fig. 2-5. Schematic of an isochronous governor

The time response of a generating unit, with an isochronous governor, when subjected to an increase in load is given in Fig. 2-6. The increase in demand (ΔP_L) causes the frequency to decay at a rate determined by the inertia of rotor. As the speed drops, the turbine mechanical power P_m begins to increase. This in turn causes a reduction in the rate of decrease of speed, and then an increase in speed when the P_m is in excess of the $P_e + \Delta P_L$. The speed will ultimately return to its reference value and the steady state P_m is increased by an amount equal to the additional load (ΔP_L).

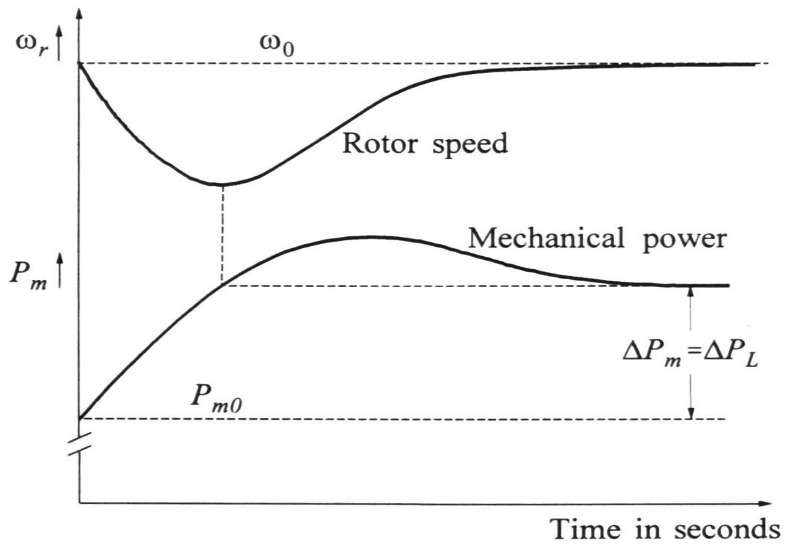

Fig. 2-6. Response of generating unit with isochronous governor

An isochronous governor works satisfactorily when a generator is supplying an isolated load or when only one generator in a multi-generator system is required to respond to changes in load. For power load sharing between generators connected to the system, speed-droop characteristic must be provided as discussed next.

2.3.1.1.2. Governors with Speed-Droop Characteristic

The isochronous governors cannot be used when there are two or more units connected to the system since each generator would have to have precisely the same frequency the same speed setting. Otherwise, they would fight each other, each trying to control system frequency to its own setting. For stable load division between two or more units operating in parallel, the governors are provided with a characteristic so that the speed drops as the load is increased.

The speed-droop or regulation characteristic may be obtained by adding a steady-state feedback loop around the integrator as shown in Fig. 2-7.

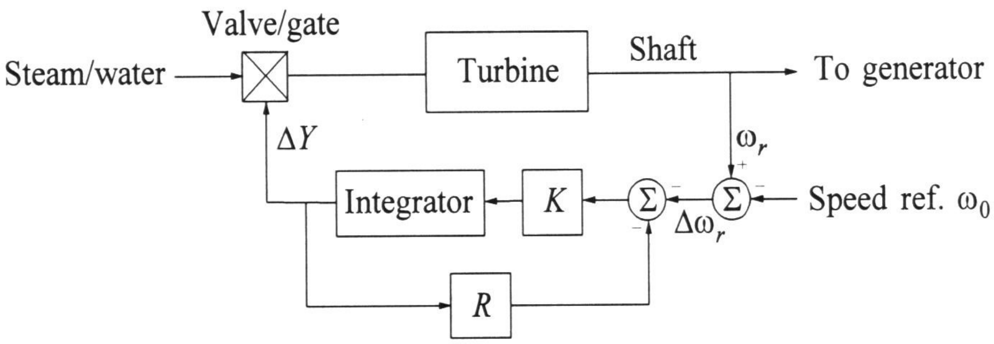

Fig. 2-7. Schematic of a governor with speed-droop characteristic

The value of *R* determines the steady-state speed versus load characteristic of the generating unit as shown in Fig. 2-8. The ratio of speed deviation (Δw_r) or frequency deviation (Δf) to change in valve/gate position (ΔY) or power output (ΔP) is equal to *R*. The parameter *R* is referred to as speed regulation or droop. It can be expressed in percentage as

$$Percent\ R = \frac{Percentage\ speed\ or\ frequency\ change}{Percentage\ power\ output\ change} \times 100 \qquad (2\text{-}1)$$

$$= \left(\frac{w_{nl} - w_{fl}}{w_o}\right) \times 100$$

where,

w_{nl} = *steady-state speed at no load*

w_{fl} = *steady-state speed at full load*

w_o = *nominal or rated speed*

The frequency and power output relation is depicted in Fig. 2-8.

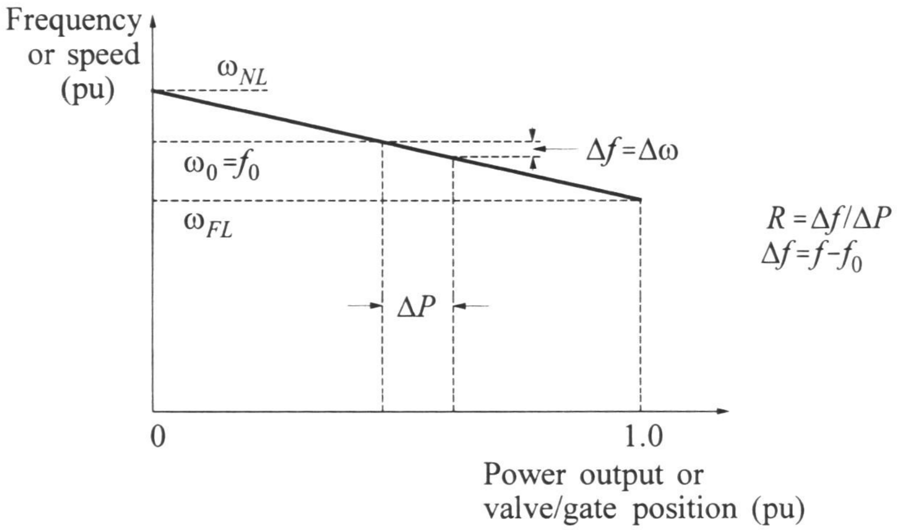

Fig. 2-8. Ideal steady-state characteristic of a governor with speed-droop characteristic

If two or more generators with speed-droop characteristics are connected to a power system, there will be a unique frequency at which they will share a load change. Consider two units with droop characteristics as shown in Fig. 2-9. They are initially at nominal frequency f_o, with outputs P_1 and P_2. When a load increase ΔP_L causes the units to slow down, the governors increase output until they reach a new common operating frequency f'. The amount of load picked up by each unit depends on the droop characteristic.

$$\Delta P_1 = P_1' - P_1 = \Delta f / R_1$$

$$\Delta P_2 = P_2' - P_2 = \Delta f / R_2$$

Hence,

$$\Delta P_1 / \Delta P_2 = R_2 / R_1 \qquad (2\text{-}2)$$

If the percentages of regulation of the units are nearly equal, the change in the outputs of each unit will be nearly in proportion to its rating.

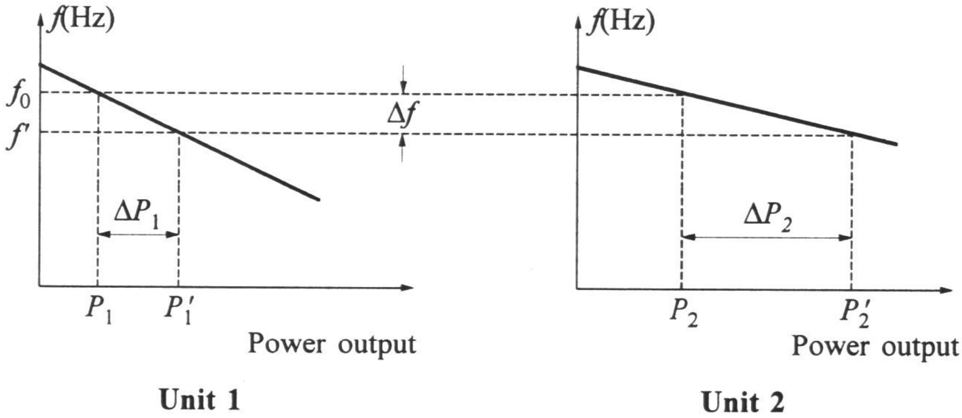

Fig. 2-9. Load sharing by parallel units with speed-droop characteristics

In conclusion, all units that are contributing to primary frequency control responds to an active power imbalance in the system relative to their speed-droop characteristic. The active power imbalance will result in a deviation in the system frequency, which will cause the primary controllers of all generators subject to primary control to respond within a few seconds. The controllers alter the power delivered by the generators until a balance between power output and consumption is re-established. As soon as the balance is re-established, the system frequency stabilizes and remains at a quasi-steady-state value as seen in Fig. 2-10, but differs from the frequency set-point because of the droop of the generators which provide proportional type of action. The speed governor also termed as the inner speed control loop and should be always active for satisfactory primary control response of the unit.

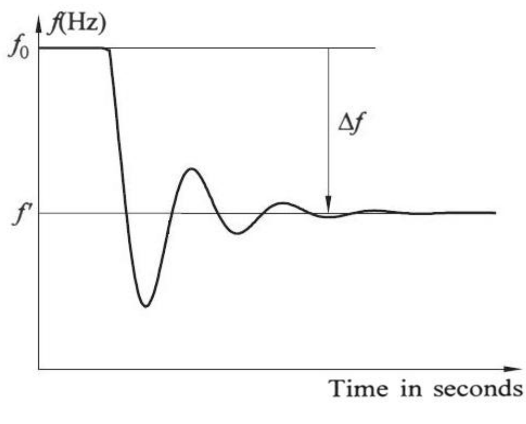

Fig. 2-10. Primary control effect after generation loss or load increase

2.3.1.2. Secondary Control

With primary control action, a change in system load will result in a steady-state frequency deviation, depending on the governor droop characteristic and frequency sensitivity of the load. All generating units on speed governing will contribute to the overall change in generation, irrespective of the location of the load change. Restoration of the system frequency from this quasi-steady-state value to nominal value requires supplementary control action which adjusts the load reference set point. Therefore, the basic means of controlling prime-mover power to match variations in system load in a desired manner is through control of the load reference set points of selected generating units. As system load is continually changing, it is necessary to change the output of generators automatically.

In an isolated power system, as in Turkish power system, the function of the secondary control (Automatic Generation Control, AGC) is to restore frequency to the specified nominal value as seen in Fig. 2-11. The secondary control action is much slower than the primary control action. As such it takes effect after the primary speed control (which acts on all units contributing to primary frequency) has stabilized the system frequency. Thus, AGC adjusts load reference settings of selected units, and hence their output power, to override the effects of the composite frequency regulation characteristics of the power system. In so doing, it restores the generation of all other units not on AGC to scheduled values. However in order to satisfactorily change the load reference setting, unit should have a closed loop power controller, which is also termed as the outer loop power controller. The outer loop power controller should be active for the satisfactory secondary control action of the unit.

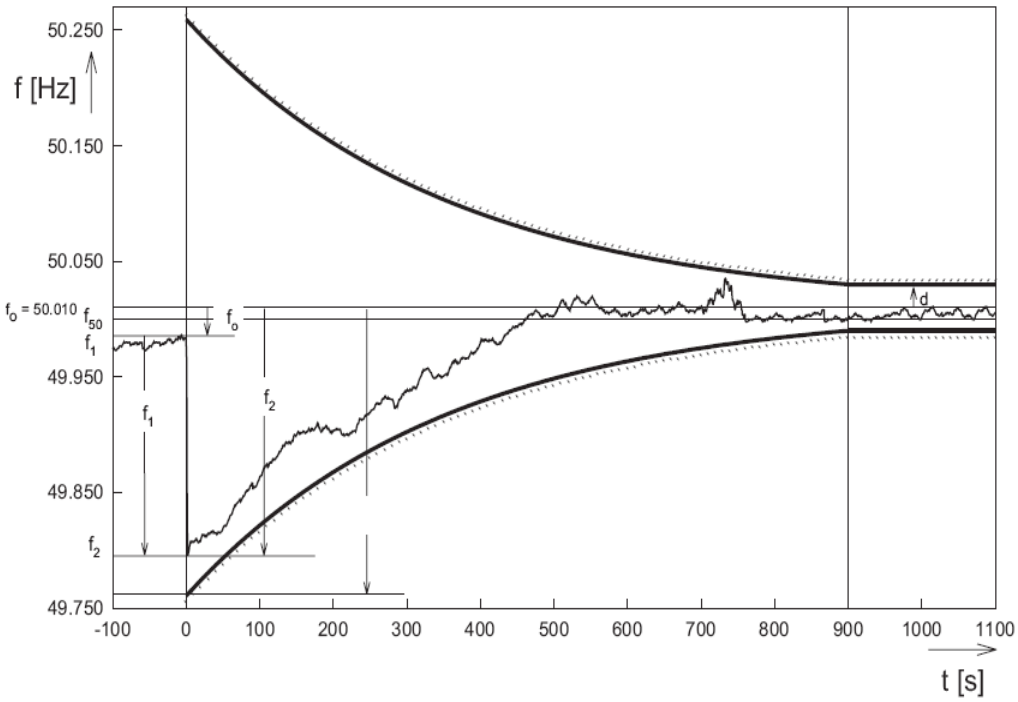

Fig. 2-11. Secondary control action

2.3.1.3. Tertiary Control

Tertiary control is any automatic or manual change in the working points of generators or loads participating, in order to:

- guarantee the provision of an adequate secondary control reserve at the right time,
- distribute the secondary control power to the various generators in the best possible way, in terms of economic considerations.

Changes may be achieved by:

- connection and tripping of power (gas turbines, reservoir and pumped storage power stations, increasing or reducing the output of generators in service);
- redistributing the output from generators participating in secondary control;
- changing the power interchange program between interconnected undertakings;
- load control (e.g. centralized telecontrol or controlled load-shedding).

Frequency Control Performance of Turkish Power System

The frequency control in Turkish power system is performed by primary (through generating units' governor action), secondary (by means of central Automatic Generation Control (AGC) System) and tertiary (manually through instruction given by National Load Dispatch Center (NLDC)) controls. The participation of the generating units to the frequency control is described in Turkish Electricity Market Grid Regulation (Grid Code) as follows;

- All generation facilities with unit capacities of 50 MW and above or total installed capacity of 100 MW and above except renewable energy resources shall be obligated to participate in primary frequency control.

- All generation facilities with unit capacities of 50 MW and above or total installed capacity of 100 MW and above except renewable energy resources and cogeneration power plants shall also participate in secondary frequency control within the scope of commercial ancillary services.

- The generation facilities with lower installed capacity may participate in frequency control only if they submit proposals to Transmission System Operator (TEİAŞ) and if their proposals are accepted [15].

In line with these regulations, currently all types of power plants are contributing to frequency control according to their reserve settings determined by the NLDC. In general, response of the Turkish Power System to the incidences is satisfactory [5]. As an example, trumpet curve (Fig. 2-12) indicating frequency control response during the generation loss of 435 MW (Units 1,2 and 3 at Berke HPP) on 25 April 2006 is given below;

Incident time	16:14:42
Power loss (ΔP_a)	435 MW
Total Power of TEIAS System	20 031 MW
Nominal Frequency (f_0)	50.00 Hz
Δf	0,265Hz
f_{min}	49,658 Hz
Δf_2	0,342 Hz
λ	1272 MW/Hz

Fig. 2-12. Trumpet curve after an incident

However the frequency response of the overall system is not satisfactory considering the UCTE requirements. The major problem about the frequency control performance of Turkish power system is the periodic oscillations with delta frequency deviation of ≤ 50 mHz and 20 – 30 seconds time period.

During the tests performed by Frequency Control Sub-Committee formed by engineers from TEİAŞ and Electricity Generation Corporation (EÜAŞ), it has been observed that there is a strong linkage between amount of HPP in service and amount of periodic oscillations in the system frequency.

Frequency records between 05:00 and 05:15 when the major HPPs were not in service on 5 January 2006 is given in Fig. 2-13.

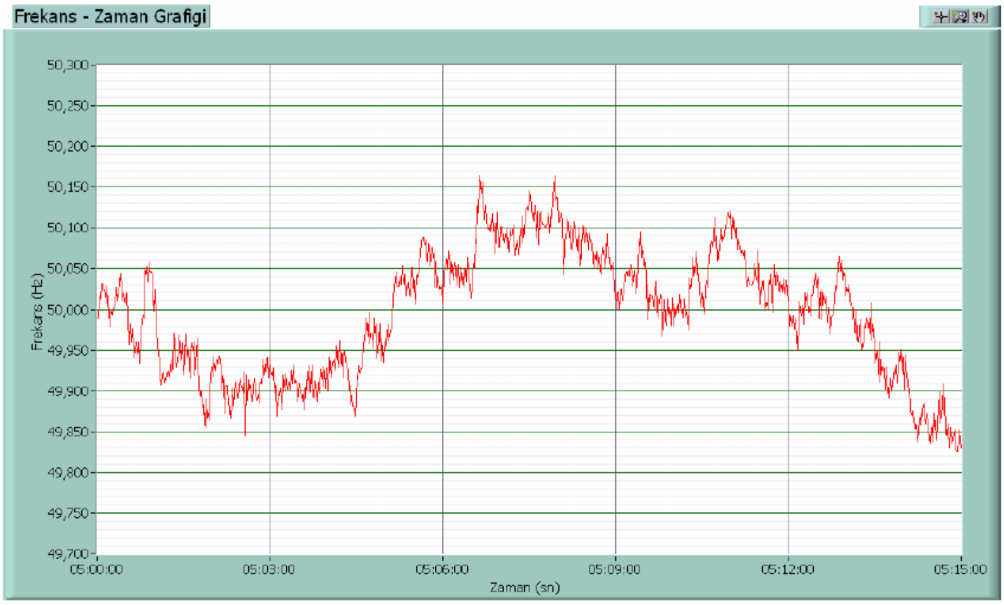

Fig. 2-13. Frequency recording when major HPP are not in service

Frequency records between 17:20 and 17:35 when the major HPPs were in service on 5 January 2006 is given in Fig. 2-14.

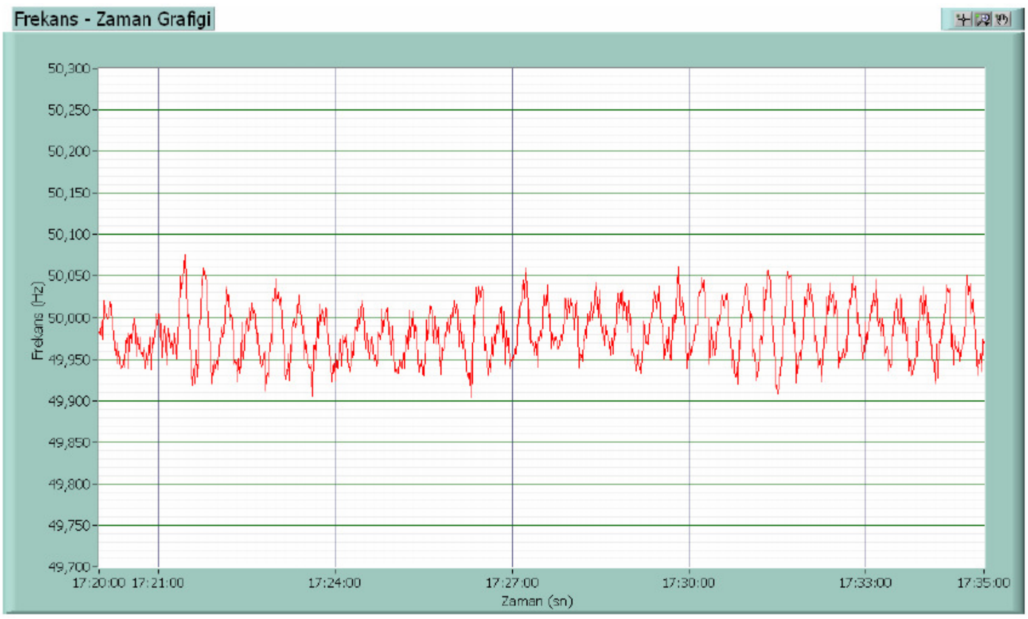

Fig. 2-14. Frequency recording when major HPP are in service

As it can be seen from the above graphics, oscillations in the system frequency are much higher during the day time when most of the HPP are in service compared to the night time when amount of HPP in service is less.

For the test purpose, AGC at NLDC was made inactive on 7 March 2006 and seen that the 50 mHz oscillations in system frequency with 20 – 30 seconds time periods still exists. This means that frequency oscillations with 20 – 30 seconds periods remain prominent independent of whether the AGC is in operation or not. Thus the studies for determining the exact reason of oscillations are focused on the HPP primary controllers.

Problem Definition

As explained in previous section Turkish power system suffers from 50 mHz oscillations in system frequency with 20 – 30 seconds time period. The oscillations are not only an obstacle before the interconnection of Turkish power system with UCTE network, but they also have various negative effects on power plants that are contributing to primary frequency regulation. As the frequency constantly changes the regulating vanes are always in operation which reduces the life time of the equipment. Further constant variation in temperature and pressure causes pipes, penstocks and boilers in power plants wear out.

In order to prevent these negative effects and to establish a sustainable connection with UCTE, the reason behind these oscillations should be determined. Hence this work mainly focuses on the possible effects of HPPs on Turkish power system frequency and possible solutions to prevent the negative contribution of HPPs to frequency stability of Turkish power system.

Contribution to the Problem Solution

In order to prepare a representative model for the Turkish power system, a Priority List of major power plants is formed. Since the frequency characteristic of the overall system is mainly determined by the major plants, it is assumed that the representative model of these plants would satisfactorily represent the overall system characteristic. The Priority List of power plants is given in Table 1-1.

Table 1-1. Priority List of Power Plants and Their Capacities

Natural Gas and Combined Cycle Power Plants (NGCCPP)			Thermal Power Plants (TPP)			Hydro Power Plants (HPP)		
Plant	**Unit**	**Rating (MW)**	**Plant**	**Unit**	**Rating (MW)**	**Plant**	**Unit**	**Rating (MW)**
GEBZE	Gas	4 x 260	ELBİSTAN	A	4 x 344	ATATÜRK		8 x 300
	Steam	2 x 282		B	4 x 362	KARAKAYA		6 x 300
ADAPAZARI	Gas	2 x 260	İSKENDERUN		2 x 660	BİRECİK		6 x 126
	Steam	1 x 282	SOMA		6 x 165	KEBAN	1-4	4 x 157
ALİAĞA	Gas	4 x 260	AMBARLI F/O	1-2	2 x 114		5-8	4 x 180
	Steam	2 x 282		3	1 x 114	ALTINKAYA		4 x 175
BURSA	Gas	4 x 239		4-5	2 x 150	OYMAPINAR		4 x 135
	Steam	2 x 237	ÇAYIRHAN	1-2	2 x 160	BERKE		3 x 175
AMBARLI	Gas	6 x 128		3-4	2 x 160	HASAN UĞR.		4 x 125
	Steam	3 x 173	KEMERKÖY	1&3	2 x 210			
HAMİTABAT	Gas	8 x 100		2	210			
	Steam	4 x 111	YATAĞAN		3 x 210			
TEMELLİ	Gas	2 x 262	SEYİTÖMER	1-2	2 x 153			
	Steam	1 x 323		3	1 x 160			
UNİMAR	Gas	2 x 168		4	1 x 160			
	Steam	1 x 169						

The representative model of Atatürk HPP is determined via field tests, which are isolated operation and step change in frequency measurement in different modes of operation. Similarly in Birecik HPP two isolated operation tests are performed and the representative model of the plant is determined and all models are validated by simulation studies. Further, stability boundaries for controller settings of these two HPPs are determined. It should be noted that the manufacturer and the technology of governor heads of Atatürk, Karakaya and Oymapınar HPPs are exactly the same. Hence by determining the controller model of Atatürk HPP, the models for Karakaya and Oymapınar HPPs are also cleared. Similarly Birecik and Berke HPPs are manufactured by the same technology and manufacturer. Hence the controller models for both plants are determined.

Further Altınkaya HPP is visited for test purposes but unfortunately due to limitations of the test equipment and signals supplied by the operator, the test could not be performed. However during the site visit period, the exact model of the governor head and the current operation settings are determined. It should also be noted that Altınkaya and Hasanuğurlu HPPs are manufactured by the same technology, Toshiba.

Unfortunately Keban HPP is not visited, but the model of the plant is determined via discussions with the representatives and experts of VaTech, who is the manufacturer of the plant. Further the current operational settings are supplied by the plant operator and the representative model is determined.

For modeling of the NGCCPP and TPP standard IEEE governor models are used according to the supplied documents and operational settings from plant operators. Certain assumptions used in the modeling will be described in further chapters.

Finally, representative model for long term frequency stability of Turkish power system is prepared and validated by previous frequency recordings. After validating the model, following studies are performed in order to determine the effects of HPP controllers on power system frequency;

- Increasing and decreasing the contribution of HPP to primary frequency control

- Changing the "Speed Droop" setting of HPP controllers ("Speed Droop" term is defined further in the chapters)

- Changing the settings of Proportional Integral (PI) controller

- Changing the structure of controller by addition of an input (derivative of frequency deviation)

After studying the effects of hydro power plants' governor settings on the Turkish power system frequency, other factors that may have negative effects on damping of frequency oscillations are introduced as future studies, together with sample simulation studies to have an idea about possible effects of these factors.

CHAPTER 3

POWER PLANT MODEL DESCRIPTIONS

Introduction

This chapter examines the characteristics of hydraulic system, which consists of turbine and penstock, generator mechanical system and controllers used on HPPs. The following sections describe the effects of water column characteristics on the hydraulic turbine performance. The main effect is water inertia in the penstock. Water column inertia causes changes in the turbine to lag behind changes in the turbine guide vane opening, which introduces a phase lag into the governor loop and has a destabilizing effect on the unit. Moreover the dynamic behavior of generator, converting the mechanical energy into electrical energy is described. Further the speed control is investigated, including the conflicts between fast primary control response to frequency deviations and positive effect on power system frequency stability. Standard IEEE models used in order to model TPPs and NGCCPPs are also described.

Modeling of Hydro Power Plants

Hydraulic System Model

3.2.1.1. Turbine Model

The oldest form of energy conversion is by the use of waterpower; the turbine converts the potential energy of the water into the rotational kinetic energy of the turbine. In the traditional hydroelectric scheme the energy is obtained free of cost as the water comes from a high level reservoir into the turbine in which the water energy is converted directly to mechanical energy. In the turbine, the tangential momentum of the water passing through a runner's blade will be changed in direction and a tangential force on the runner is produced. The runner therefore rotates and the energy is transferred from the water to the runner and hence to the output shaft. The water is discharged with reduced energy. The hydraulic turbine may be classified into one of two general categories: impulse and reaction [6]. Although there are many applications of impulse turbines around the world none of the priority list HPPs has an impulse type turbine. Hence the impulse turbine model is not investigated in this study.

All HPPs in priority list are equipped with a certain type of reaction turbines which is Francis turbine, illustrated in Fig. 3-1. The water enters a spiral casing (volute) which surrounds the runner, whose cross sectional area decreases along the water path in such a way to keep the water velocity constant in magnitude. Departing the volute the water is directed on the runner by the guide vanes mounted all around the periphery of the runner. Each vane is pivoted and all will be turned in synchronism to alter the flow rate throughout the turbine, and hence the power output as required by governor action. The runner blades deflect the water so that its angular momentum is changed. From the centre of the runner, the water is turned into the axial direction and flows to the tailrace via the draft tube. In order to ensure the hydraulic turbine is full of water, the lower end of the draft tube is always submerged below the water level in tailrace [7].

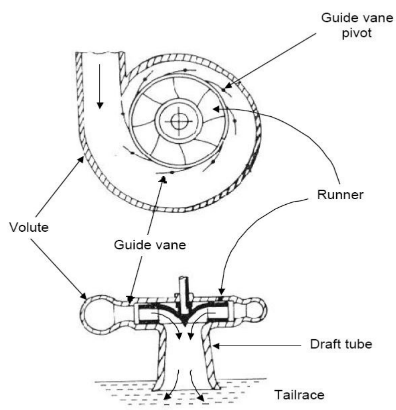

Fig. 3-1 Francis Turbine

The mechanical power (P_m) available from an ideal hydraulic turbine is the product of hydraulic head available (h) and mass flow rate (q) but in practice this is reduced by an efficiency factor, h, to account for power losses. The turbine torque at rated speed and head is almost linearly related to guide vane position for most turbines in the range from no-load to rated load but only approximately in the range from fully closed guide vane to no load guide vane, as shown in Figure 3-2. The turbine model is based on the equation for steady state operation relating the output power to water flow and head [6].

$$P_m = \eta q \rho g_a h \tag{3-1}$$

where:

P_m = Turbine output power

η = The turbine efficiency

ρ = Water density

g_a = Acceleration due to gravity, m2/s

h = The head at the turbine admission, m

q = Actual turbine flow, m3/s

The fact that the turbine is not 100% efficient is taken into account by subtracting the no load flow q_{nl} from the net flow to give the effective flow which, when multiplied by the head, produces mechanical power. There is also a turbine damping effect, which is a function of guide vane opening, to be included. Therefore the per unit turbine power, Pm can be expressed as:

$$\overline{P_m} = A_t \overline{h}\left(\overline{q} - \overline{q_{nl}}\right) - D_n \overline{G}\overline{\Delta n} \tag{3-2}$$

The turbine MW rating is used as power base, q_{base} is chosen as the turbine flow rate, with guide vanes fully open (guide vane position =1) and h_{base} is equal to the static head of water column h_0. The parameter D_n accounts for the effect of the speed variation Δn on the turbine efficiency; typical values of D_n fall in the range

$0.5 \leq D_n \leq 2.0$. The turbine gain A_t is obtained from the ratio of effective gate position to the actual gate position and can be calculated using equation (3-3).

$$A_t = \frac{1}{G_{fl} - G_{nl}} \times \frac{Turbine \quad MW \quad rating}{Generator \quad MW \quad rating} \tag{3-3}$$

where G_{fl} is the guide vane position at full load and G_{nl} is the guide vane position at no load both are calculated at rated speed and head. The relationship between idealized and real guide vane position is shown in Fig. 3-2.

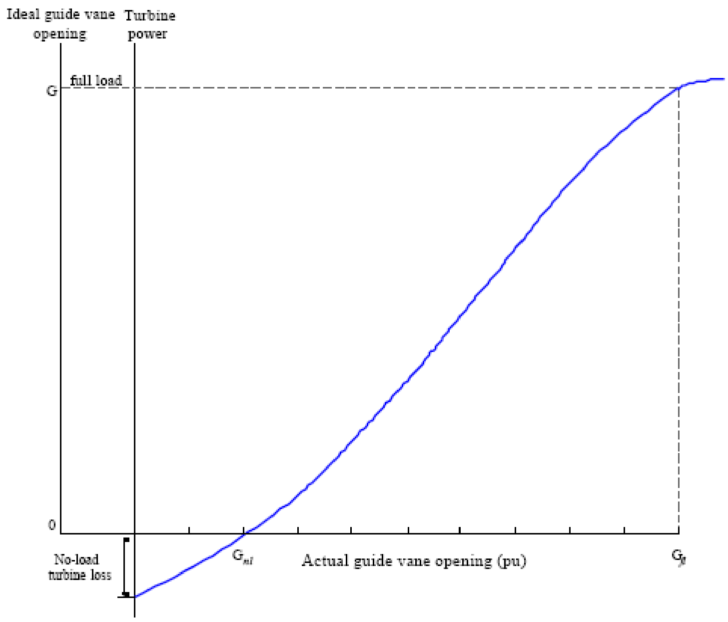

Fig. 3-2 Typical torque/guide vane characteristic

The turbine characteristics define base flow through the relationship between the flow (q), guide vane (G) position and head (h). The per unit flow rate through the turbine using q_{base} as the turbine flow rate and h_{base} is equal to the static head h_0, is given by its valve characteristic,

$$\bar{q} = \bar{G}\sqrt{\bar{h}} \tag{3-4}$$

3.2.1.2. Modeling the Water Column

The performance of a hydraulic turbine is greatly influenced by the characteristics of the water column which feeds it, including the effect of water inertia in the penstock. The effect of water inertia is to cause changes in turbine flow to lag behind changes in the guide vane opening. In fact, the power has a transient response which is initially in the opposite sense to that intended by changing the guide vane position. Although the turbine guide vane opening may change rapidly, the water column inertia prevents the flow from changing as rapidly. Consequently, after a rapid increase in guide vane opening, and before the flow has had time to change appreciably, the velocity of water into the wheel drops because of the increased area of the guide vane opening. The power transfer to the wheel actually drops before it increases to its required steady state value. This is the most prominent factor, which makes a hydraulic turbine such an uncooperative component in a speed control system [9].

The turbine and penstock characteristics are determined by three basic equations relating to the velocity of water in the penstock, acceleration of the water column under the influence of gravity and the production of mechanical power in the turbine. First, a non-linear representation is developed which is appropriate when large changes in speed and power are to be considered, such as in islanding, load rejection and system restoration studies.

The basic water column model represents a single penstock with a very large or no surge tank. The penstock is modeled on the assumption that the water acts as an incompressible fluid so that here the water hammer effect may be neglected. Consider here a rigid conduit of length l and cross-section area A, where the penstock head losses h_f due to the friction of water against the penstock wall are proportional to flow (q) squared.

$$h_f = f_p\, q^2 \tag{3-5}$$

where f_p, is the head loss coefficient in the penstock due to friction [10]. Assuming that the water in the penstock can be treated approximately as a solid mass, the rate of change of flow can be related to the head of water using Newton's 2[nd] law of motion. The force on the water mass is

$$\left(h_0 - h - h_f\right)\rho g_a A = \rho A l \frac{dv}{dt} \tag{3-6}$$

where

h_0 = The static head of water column, m

h = The head at the turbine admission, m

h_f = The head loss due to friction, m

f_p = head loss coefficient, m/(m3/s)^2

v = The water velocity, m/s

The rate of change of the flow in the penstock can be determined as:

$$\frac{dq}{dt} = \left(h_0 - h - h_f\right)\frac{g_a A}{l} \tag{3-7}$$

Equation (3-7) can be written in per unit form in order to normalize system representation. Compared to the use of physical units, the per unit format offers computational simplicity by eliminating units and expressing the system quantities as dimensionless ratios. The base values are chosen so that the principle variables will be equal to one per unit under rated conditions. Here the base head h_{base} is chosen to be the available static head h_0 which is equal to the reservoir head minus the tailrace head, and the base flow q_{base} is equal to the turbine flow with guide vane fully open. Expressing equation (3-7) in per unit yields

$$\frac{d\overline{q}}{dt} = \left(\overline{1} - \overline{h} - \overline{h_f}\right)\frac{h_{base} g_a A}{l q_{base}} \tag{3-8}$$

$$\frac{d\overline{q}}{dt} = \frac{\left(\overline{1} - \overline{h} - \overline{h_f}\right)}{T_w} \tag{3-9}$$

where $T_w = \dfrac{lq_{base}}{h_{base} g_a A} = \dfrac{lv_{base}}{h_{base} g_a}$ is the water starting time.

The water starting time represents the time required for a head h_{base} to accelerate the water in the penstock from standstill to the velocity v_{base}. This is calculated between turbine inlet and the forebay or the surge tank if a large one exists [11]. Consider a simple penstock supplied from an open reservoir discharging into the atmosphere as shown in Fig. 3-3. Opening the guide vane in a time Δt causes the velocity of the water in the penstock to increase by Δv and the head at the turbine inlet to drop by Δh.

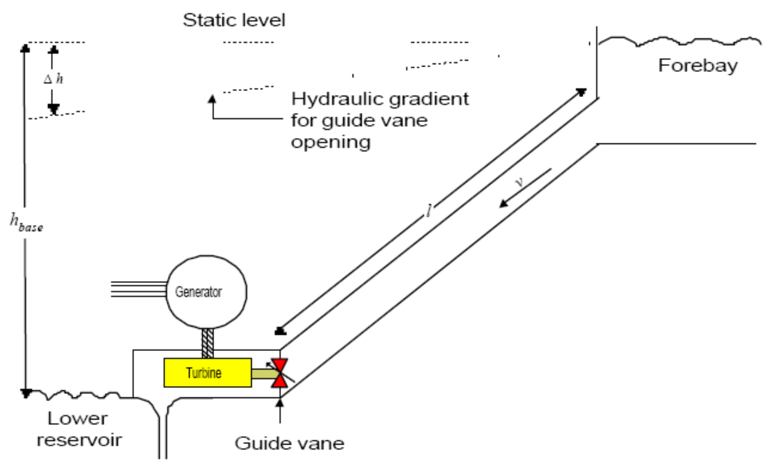

Fig. 3-3 Schematic of a HPP

The acceleration of water due to change in head at the turbine, characterized by Newton's

2nd law of motion may be expressed as

$$\rho A l \frac{d\Delta v}{dt} = -\rho g_a A \Delta h \tag{3-10}$$

The acceleration equation can be converted to per unit form by dividing by v_{base} and h_{base} to give:

$$\left(\frac{lv_{base}}{g_a h_{base}}\right)\frac{d\Delta\bar{v}}{dt} = -\Delta\bar{h} \tag{3-11}$$

Writing in terms of per unit variables

$$T_w \frac{d\Delta\bar{v}}{dt} = -\Delta\bar{h} \tag{3-12}$$

This equation represents an important characteristic of the hydraulic plant. Inspection of equation (3-12) shows that, if the guide vane is closed, a back pressure will arise causing the water to decelerate. That is, if there is a positive pressure change, there will be a negative acceleration change. Similarly, a negative pressure change will cause a positive acceleration change. The maximum acceleration occurs immediately after the guide vane opening because the entire difference in pressure is available for accelerating the water. For a non-uniform penstock with different cross sectional areas, the water inertia time constant is calculated as [12]:

$$T_w = \frac{\sum lv}{g_a h} \tag{3-13}$$

where $\sum lv$ is the summation of length and velocity of sections in the water passage.

3.2.1.3. Combined Turbine / Penstock Model

The hydraulic system can be modeled by combining equations (3-2) for the turbine and (3-9) for the inelastic water column. The block diagram of Fig. 3-4 is a nonlinear representation showing how the generated power depends on the guide vane position. Note that the power also depends on additional inputs Δn, h_0 and q_{nl} but that these change slowly compared to the primary control input. The value for water starting time of the penstock (Tw) is obtained at rated conditions using rated head and rated flow as the base values.

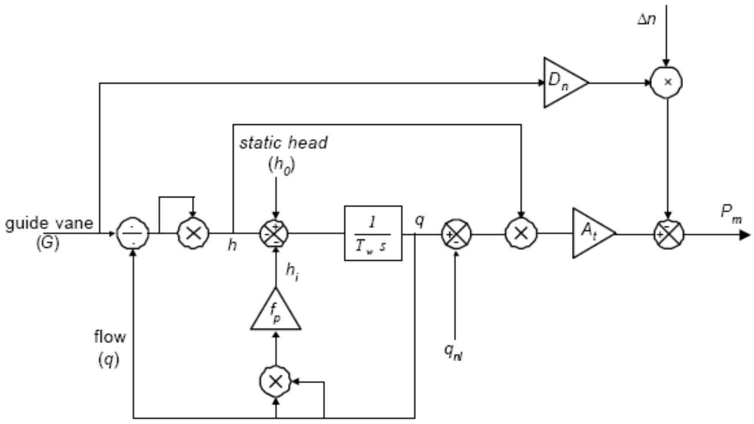

Fig. 3-4 Model of penstock and turbine

3.2.1.4. Linearised Turbine / Penstock Model

A better understanding of the model is possible via linearised representation. The water column transfer function is obtained by linearising the basic penstock–turbine equations, (3-4) and (3-9) as presented in Appendix-A. This results in the first order transfer function of equation (3-14) relating small changes in the mechanical power to changes in the guide vane opening. Note that the water time constant Tw here corresponds to the operating condition rather than the rated condition. Thus to model the unit correctly in stability simulations, it is necessary to adjust the value of Tw each time the initial operating conditions are changed [17].

$$\frac{\Delta P_m(s)}{\Delta G(s)} = \frac{1 - T_w s}{1 + 0.5 T_w s} \tag{3-14}$$

The system's dynamic characteristic is illustrated in Figure 3-5, this shows the change in the turbine mechanical power for a step change in the guide vane position applied at t = 0 for a system with a water time constant Tw. A transient change in power occurs which is opposite to the direction of change in guide vane position and the change in the turbine power is twice as large and in the opposite direction to the final change. The subsequent power increase depends on the value of Tw, as the water accelerates until the flow reaches the new steady state value that establishes the new power output [7].

The initial and final power values for a unit step change in guide vane position can be determined as follows. The initial value theorem gives [2].

$$P_m(0) = \lim_{s\to\infty} s\frac{1}{s}\left[\frac{1-T_w s}{1+0.5T_w s}\right] = -2$$

while the final value theorem gives,

$$P_m(\infty) = \lim_{s\to 0} s\frac{1}{s}\left[\frac{1-T_w s}{1+0.5T_w s}\right] = 1$$

The step time response can be determined as

$$\Delta P_m(t) = \left[1 - 3e^{-\frac{2t}{T_w}}\right]$$

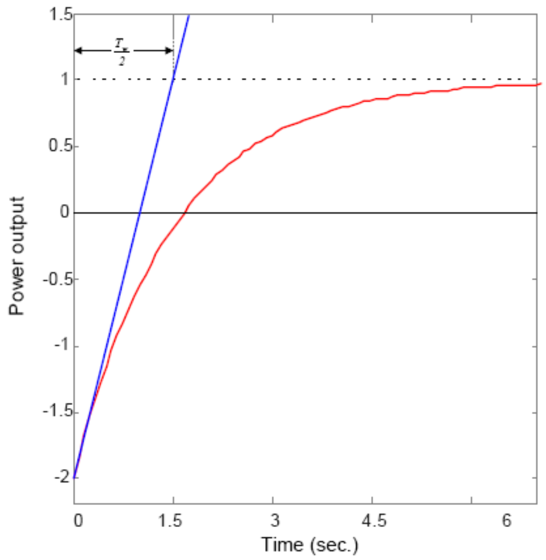

Fig. 3-5 Turbine power change due to step guide vane opening

Generator Mechanical Model

The dynamic behavior of the generators within a power system is of fundamental importance to the overall quality of the power supply. The synchronous generator converts mechanical power to electrical power at a specific voltage and frequency. The source of the mechanical power, the prime mover, may be a diesel engine, a steam turbine or a water turbine. Whatever the source, it must have the basic property that its speed is almost constant regardless of the power demand. The analysis of any power system to determine its long term frequency stability involves the mechanical properties of the machines.

The mechanical equations of a rotating machine are very well established and they are based on the swing equation of the rotating inertia. The equation is based on the elementary principle in dynamics which states that accelerating torque is the product of moment of inertia of the rotor times its angular acceleration. [14]. Constant shaft speed for a given machine is maintained when there is equilibrium between the mechanical shaft and electrical torques. Any imbalance between the torques will cause the acceleration or deceleration of the machine according to the equation (3-14).

$$T_{acc} = J\frac{d^2\delta_m}{dt^2} = T_{mech} - T_{elec} \qquad (3\text{-}14)$$

where:

T_{acc} = Accelerating torque, N.m.

J = Combined moment of inertia of the generator and turbine, Kg.m2

δ_m = Mechanical torque angle of the rotor, rad.

t = Time, seconds

T_{mech} = Mechanical torque, N.m.

T_{elec} = Electromagnetic torque, N.m

The mechanical angular velocity ω_m is the time derivative of the torque angle. Rewriting

(3-14) yields,

$$J\frac{d\omega_m}{dt} = T_{mech} - T_{elec} \tag{3-15}$$

The kinetic energy of a rotating body is equal to ½ J ω_m^2, thus equation (3-15) can be normalized in terms of the per unit inertia constant H, which is defined as the kinetic energy of the machine at rated speed per machine volt-ampere rating. Using w_{m0} to denote rated angular velocity in mechanical radians per second gives

$$\frac{2HVA_{base}}{\omega_{m0}^2}\frac{d\omega_m}{dt} = T_{mech} - T_{elec} \tag{3-16}$$

The angular velocity of the rotor in electric rad/sec ω is related to the rotor mechanical angular velocity by $\omega = \frac{\omega_m}{p_n}$, where P_n is the number of generator poles. The equation of motion in per unit form can be written using the angular velocity of the rotor in electric rad/sec.

$$2H\frac{d\overline{\omega}}{dt} = \overline{T}_{mech} - \overline{T}_{elec} \tag{3-17}$$

where $T_{base} = \frac{VA_{base}}{\omega_{m0}}$

It is preferable to express the relationship of equation (3-17) in term of mechanical and electrical power rather than torque. Since the power is equal to torque times angular velocity, P=Tω, expanding for small oscillations around the operating point and neglecting the second order terms gives,

$$\Delta P = \overline{\omega_o}\Delta\overline{T} + \overline{T_0}\Delta\overline{\omega} \tag{3-18}$$

At steady state, the mechanical torque is equal to the electrical torque ($T_{mec0} \cong T_{elec0}$). Combining equations (3-17) and (3-18), the deviation in per unit speed

$\Delta\omega$ of the rotor as a function of deviations in the mechanical and electrical powers can be represented as

$$\Delta\overline{P}_m - \Delta\overline{P}_e = 2Hs\Delta\overline{\omega} \qquad (3\text{-}19)$$

3.2.1.5. Mechanical Starting Time

The mechanical starting time of the machine T_m, can be calculated using equation (3-17) where,

$$\frac{d\overline{\omega}}{dt} = \frac{\overline{T}_{acc}}{2H}$$

Let T_m be the time required by the rated torque to accelerate the rotor from stand still to rated speed. Integrating with respect to time with $\omega = 1.0$ pu, and $T_{acc} = 1.0$ pu results in:

$$1 = \frac{1}{2H}\int_0^{T_m} 1 \quad dt$$

Therefore, the mechanical starting time $T_m = 2H$

Speed Controller Models

The frequency of a power system is dependent on the balance between the generated and demanded power. In case of an imbalance the difference should be eliminated by the controllers in each plant according to their speed droop settings, which is referred as primary control as previously explained

The primary speed control function involves feeding back speed error to control the gate position. In order to ensure satisfactory and stable parallel operation of multiple units, the speed controller is provided with a droop characteristic as discussed in previous chapters. Fig. 2-7 also indicates the schematic of a speed controller with speed-droop characteristic.

However this structure is not sufficient for stable operation of hydro units. Hydraulic turbines have a peculiar response due to water inertia: a change in gate position produces an initial turbine power change which is opposite to that sought. For stable control performance, a large transient (temporary) droop with a long resetting time is therefore required. This is accomplished by the provision of a rate feedback or transient gain reduction compensation [2]. The transient droop is introduced as shown in Fig. 3-6.

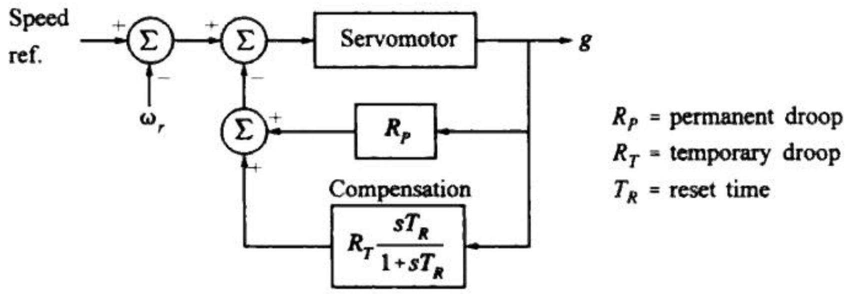

Fig. 3-6. Speed controller with transient droop compensation

The effect of transient droop is to reduce the initial response of the controller. The unit initially responds to a frequency deviation as if its droop setting is $R_P + R_T$. Thus the guide vanes will open less and the initial inverse pressure effect of water inertia is reduced. The duration of this limitation on initial response is dependent on T_R setting. According to T_R setting, the effect of temporary droop will be reduced leaving the permanent droop to determine the steady state response of the unit. As seen in Fig. 3-7a and Fig. 3-7b the transient droop compensation stabilizes the controller.

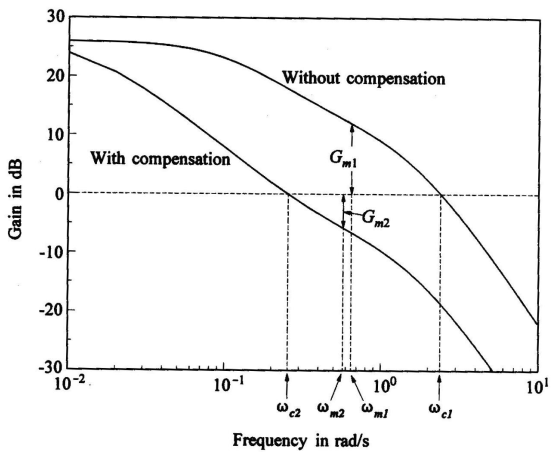

Fig. 3-7a. Open-loop frequency response characteristic with and without transient droop

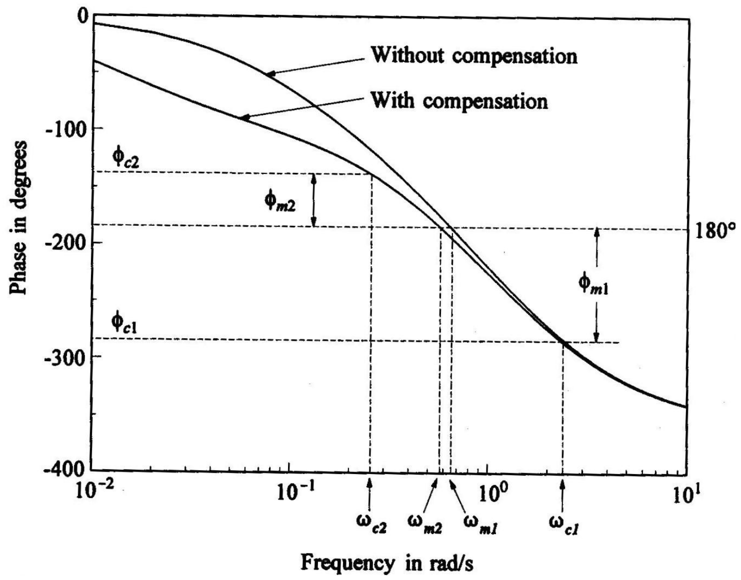

Fig. 3-7b. Open-loop frequency response characteristic with and without transient droop

It is obvious that a HPP unit operating in island condition (i.e. a single generator feeding a load) with unstable controller will trip due to over or under speed protections. However if the unit with the same controller is connected to a strong grid, the unit will not trip and be able to supply its primary response probably faster than stable HPP units. This is mainly due to the fact that a single unit is not able to change the overall system frequency. Hence observing a unit operating without problem in gird operation does not give any information about the stability of controller.

In order to keep the unit stable the R_T and T_R parameters are required, as explained above. However limiting the initial response of the unit with R_T and T_R also has its price. Although the unit becomes stable, the primary response of the unit to frequency deviations slows down. In order to observe this effect the step responses of a sample controller for different R_T and T_R settings are determined considering the unit is connected to a very large grid. Also the model is linearised around the equilibrium point and the pole positions are observed. As seen in Fig. 3-8 and 3-9 the unit becomes stable by increasing R_T and T_R whereas the step response of the unit in grid operation slows down.

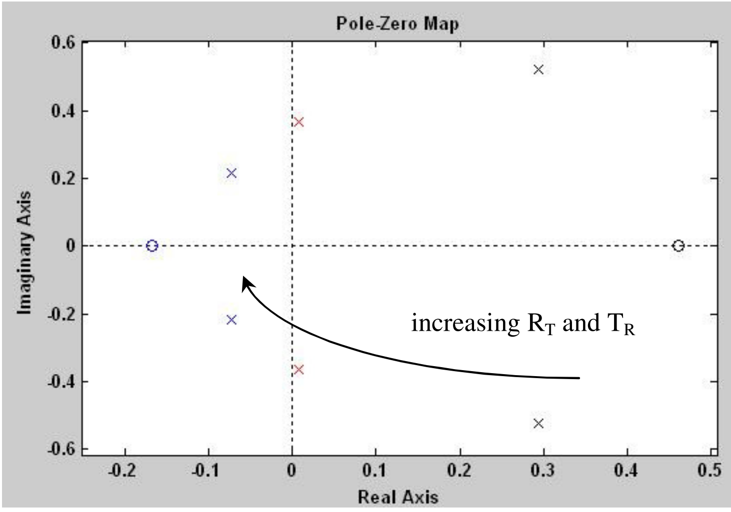

Fig. 3-8. Pole positions for different R_T and T_R settings

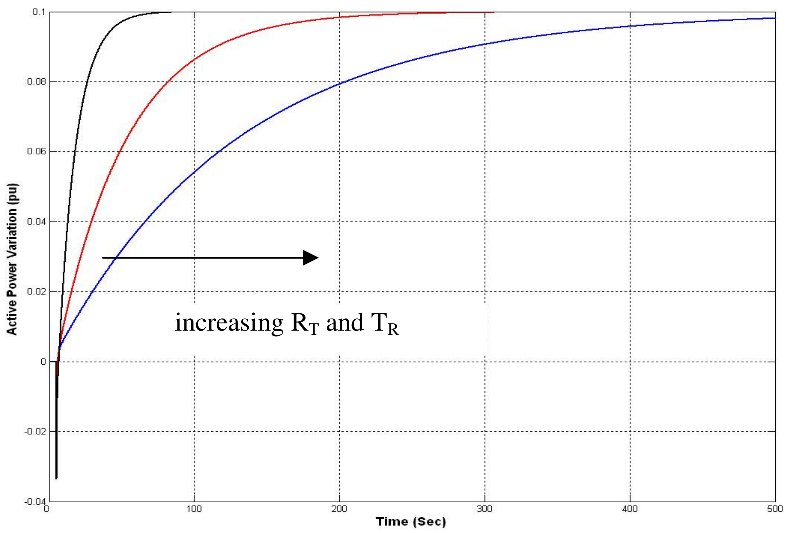

Fig. 3-9. Unit response to -200mHz step frequency change for different R_T and T_R settings

As seen in Fig. 3-8 and 3-9 although the unit is unstable in island conditions, it operates perfectly while connected to a very large grid. This does not cause an observable problem on overall system frequency, if a single unit or a few percents of units are operated in this way, however as the percentage increase the system frequency becomes oscillating as explained in [4]. This problem will be investigated in further chapters but it could be concluded that there is an obvious conflict between the stable operation and fast controller response for HPPs.

The speed control is performed by mechanical and hydraulic components in older units via flying ball and dashpot. New units perform the same function with

Proportional-Integral-Derivative (PID) action with D is usually set to zero as shown in Fig. 3-10. The logic behind the controllers and the overall transfer functions are equivalent and the parameters (PI) can easily be selected to result in desired R_T and T_R as shown in [4].

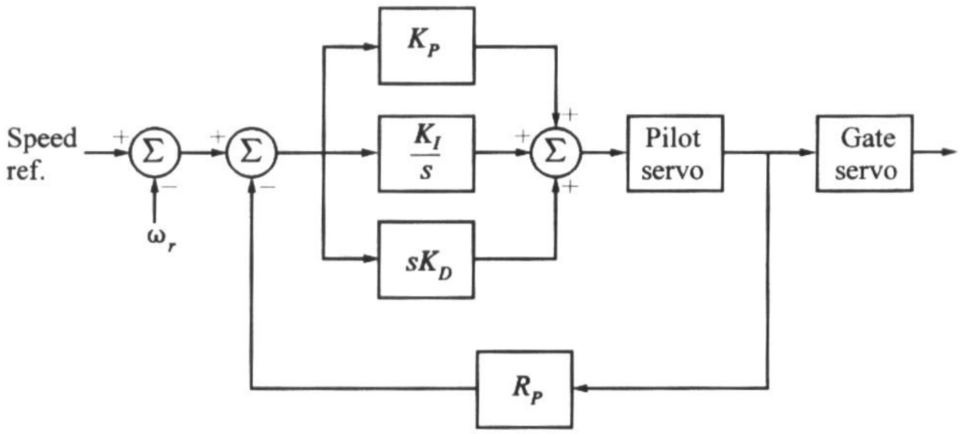

Fig. 3-10. PID speed controller

Where K_p, K_I and K_D are PID parameters respectively

Modeling of Thermal Power Plants

The thermal power plants mainly consist of two major parts, the boiler and the turbine. The basic configuration of TPPs is given in Fig. 3-11.

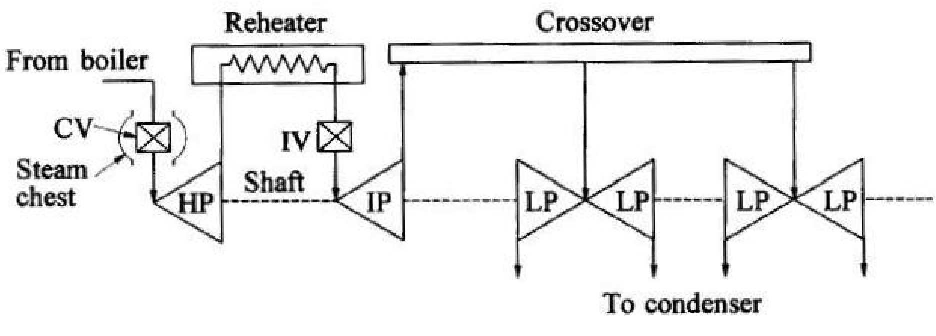

Fig. 3-11. Turbine configuration

Steam enters the High Pressure (HP) section through the Control Valve (CV) and the inlet piping. The housing for the control valves is called the steam chest. A substantial amount of steam is stored in the chest and the inlet piping to the HP section. The HP exhaust steam is passed through the reheater. The reheat steam flows into the Intermediate Pressure (IP) turbine section through the reheat Intercept Valve (IV) and the inlet piping. The crossover piping provides a path for the steam from IP section exhaust to the Low Pressure (LP) inlet [2].

During the operation boiler controllers keeps the pressure constant whereas the turbine controllers operates on output power. In case of a disturbance in the system, the turbine controllers respond to the frequency deviation which affects the pressure before the turbine. This change in pressure is also observed in power output but it is compensated by the boiler control in order to avoid high or low pressure, which may damage the turbine. Although the boiler controller has a certain effect on the power output, a standard model with the assumption of perfectly constant pressure is utilized. That is mainly due to the fact that the study is concentrated on the effects of HPPs on sustained oscillations and the negative effects of boiler controllers are out of the scope.

The thermal power plants are modeled utilizing the IEESGO, standard IEEE model, which is given in Fig 3-12.

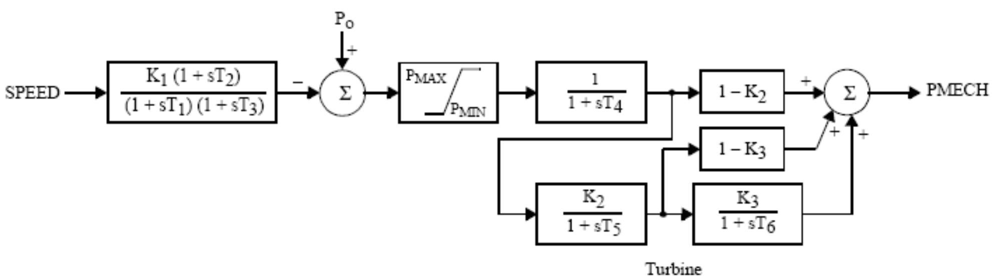

Fig. 3-12. IEEE standard IEESGO controller and turbine model

where

T_1 = Controller lag, seconds

T_2 = Controller lead compensation, seconds

T_3 = Governor lag, seconds

T_4 =Time constant of main inlet volumes and steam chest, seconds

T_5 = Reheater delay, seconds

T_6 = Delay due to IP-LP turbine, crossover pipes and LP end hoods, seconds

K_1 = 1/ speed droop

K_2 and K_3 =Constants determining fractions of HP, IP, LP on total power generation, pu

P_0 = Power set value, pu

P_{max} and P_{min} = Power output limits, pu

P_{mech} = Mechanical output power of turbine, pu

The speed controller regulates the control valves according to the variation in system frequency. The speed error is multiplied by K_1 to get the target power deviation in response to the speed error. The controller has a lead-lag compensation that could be tuned to desired response by T_1 and T_2 and the governor lag is represented by T_3 which is usually less than 1 second. After these the target power deviation is added to P_0 summing up to target power of the unit

As indicated earlier, the control valves modulate the steam flow through the turbine for load/frequency control during grid operation. The response of steam flow to a change in control valve opening exhibits a time constant T_4 due to the charging time of the steam chest and the inlet piping to the HP section which is in the order of 0.2 to 0.3 seconds. The steam flow in the IP and LP sections can change only with the buildup pressure in the reheater volume. The reheater holds a substantial amount of steam and T_5 is in the order of 5 to 10 seconds. The steam flow into the LP sections experiences an additional time constant T_6 associated with the crossover piping in the order of 0.5 seconds.

The parameter values for the models are determined from the plant operators and applied to the system model. The generators of the TPPs are modeled as described in section 3.2.2.

Modeling of Natural Gas Combined Cycle Power Plants

A gas turbine is comprised of three major components, which are the axial compressor, combustor(s) and the turbine. Air compressed through the compressor goes through the combustor and gets burnt with input fuel resulting in high temperature, high pressure exhausts gas. This exhaust gas does its work while expanding through the turbine (and through the heat recovery steam generator in combined cycle applications) back to the atmosphere [16]. The configuration of NGCCPP is given in Fig. 3-13.

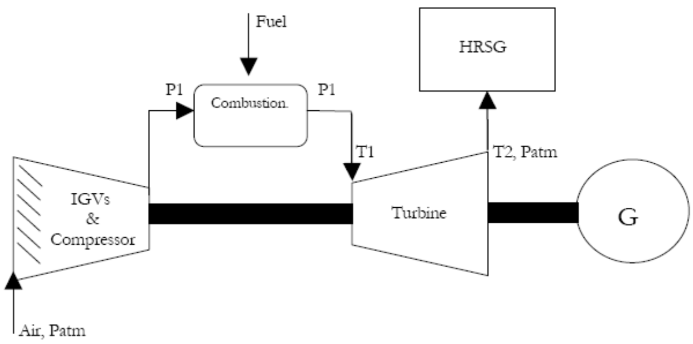

Fig. 3-13. A general NGCCPP configuration

In order to model the controller and the turbine of NGCCPPs, standard IEEE GAST model is utilized. Primary inputs of the system are "fuel flow" and "airflow". Fuel flow is a completely controllable parameter whereas airflow which is a function of ambient temperature together with shaft speed (or power system grid frequency) can be regulated with the help of compressor inlet guide vanes up to a certain degree. However in the GAST model the airflow is assumed to be constant, which eliminates the power output variation depending on system frequency. The model is presented in Fig. 3-14.

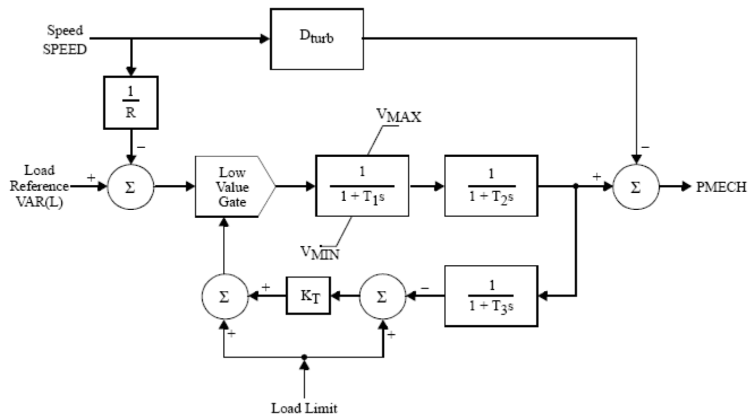

Fig. 3-14. IEEE standard GAST controller and turbine model

where

R = Speed droop

T_1 = Governor time constant, seconds

T_2 = Combustion chamber time constant, seconds

T_3 = Exhaust gas temperature measurement time constant, seconds

V_{max} and V_{min} = fuel valve opening limits, pu

K_T = Gain of the load limiting feedback path

P_{mech} = Mechanical output power of turbine, pu

D_{turb} = Speed damping of gas turbine

The GAST model represents the principal dynamic characteristics of gas turbines driving generators connected to power systems. The error signal is determined by the deviation in system frequency. The deviation is divided by R and added to the load reference and the governor responds to the deviation via a forward path with a time constant, T1, and drives a combustion chamber with a time constant T2. Also the model includes a load-limiting feedback path. The load limit is sensitive to turbine exhaust temperature, and T3 represents the time constant of the exhaust gas measuring system. Further K_T represents the gain of the load limiting feedback. Finally D_{turb} represents speed damping introduced by the gas turbine rotor.

The parameter values for the models are determined from the plant operators and applied to the system model. The generators of the NGCCPPs are modeled as described in section 3.2.2.

CHAPTER 4

MODELING AND SIMULATION STUDIES

Introduction

After describing the dynamical behavior of power plants focusing on the HPPs, this chapter proceeds with the results of performed field tests on speed controllers. During the visit of experts from UCTE to Turkey, two island operations tests were performed in Birecik and Atatürk HPPs in order to observe the ability of plants to operate in island mode. Both tests resulted in unit trips. The theoretical studies indicated that the unit trips were due to unstable operational settings of the plants. This chapter describes the theoretical studies performed in order to determine the model and the effects of controller parameters on stability of the unit.

As the data of other major HPPs are acquired from plant operators, the simulations indicated that most of the HPPs are operating with unstable settings. In order to observe the effects of HPPs with unstable settings on power system frequency, the power system model to analyze the long term frequency stability is determined. The derivations regarding the model are also given in this chapter. After determination, the model is verified by measurements of real events. Having the model validated, the effects of changes on governor settings are simulated and results are presented further in this chapter.

Additionally the power controllers, which are necessary for the secondary control operation as described before, are investigated. The current operation of power controller is described. The stability criteria considering this current structure and the negative effects of the controller are discussed theoretically. The affects of power controllers on system frequency is studied with long term frequency stability model and assumptions on controllers of TPP and NGCCPP.

Field Tests on Atatürk Hydro Power Plant

Atatürk HPP is the biggest power plant in Turkey, with a total rated power of 2400 MW. The power is generated via eight 300 MW units and transferred to the system by a 400 kV transmission substation.

Island Operation Test

In order to observe the ability of Atatürk HPP to operate in island conditions a field test is organized by TEİAŞ. The test scenario was to form an island of demand approximately 500 MW and to feed this load by two units of Atatürk HPP. The island prepared by TEİAŞ is given in Fig. 4-1.

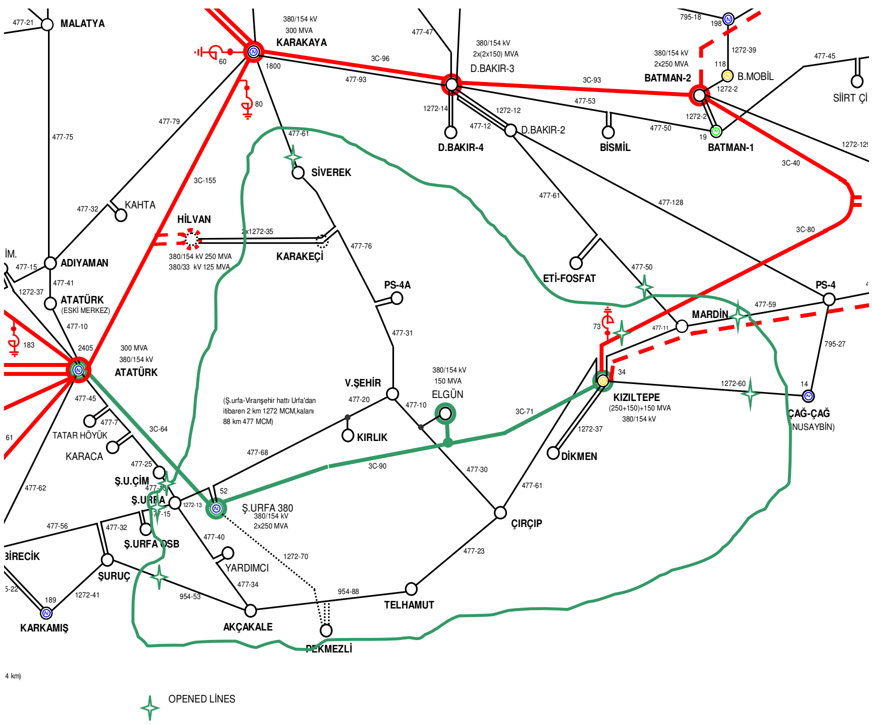

Fig. 4-1. The islanded region during test in Atatürk HPP

During the test power output, wicked gate opening and unit speed is measured with 6400 samples/second resolution. Speed droop setting of the controllers was 8% and units were loaded at approximately 250 MW each.

The switchyard of Atatürk HPP is organized leaving two units and the feeder for the region to be islanded on one bus. All the lines that connect the region shown in Fig. 4-1 to the grid are tripped one by one, leaving only one connection to grid and to Atatürk HPP. The flow through the last line was approximately 5MW when the region is completely islanded from the grid by tripping this line.

After the trip of the last connection, the island frequency began oscillating and the grow rate of oscillations was increased by the tripping of an under frequency relay in Mardin substation. Finally both units tripped causing a blackout in the region. The frequency measurement during the test is given in Fig. 4-2.

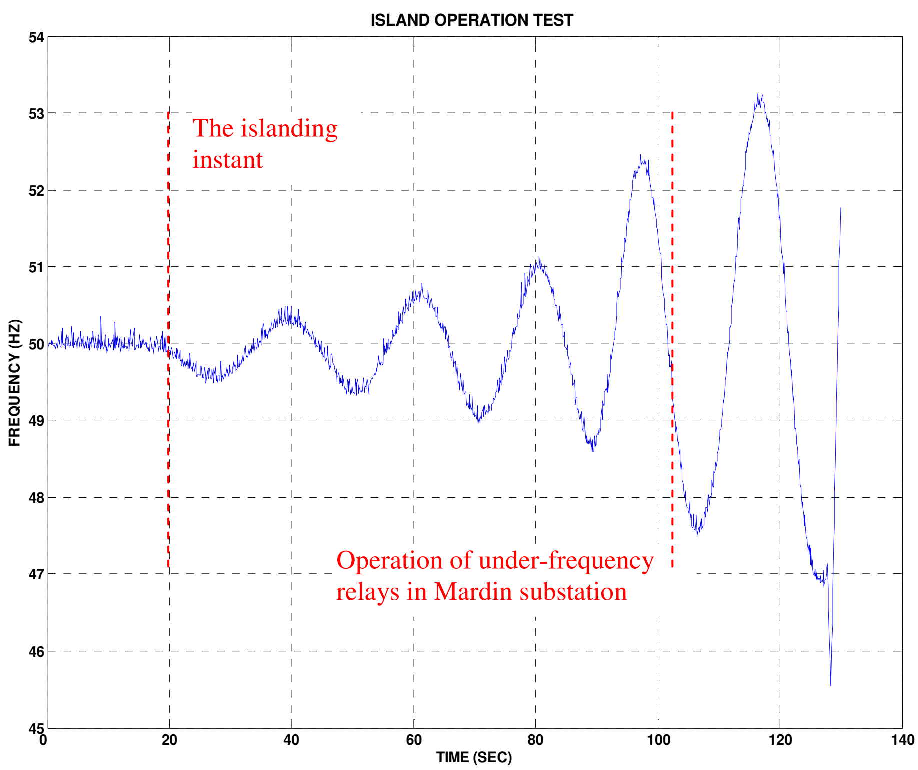

Fig. 4-2. The frequency of the islanded region during test in Atatürk HPP

The Step Response Test

In order to understand the reason of trip a modeling study is performed on the plant. The exact controller structure is determined via plant documentation. As seen in Fig. 4-3 the PI speed controller is followed by a PID position controller.

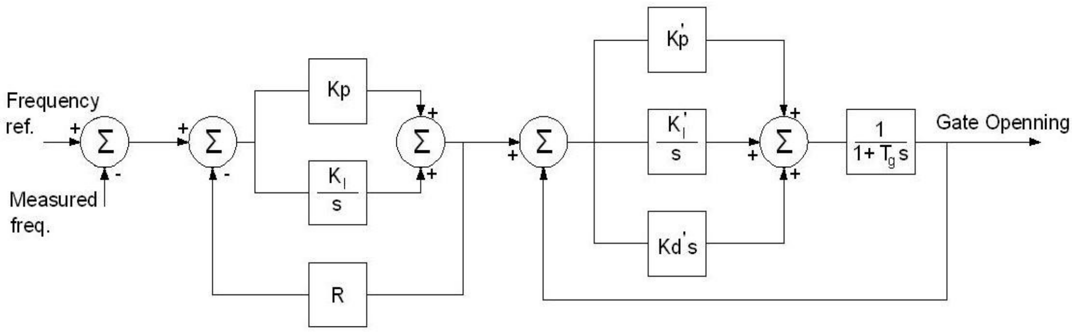

Fig. 4-3. The speed controller block diagram of Atatürk HPP

where K_P’, K_I’ and K_d’ are the PID gains of the position controller and T_g represents the time delay between position controller output and actual position of gate.

The speed measurement signal of the controller is disabled and an artificial speed signal is supplied to the speed measuring system by utilizing a signal generator. Applying 50 Hz to the speed measurement system, the steady state operation is reached. Then step changes of ±200 mHz are applied and the response of the unit is recorded.

The records are compared with simulation results. The settings of the controller and the characteristic of the water column are determined. The comparison of simulation results with measurements is given in Fig. 4-4.

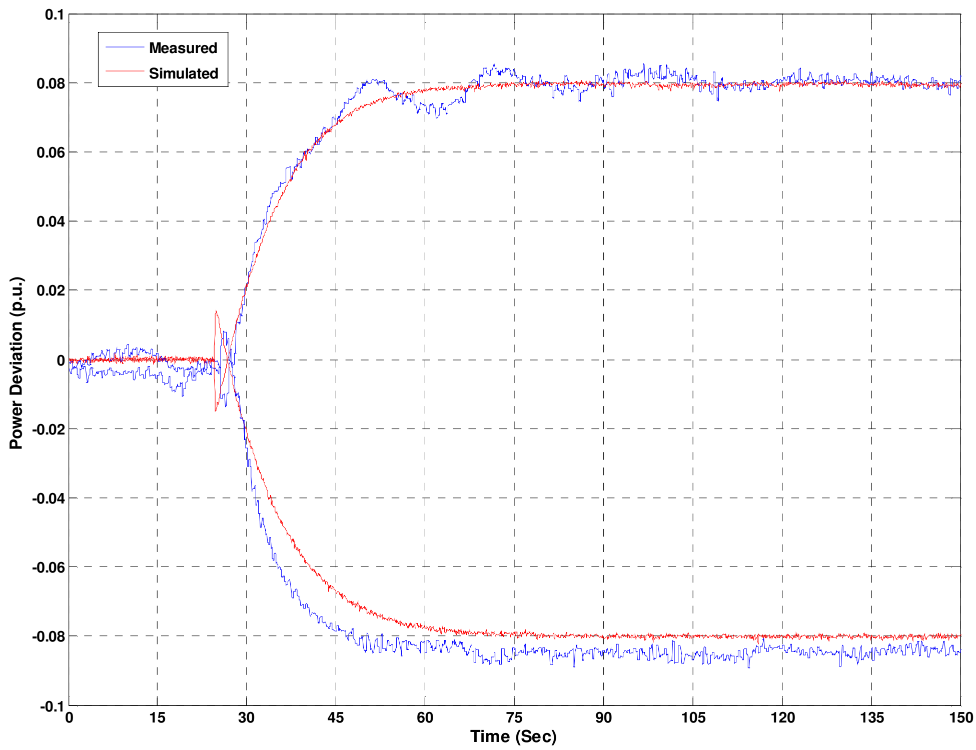

Fig. 4-4. The ±200 mHz step response of Unit 8 in Atatürk HPP

After determining the model of the units, the transmission system and loads of the islanded region are modeled neglecting the effect of frequency deviation on demand power. The islanded region transmission system model and load flow results are presented in Appendix-B.

The Island Operation Simulations

The simulations are performed with Power System Simulator for Engineering (PSS/E) Version 30.3. PSS/E is a package software used for many studies like load flow, fault analysis and dynamic studies. TEİAŞ also performs the required system studies by the PSS/E software

The connection of the island to the power system is represented by a bus connected to 400 kV bus of Atatürk HPP for studies. The flow through the line is set equal to the pre-islanding conditions and the line is tripped. Also the demand loss in Mardin substation is modeled by tripping of a bulk load. The results of the simulation are given in Fig. 4-5.

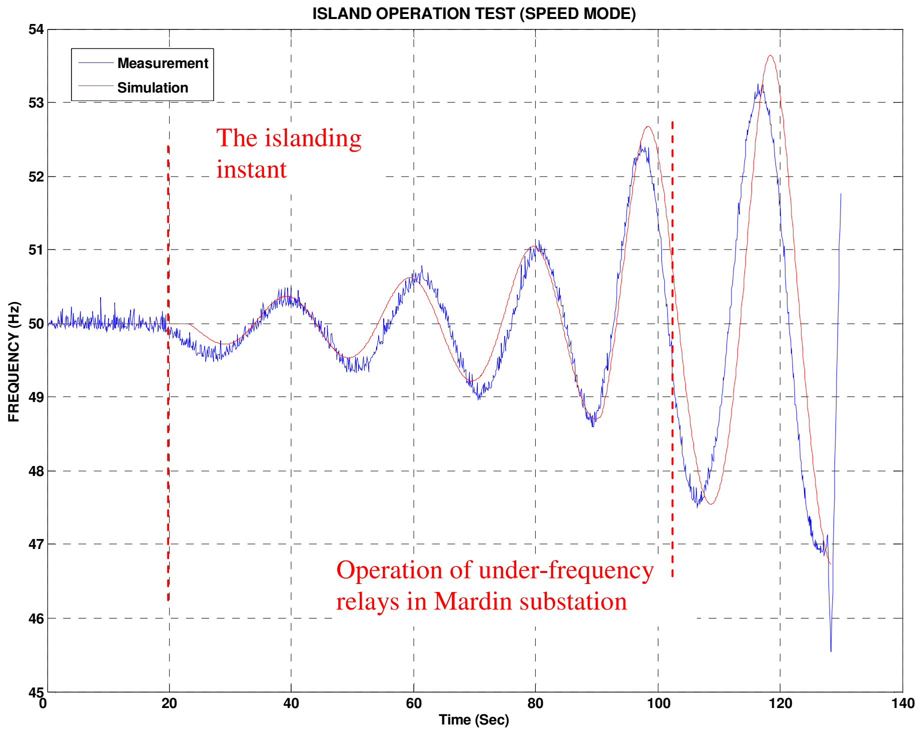

Fig. 4-5. The island operation simulations for Atatürk HPP

After reaching satisfactory results in simulations, a study is performed in order to determine the limits of PI and speed droop for stable operation of HPPs.

Stability Limits of a Atatürk HPP

Generally, generators are connected to a large power system and the frequency is dependent on the dynamic behavior of the system. Hence the true response characteristic of units cannot be observed during grid operation. However during island operation the unit must act to maintain the system frequency. Although the island operation is usually performed by zero speed droop (isochronous operation) and the speed droop is active only during grid operation, the effect of speed droop to stability of a unit in island operation is also studied. The main reason of this study is to observe the characteristic of the unit settings for grid operation, during island conditions.

In order to determine the stability limits for controller settings a linearised model is utilized with assumptions such as;

- The full load water time constant is utilized and held constant.
- The relation between the power output and the gate opening is assumed to be linear
- The guide vane dynamics are assumed to be fast enough to be ignored.

Hence after the assumptions the block diagram given in Fig. 4-6 is formed for studies.

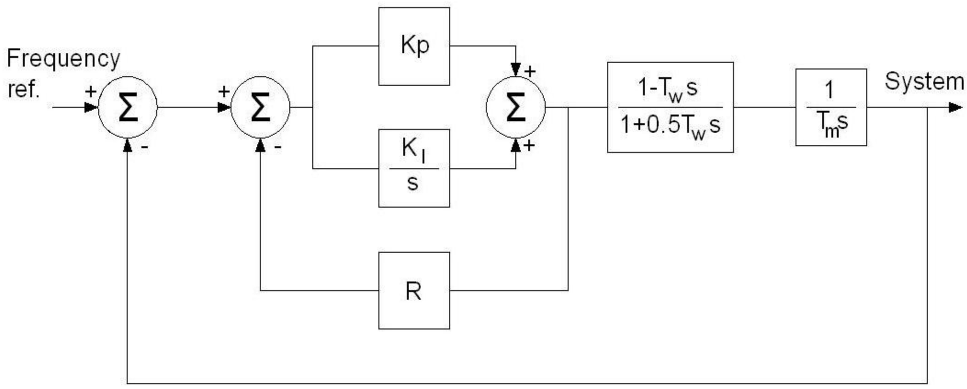

Fig. 4-6. The block diagram of HPP

The transfer function can be written as,

$$G(s) = \frac{(K_P s + K_I)(1 - T_w s)}{[R(K_P s + K_I) + s](1 + 0.5T_w s)T_m s} \tag{4-1}$$

4.2.1.1. Routh-Hurwitz Stability Criterion

It is well known that the stability of a linear closed-loop system is determined by the locations of its poles. In case of a pole located at right hand side of the complex plane, the system is unstable. Hence the necessary condition for stability is to have poles with negative real parts. The closed-loop pole locations can be determined by solving the characteristic equation (4-2)

$$1 + GH(s) = 0 \tag{4-2}$$

However Routh-Hurwitz method can determine the number of right hand side poles, without solving the equation. For a characteristic equation of form,

$$A(s) = A_n s^n + A_{n-1} s^{n-1} + ... + A_1 s + A_0 \tag{4-3}$$

In order to have roots of the characteristic equation (4-3) with negative real parts, all coefficients $\{A_i\}$ should be positive. Further Routh-Hurwitz criterion requires the calculation of Routh's array. The array is formed by placing the even numbered coefficients to first row starting from the A_n and the second row is formed by placing the odd numbered coefficients in the second row. The rest of the rows are filled by the following equations (4-4) and (4-5).

Routh's Array;

$$\begin{array}{llll} A_n & A_{n-2} & A_{n-4} & \ldots \\ A_{n-1} & A_{n-3} & A_{n-5} & \ldots \\ B_1 & B_2 & \ldots & \\ C_1 & C_2 & \ldots & \\ \ldots & & & \end{array}$$

where

$$B_i = -\frac{\det\begin{bmatrix} A_n & A_{n-2i} \\ A_{n-1} & A_{n-2i-1} \end{bmatrix}}{A_{n-1}} \tag{4-4}$$

$$C_i = -\frac{\det\begin{bmatrix} A_{n-1} & A_{n-2i-1} \\ B_1 & B_{i+1} \end{bmatrix}}{B_1} \tag{4-5}$$

For the transfer function (4-1), the characteristic equation is in the form of equation 4-6. The derivation of the equation can be found in Appendix-C;

$$s^3 0.5(1+X_1)+s^2(X_1+0.5X_2-X_3+1)+s(X_2+X_3-X_3X_4)+X_3X_4=0 \quad (4\text{-}6)$$

where,

$$X_1 = RK_P$$
$$X_2 = RK_I T_w$$
$$X_3 = \frac{T_w K_P}{T_m}$$
$$X_4 = \frac{K_I T_w}{K_P}$$

In the Routh's array the elements of first column should not change sign. Also for negative real parts the coefficients $\{A_i\}$ should be positive. Applying the criterion to the characteristic equation (4-6), for stability;

- For $A_3 > 0 \rightarrow X_1 > -1$ (which is always true)
- For $A_2 > 0 \rightarrow X_1 + 0.5X_2 + 1 > X_3$
- For $A_1 > 0 \rightarrow X_2 + X_3 > X_3X_4$
- For $A_0 > 0 \rightarrow X_3X_4 > 0$
- For $B_1 > 0 \rightarrow A_1A_2 - A_3A_0 > 0$
- For $C_1 > 0 \rightarrow A_0 > 0$

If all conditions are satisfied, the stability boundaries can be found by equating $A_1A_2 - A_3A_0$ to zero, which gives;

$$X_3^2(X_4-1) + X_3(X_1-1.5X_1X_4-0.5X_2-0.5X_2X_4-1.5X_4+1) + (X_2+X_1X_2+0.5X_2^2) = 0 \quad (4\text{-}7)$$

The calculated stability boundaries for Atatürk HPP are given in Fig. 4-7.

From the simulation studies it is calculated that $K_P = 2.5$ and $K_I = 2.3$. As seen in Fig. 4-7. The current operational setting of Atatürk HPP determined by modeling studies is above the stability boundary for 8% speed droop.

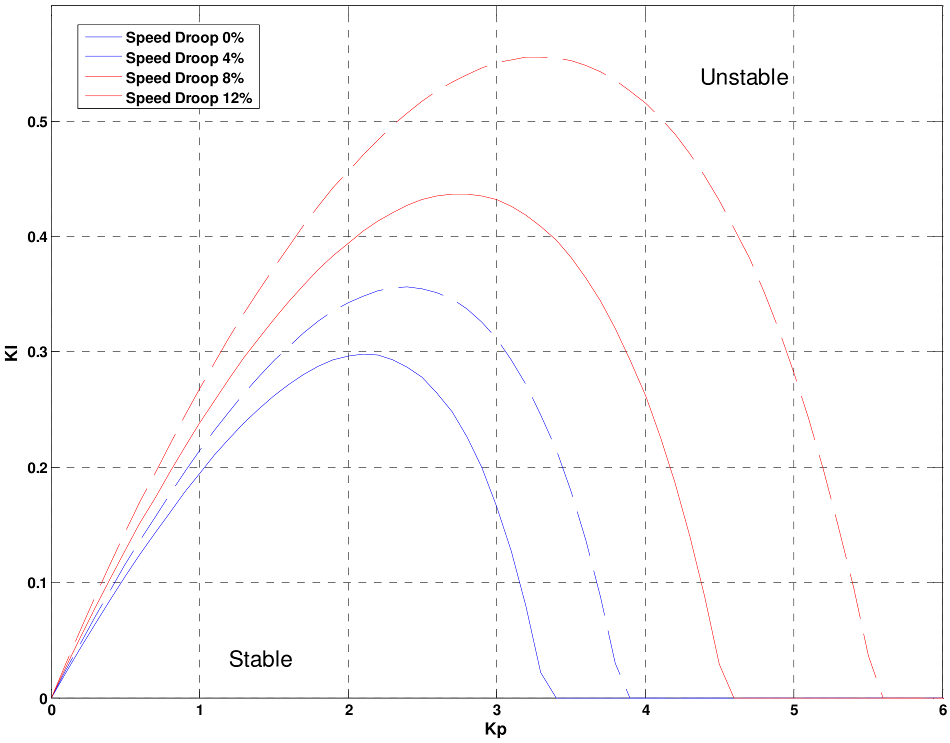

Fig. 4-7. The stability boundaries for Atatürk HPP

Further it is observed that by increasing the speed droop, the stability boundary is increased. However it should be noted that the increase in speed droop corresponds to a lesser primary response of the unit.

Field Tests on Birecik Hydro Power Plant

Birecik HPP is also one of the biggest HPPs in Turkey with a rated capacity of 690 MW. The six generators of the plant, each has a rating of 115 MW, are connected to the system by three 400 kV step-up transformers.

The Island Operation Test

Similar to the island test in Atatürk HPP, Birecik HPP is also tested in island conditions. For the test purposes another island is formed by TEİAŞ. The total demand within the islanded region was about 200 MW and this load was supplied by two units of Birecik HPP. The islanded region is given in Fig. 4-8.

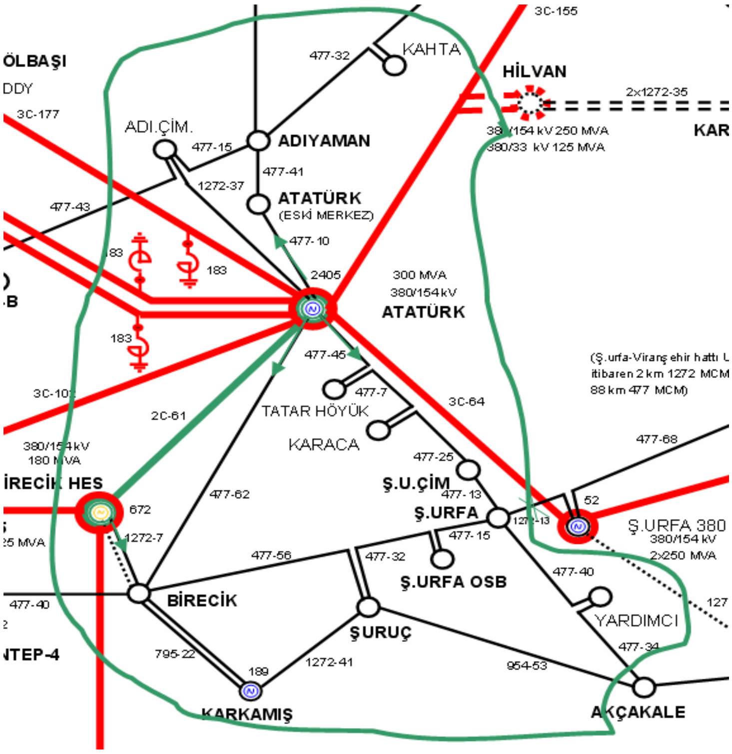

Fig. 4-8. The islanded region during test in Birecik HPP

During the test, connection of the measurement system used in Atatürk HPP was not possible due to technical limitations. Hence measurements are taken with 1 sample/second resolution by the recording system of the plant. The speed droop of units was 4% and the units are loaded to 100 MW.

The required maneuvers are organized by TEİAŞ and the Birecik HPP fed the island through the substation of Atatürk HPP as shown with a solid green line in Fig. 4-5. The region is isolated by tripping of the interconnection lines one by one. The flow through the final line was approximately 5 MW when the line is tripped and the system is isolated. The islanded region transmission system model and load flow results are presented in Appendix-B.

After the tripping of the last line the system frequency begun oscillating much faster than the test in Atatürk HPP. The units tripped due to the over speed protection of the plant. The island frequency during test is given in Fig. 4-9.

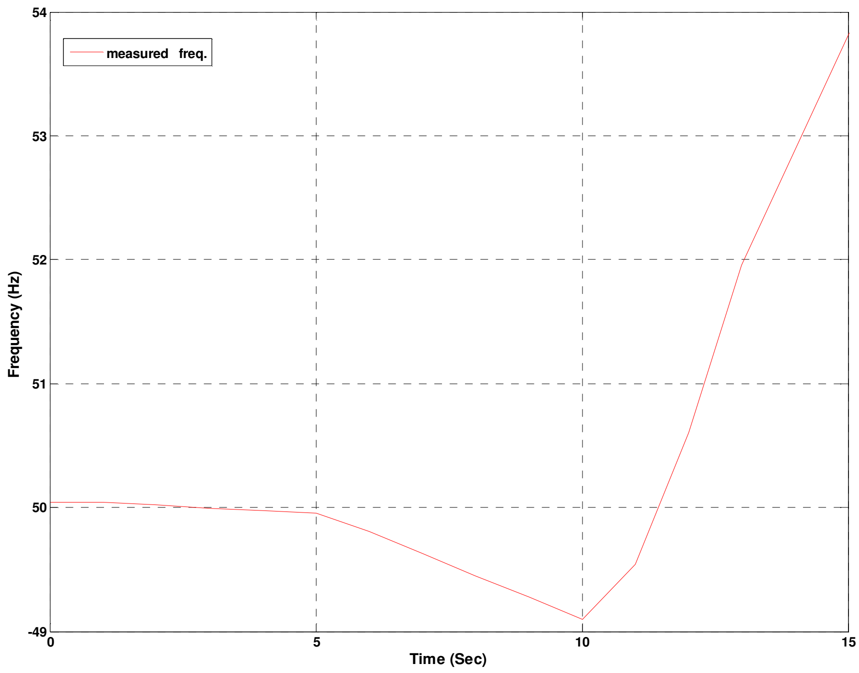

Fig. 4-9. The island frequency during test in Birecik HPP

Since the recording system of the plant is limited and external recording systems create problems on controller, the system is modeled according to the trip data.

The Island Operation Simulations

The controller structure of Birecik HPP is also determined from the plant documentation. One important difference between the structures of Atatürk HPP and Birecik HPP is an additional input to the speed controller. In Birecik HPP speed controller the derivative of speed measurement is also added to the error signal. The effect of derivative signal is investigated further in this chapter. The speed controller structure of Birecik HPP is given in Fig. 4-10.

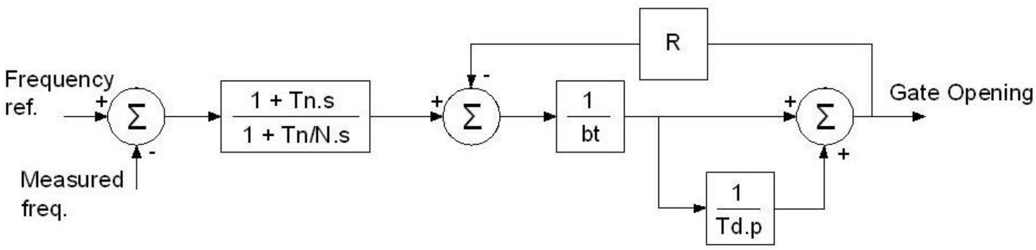

Fig. 4-10. The speed controller block diagram of Birecik HPP

where

T_n = Derivative time constant, seconds

N = Differentiator gain

b_t = Transient speed droop

T_d = Integration time constant, seconds

The parameters b_t and T_d can easily be represented by K_P and K_I of the regular PI controller such as;

$$K_P = \frac{1}{b_t} \tag{4-8}$$

$$K_I = \frac{1}{b_t T_d} \tag{4-9}$$

After determining the structure of the controller, the pre-islanding conditions are modeled as in the case of Atatürk HPP. The result of island operation simulation is given in Fig. 4-11.

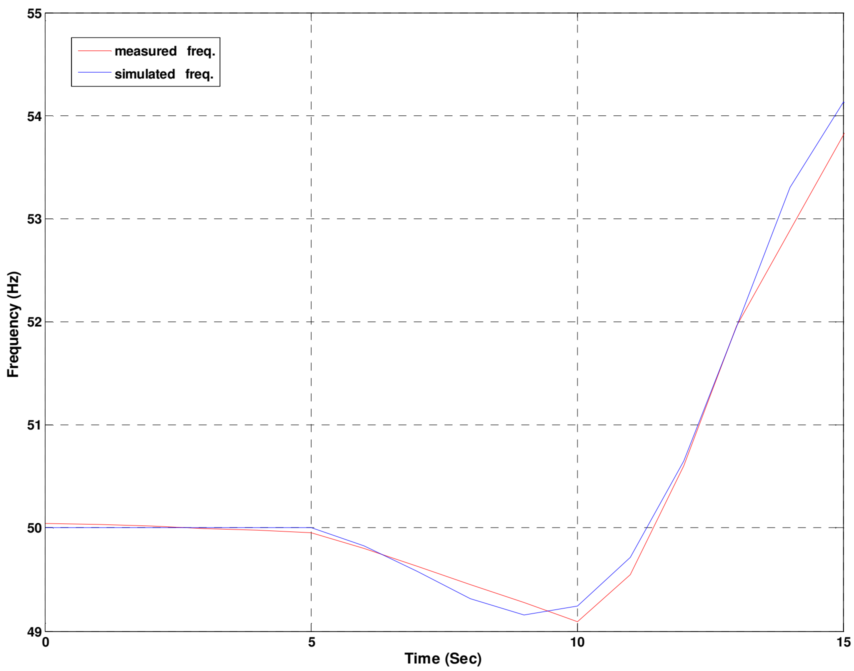

Fig. 4-11. The island operation simulations for Birecik HPP

After achieving satisfactory results, another study is performed to determine the stability limits for Birecik HPP. Also this study indicates the effects of derivative input on stability of unit.

Stability Limits Studies for Birecik HPP

The stability limits for Birecik HPP are determined by the same method used in Atatürk HPP. However the controller structure is slightly changed as given in Fig 4-12. The assumptions used in Atatürk HPP case are also valid for Birecik HPP but due to the change in structure, an additional assumption is made;

- The Differentiator gain, N, is assumed to be high enough to model the input as the addition of the difference between the reference and measured frequency and its derivative.

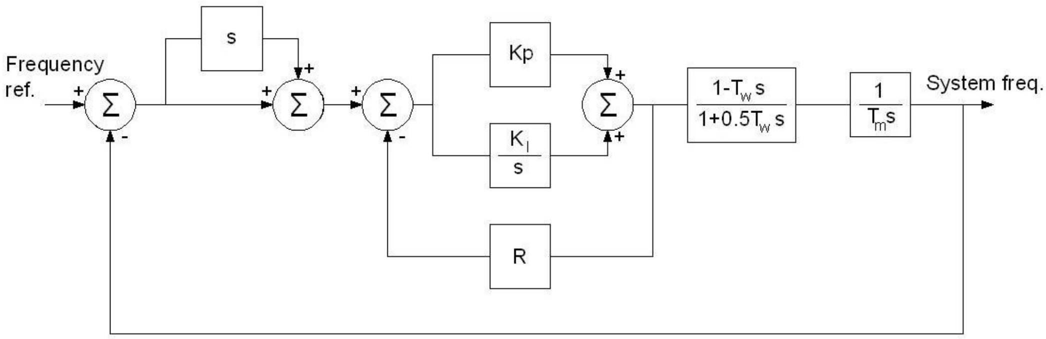

Fig. 4-12. The block diagram of HPP with derivative input

As the structure changes the transfer function is also changed to;

$$G(s) = \frac{(s+1)(K_P s + K_I)(1 - T_w s)}{[R(K_P s + K_I) + s](1 + 0.5T_w s)T_m s} \tag{4-10}$$

For the transfer function (4-10), the characteristic equation is in the form of equation 4-11. The derivation of the equation can be found in Appendix-D;

$$\begin{aligned} &s^3[0.5(1+X_1)+X_3X_5]+s^2(X_1+0.5X_2-X_3+1+X_3X_5-X_3X_4X_5)+ \\ &s(X_2+X_3-X_3X_4+X_3X_4X_5)+X_3X_4=0 \end{aligned} \tag{4-11}$$

where,

$$X_1 = RK_P$$
$$X_2 = RK_I T_w$$
$$X_3 = \frac{T_w K_P}{T_m}$$
$$X_4 = \frac{K_I T_w}{K_P}$$
$$X_5 = \frac{1}{T_w}$$

As in the case of Atatürk applying the criterion to the characteristic equation (4-11) for Birecik HPP, for stability;

- For $A_3 > 0 \rightarrow 0.5X_1 + X_3X_5 > -0.5$ (which is always true)
- For $A_2 > 0 \rightarrow X_1 + 0.5X_2 + 1 + X_3X_5 + X_3X_4X_5 > X_3$
- For $A_1 > 0 \rightarrow X_2 + X_3 + X_3X_4X_5 > X_3X_4$
- For $A_0 > 0 \rightarrow X_3X_4 > 0$
- For $B_1 > 0 \rightarrow A_1A_2 - A_3A_0 > 0$
- For $C_1 > 0 \rightarrow A_0 > 0$

If all conditions are satisfied, the stability boundaries can be found by equating $A_1A_2 - A_3A_0$ to zero, which gives;

$$X_4^2(X_3^2X_5^2 - X_3^2X_5) + X_4(X_1X_3X_5 - 1.5X_1X_3 - 0.5X^2X^3 + 1.5X_2X_3X_5 - X_3 + X_3X_5 + X_3^2 - 2X_3^2X_5 + X_3^2X_5^2 - 0.5X_3) + (X_1X_3 + X_1X_2 + 0.5X^2 - 0.5X_2X_3 + X_2 + X_3 - X_3^2 + X_2X_3X_5 + X_3^2X_5) = 0 \quad (4\text{-}7)$$

The calculated stability boundaries for Birecik HPP are given in Fig. 4-13.

As seen in Fig. 4.13. the PI settings of Birecik HPP is out of the stability boundary for 4% speed droop.

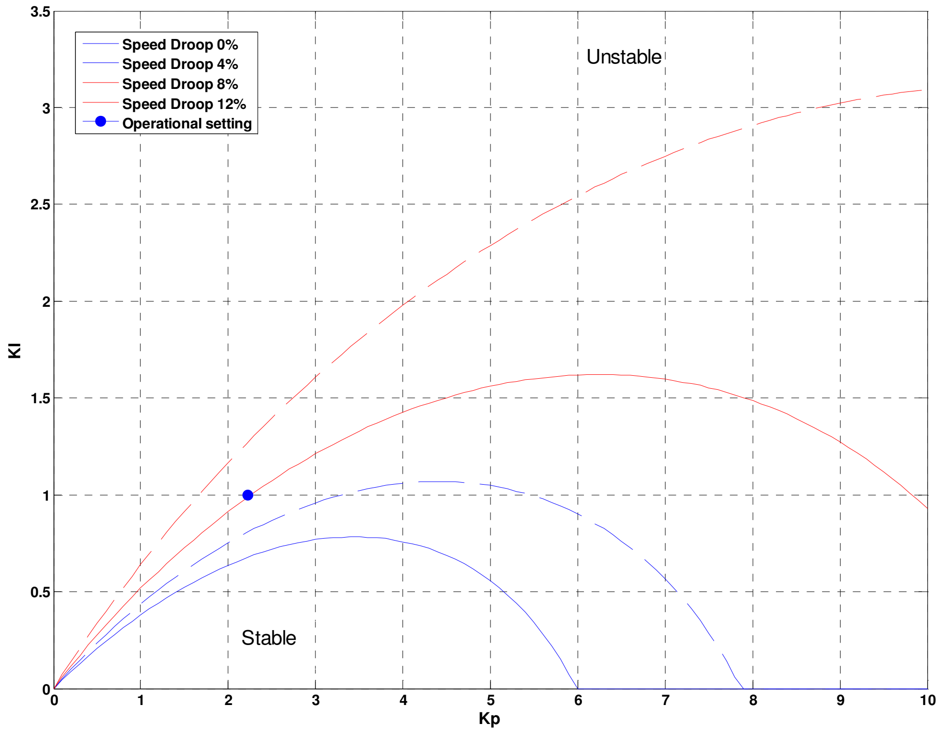

Fig. 4-13. The stability boundaries for Birecik HPP

After the discussion with plant operators and TEİAŞ representatives, it is understood that the controller settings of the plant are changed in order to satisfy the grid code requirement. I order to observe the response with old settings; TEİAŞ organized another island operation test for Birecik HPP.

The Second Island Operation Test

The second island operation test is performed after the modification of settings. The unit controller settings are turned into the commissioning values and the test described in section 4.3.1 is performed again. Unfortunately the plant operator was unable to supply the frequency recordings, hence the recordings of NLDC is utilized for comparison. The measurements and simulation results are given in Fig. 4-14.

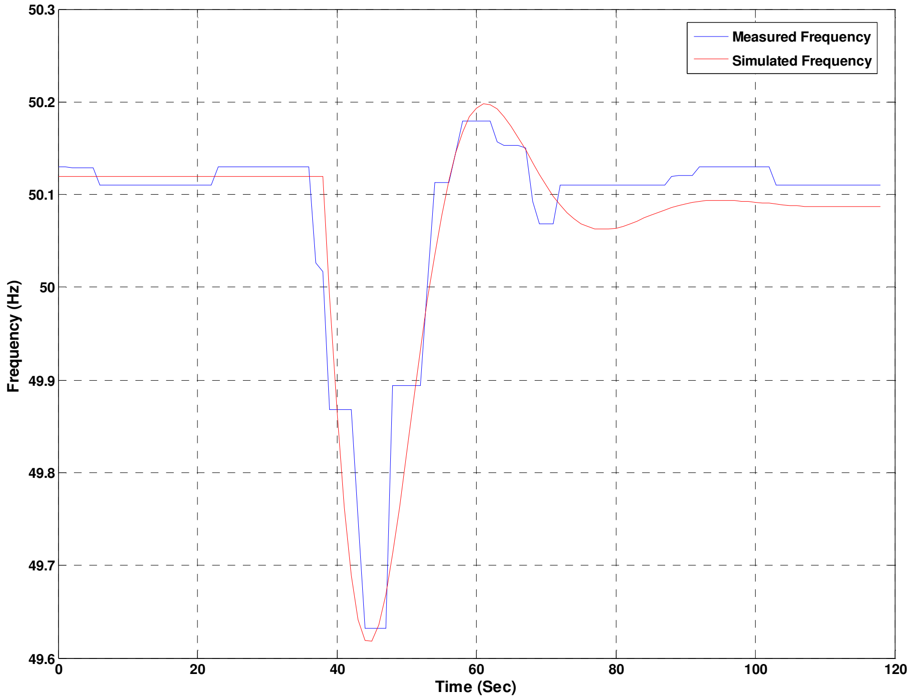

Fig. 4-14. The second island test in Birecik HPP

As seen in Fig. 4-14. with the commissioning controller settings the unit was able to supply the island. The new settings are also shown on the stability margin curves in Fig. 4-15.

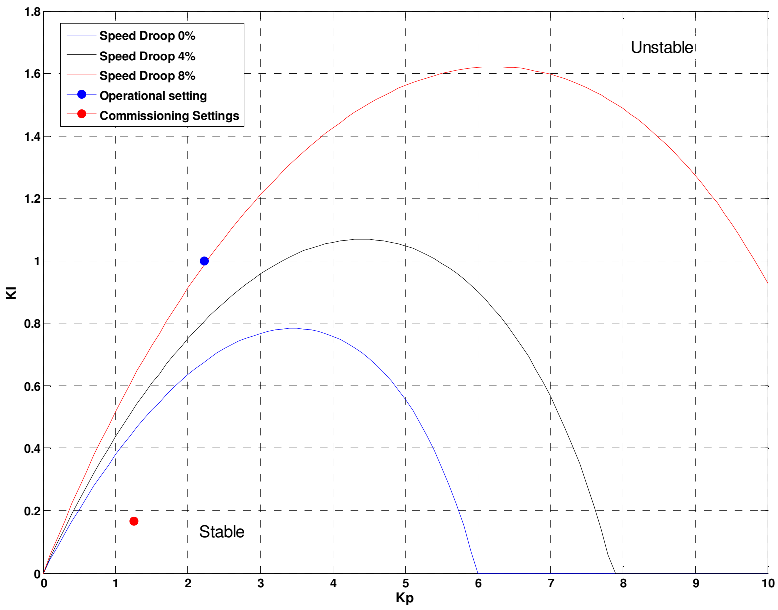

Fig. 4-15. The stability limits for Birecik HPP

However changing the PI settings of the controller does not only affect the stability of the unit, but also the response time.

The Effect of PI Parameters on Unit Response Time

As stated in previous chapters increasing the temporary droop and integration time constant slows down the unit response but increases the stability margins. Increasing the temporary droop and integration time constant corresponds to a reduction in K_P and K_I values, which is the case for Birecik HPP as seen in Fig. 4-15. In order to observe this effect the response of controller to a ±200 mHz step change in frequency is simulated for grid operation. Both operational and commissioning settings simulation results are given in Fig. 4-16.

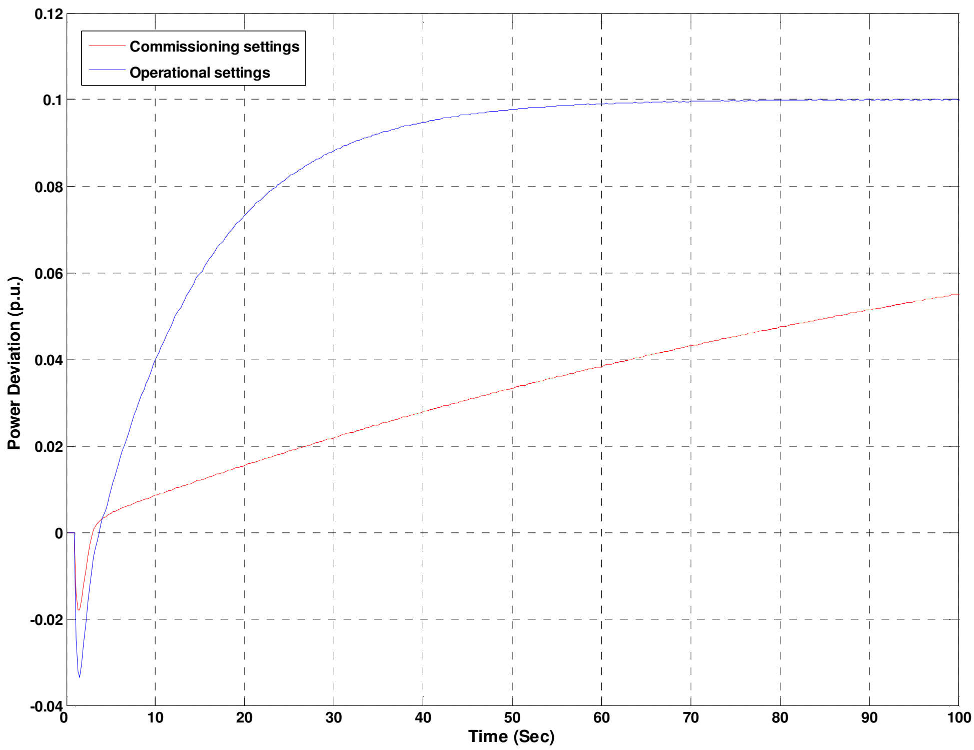

Fig. 4-16. The step response simulation of Birecik HPP

As seen in Fig. 4-16. the stable settings are much slower than the settings that are unstable during grid operation. Hence there is a conflict between stable operation and fast response in hydro power plants.

However the grid code has direct commands about the primary response of HPPs. The grid code indicates that all power plants should supply their primary reserve within 30 seconds and the speed droop of HPPs should be between 2% - 6% [15]. In order to satisfy this criteria nearly all of the HPPs in Turkish power system is operating with settings that are unstable in grid operation. The effects of this operation philosophy on power system frequency stability will be discussed further in this chapter.

The Effect of Derivative Input on Controller Stability

In order to observe the effect of derivative input on controller stability the stability margins for Birecik are re-calculated utilizing the transfer function 4-1. The calculated results show the stability margin of Birecik HPP without the derivative input. Hence comparison of results indicates the effect of derivative input as shown in Fig. 4-17.

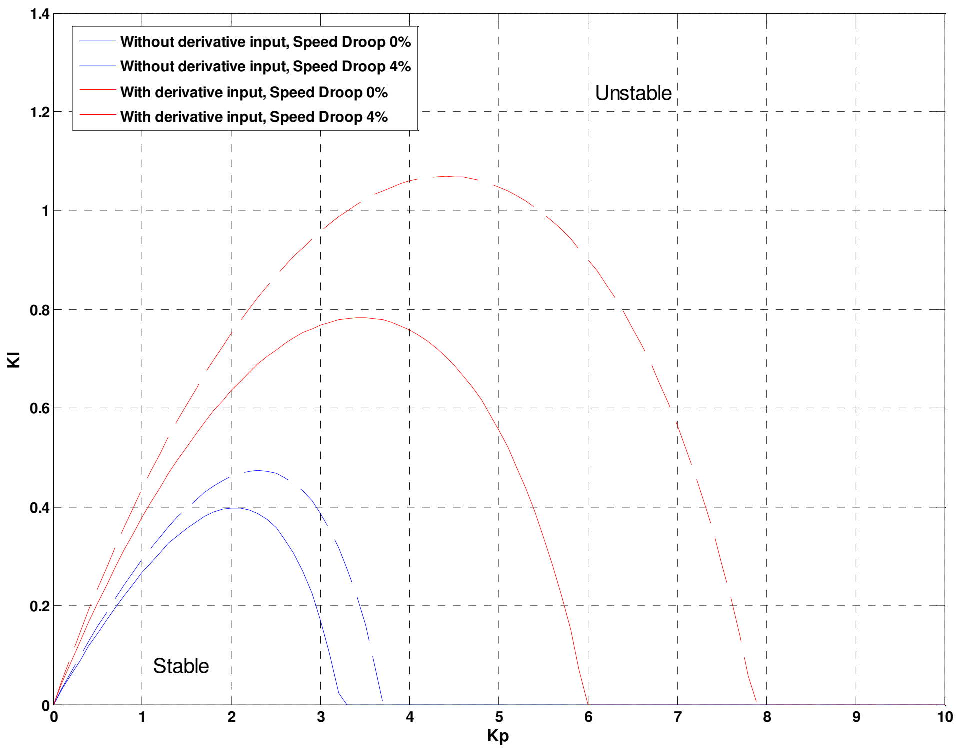

Fig. 4-17. The stability boundary comparison of Birecik HPP

As seen in Fig. 4-17 the derivative input has a very important effect on the stability boundary for PI parameters. Since an increase in PI parameters results in a decrease in response time of unit, the derivative input can improve the response time of the unit without making it unstable in island operation.

Effects of Controller Settings of Hydro Power Plants on System Frequency

In the analysis of load-frequency controls, the area of interest is the collective performance of all generators in the system [2]. The consideration of inter-area oscillations and transmission system performance may be required for weak systems. However the frequency measurements of Wide Area Measurement System (WAMS) indicates Turkish power network is a strong system without any inter-area oscillation. Fig. 4-18 presents the frequency measurements from Babaeski and Keban substations after a generation loss of 600 MW.

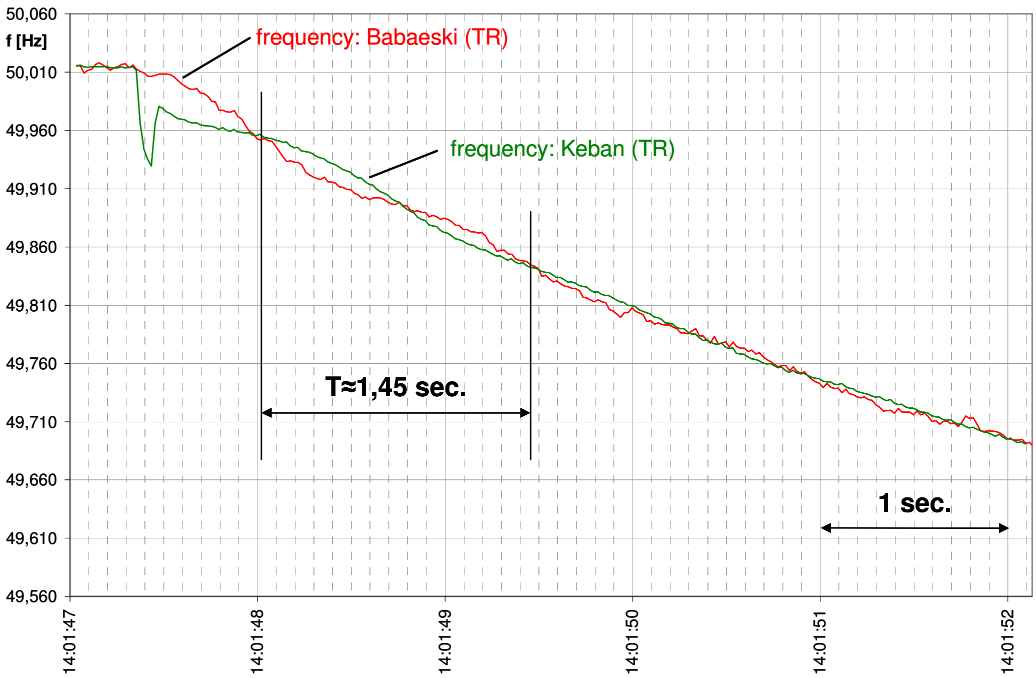

Fig. 4-18. The measured frequency in different buses after a disturbance

As seen in Fig. 4-18 the inter-area oscillations are damped rapidly and can easily be neglected for long term frequency stability studies.

Hence utilizing this approach, (i.e., coherent response of all generators to changes in demand) all generators in the system are modeled by a single equivalent rotating mass. Similarly the dependency of system load to frequency changes is represented by a single damping constant.

Representative Power System Model

Starting from the well known swing equation in Laplace domain, equation 3-19, and adding the effect of the damping coefficient equation becomes,

$$2H_i s\Delta\overline{w} = \Delta\overline{P}_{i\,m} - (\Delta\overline{P}_{i\,e} - D\Delta\overline{w}) \tag{4-12}$$

where D is the damping coefficient and *i* is the generator index. Note that this equation is determined utilizing machine ratings as base values. However for system simulation the active power base is changed to system total generation and then all equations for each generator is summed up to get;

$$\left(2\frac{\sum_{i=1}^{g} VA_{i\,base} H_i}{\sum_{i=1}^{g} VA_{i\,base}} + D\right) s\Delta w = \frac{\sum_{i=1}^{g} VA_{i\,base}\Delta\overline{P}_{i\,m}}{\sum_{i=1}^{g} VA_{i\,base}} - \frac{\sum_{i=1}^{g} VA_{i\,base}\Delta\overline{P}_{i\,e}}{\sum_{i=1}^{g} VA_{i\,base}} \tag{4-13}$$

where *g* is the total number of generators. Arranging the equation 4-13 to get;

$$(2\tilde{H}s + D)\Delta w = \sum_{i=1}^{g} k_i \Delta P_{i\,m} - \Delta\tilde{P}_e \tag{4-14}$$

where;

$$\tilde{H} = \frac{\sum_{i=1}^{g} VA_{i\,base} H_i}{\sum_{i=1}^{g} VA_{i\,base}} \tag{4-15}$$

$\tilde{H}$ is the weighted average inertia of all generators.

$$k_i = \frac{VA_{i\,base}}{\sum_{i=1}^{g} VA_{i\,base}} \tag{4-16}$$

k_i is the ratio of rated power of i[th] unit to total system rating. Note that for generators that do not contribute to primary frequency regulation mechanical power does not change. Thus for such generators this value has no effect on frequency deviation.

$$\Delta \tilde{P}_e = \frac{\sum_{i=1}^{g} VA_{i\,base} \Delta P_{i\,e}}{\sum_{i=1}^{g} VA_{i\,base}} \tag{4-17}$$

ΔP_{i_e} is the total electrical load change in p.u.

The final model determined according to the above equations is given in Fig. 4-19

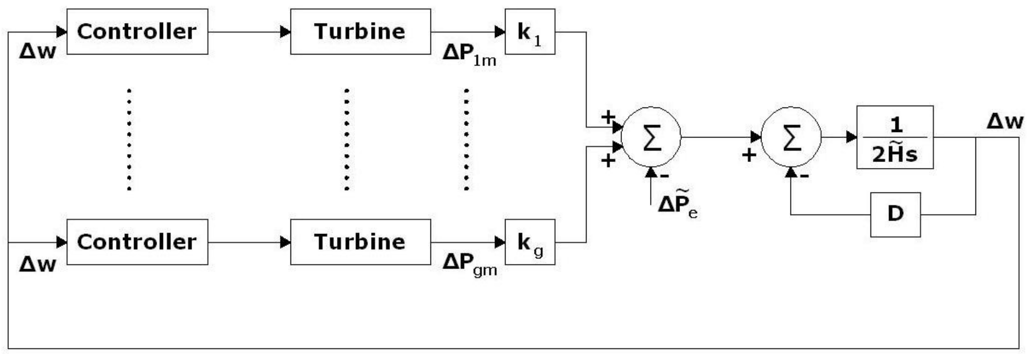

Fig. 4-19. The model utilized for system wide studies.

Model Validation

Utilizing the MATLAB/SIMULINK software, which is commonly used for computational tasks and model based dynamic simulations, the power system model is prepared as described above.

The model is verified by three different events in January, March and April 2006. Simulations studies are performed, utilizing the generation and frequency data supplied by NLDC. The generation data includes the hourly generated energy by the major units. Although not exact, this data gives an idea about the number of units of major plants in service. The loadings of units however are assumed according to the common loading of the plants, which is determined by interviews with NLDC representatives. The frequency data is the recorded measurement with one sample/second resolution.

The first data (Case-1) belongs to the generation loss in January 2006. Three units in Keban HPP were tripped and a total of 500 MW generation is lost. The total system load at the trip instant was approximately 17500 MW. The generations of major power plants are modeled according to the generation data supplied by NLDC and given in Appendix-F, and the system wide simulations are performed. The comparison of simulation results and measurements are presented in Fig. 4-20.

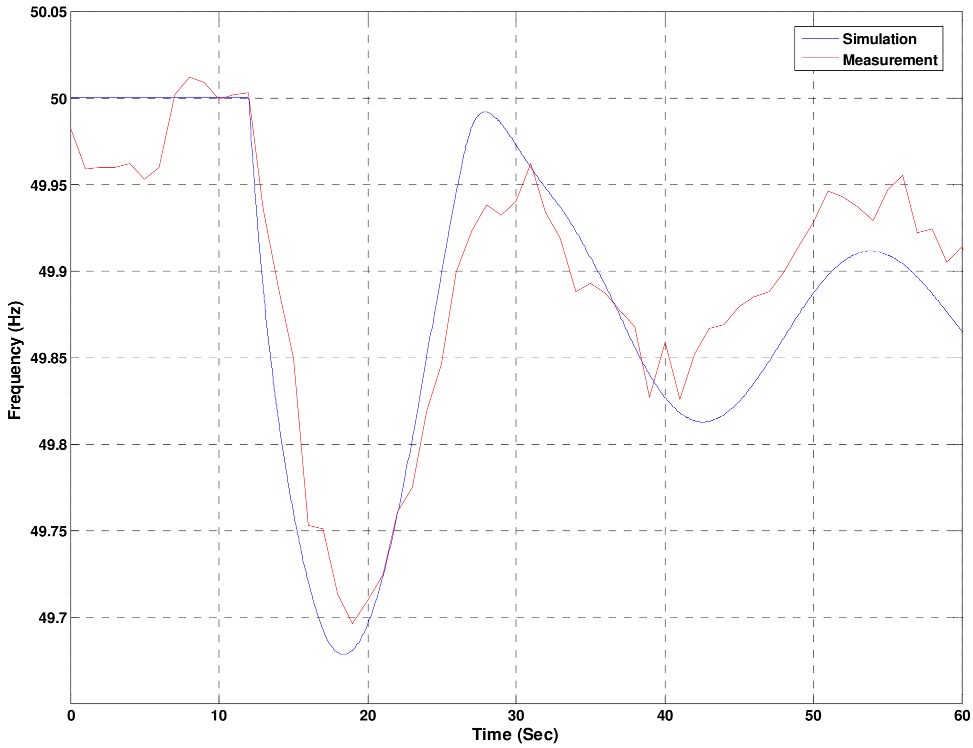

Fig. 4-20. The measurement and simulation of generation loss in January 2006 (Case-1).

Another generation loss data is utilized for testing the model at higher system load. The second data (Case-2) belongs to the generation loss in April 2006. Three units of Berke HPP were tripped leading to an approximately 430 MW generation loss. The total system generation at the fault instant was approximately 20000 MW and details about the plant generations are given in Appendix-F. The comparison of simulation results with measured frequency data is given in Fig. 4-21.

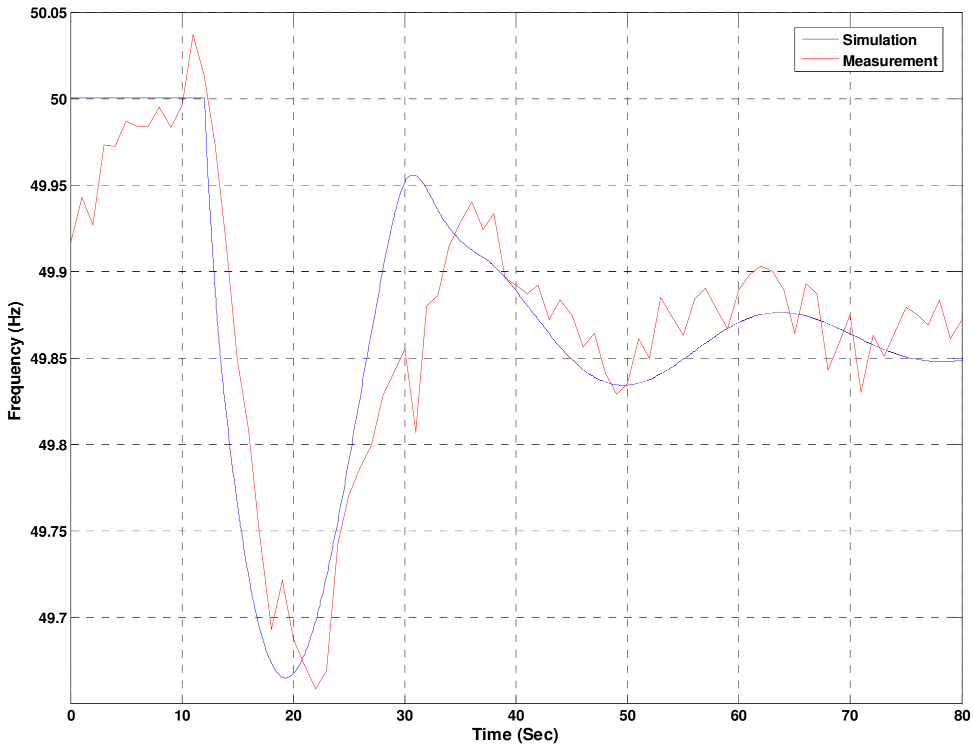

Fig. 4-21. The measurement and simulation of generation loss in April 2006 (Case-2).

The final case (Case-3) is the measurements of an outage in Karakaya HPP. Two units of plant were tripped and a total of 600 MW generation was lost. The total system load was approximately 21500 MW (details about the plant generations are given in Appendix-F). The same scenario is formed in the model and simulation is performed. The results are compared with the measured data as shown in Fig. 4-22.

As seen in figures 4-20, 4-21 and 4-22, the model gives satisfactory results for three different cases, representing the low, medium and high total system demand. Hence further studies are performed by the above described model.

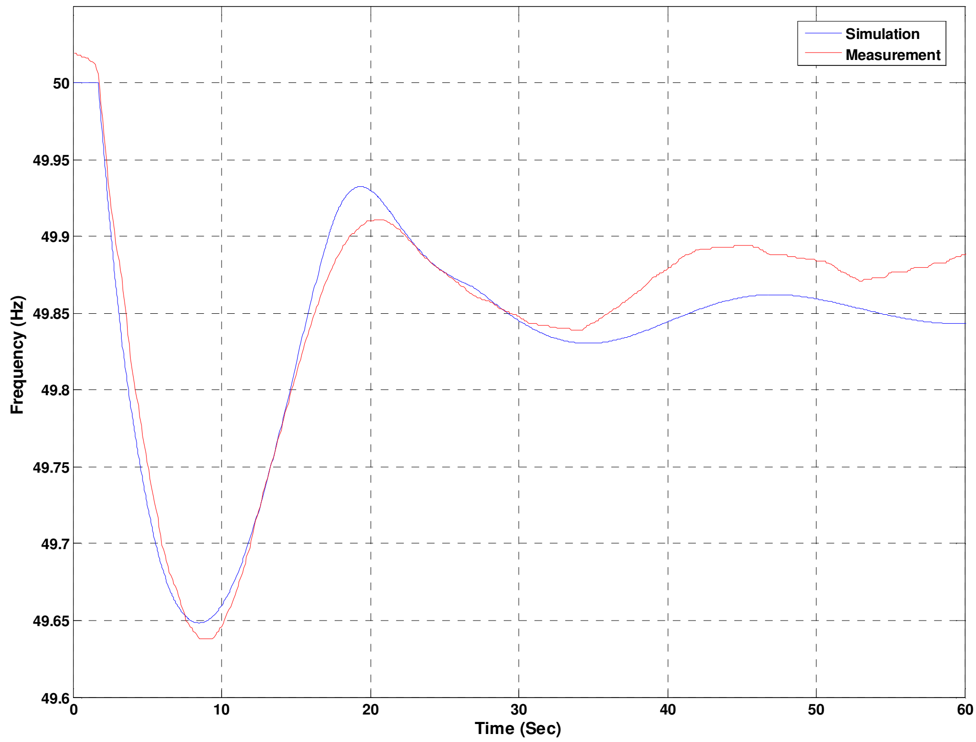

Fig. 4-22. The measurement and simulation of generation loss in March 2006 (Case-3).

It should be noted that the model does not contain a secondary controller loop. Since only primary control is active in simulations, simulated frequency will never reach back to 50 Hz. The real system, on the other hand, is equipped with a secondary controller, which will respond to frequency changes and bring the system frequency back to 50 Hz. This difference between the model and real system also results in a difference between simulated and measured frequencies. The error grows larger as the time after generation loss increases. The increase of error, as time increases, in comparison figures (Fig. 4-20, 4-21 and 4-22) can be explained by this secondary control action of the real system.

Simulation Studies

Although oscillations with 20 – 30 seconds period are common at all cases described in previous section, the damping characteristics is different. Case-1 shows lesser damping than Case-2 and Case-3, and Case-3 has the best damping of all three cases. As seen in Appendix-F and figures 4-20, 4-21 and 4-22, the damping of oscillations increase as the primary reserve contribution percentage of HPP decrease.

4.4.1.1. Effects of Changing Hydro Power Plant Contribution

In order to better observe the effect of HPP contribution on oscillations with 20 – 30 seconds period, Case-1 is simulated again with increased and decreased HPP generation and reserve without changing the total system demand. First the contribution of HPP is reduced by 1000 MW; case is referred as Case-1-a. Than HPP generation is further reduced by another 1000 MW; case is referred as Case-1-b. The details about the plant generations are given in Appendix-F for both cases. Simulations results are compared to Case-1 and results are presented in Fig. 4-23.

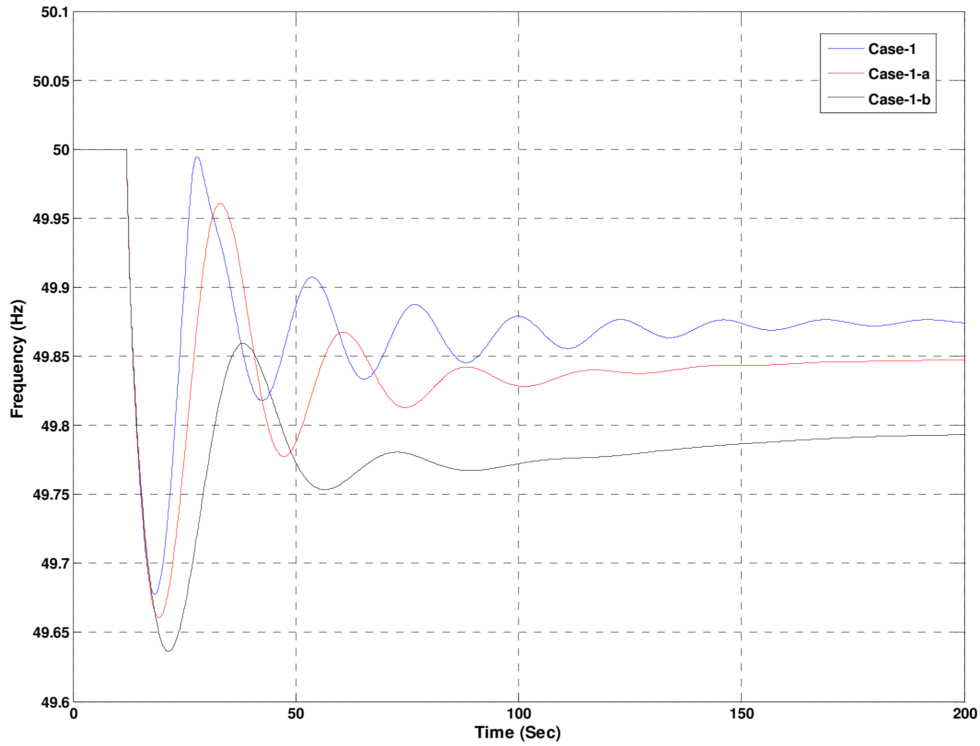

Fig. 4-23. Comparison of Case-1 with Case-1-a and Case-1-b

As seen in Fig. 4-23, the damping of oscillations increases and oscillations die out faster in Case-1-b, which is minimum HPP contribution case. In order to be sure about the negative effect of HPPs, the contribution of HPPs is increased by 1000

MW as Case-1-c. Further the contribution is increased by another 1000 MW and results are recorded as Case-1-d. The generation scenario is given in Appendix-F. The comparison of results with Case-1 is given in Fig. 4-24.

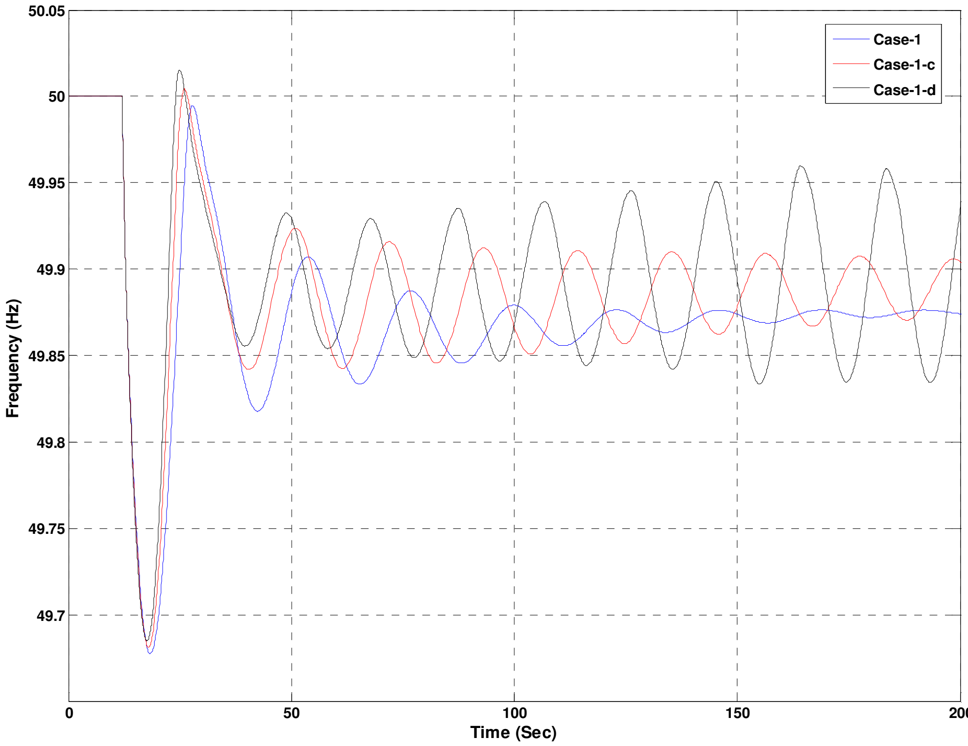

Fig. 4-24. Comparison of Case-1 with Case-1-c and Case-1-d

As seen in figures 4-23 and 4-24, the damping of these oscillations highly dependent on HPP contribution to primary frequency control.

4.4.1.2. Effects of Changing Hydro Power Plant Controller Settings

As previously stated, HPP speed controllers are set to give their primary frequency response in 30 seconds and with a speed droop between 2 – 6%. It is also previously discussed that these settings are contradicting with the stable operation of units. Hence increasing the speed droop setting and slowing the unit down, the units should have less negative effect on system frequency.

In order to test first part of this statement, two more simulations are performed. The Case-1-d is chosen as the base case, for better observation of the effect, speed droop of some HPPs are increased from 4% to 10%; case is referred as Case-1-e. Finally the speed droop of all units are increased to 10% and case is referred as Case-1-f. The detailed speed governor settings are presented in Appendix-F. The comparison of simulation results are given in Fig. 4-25.

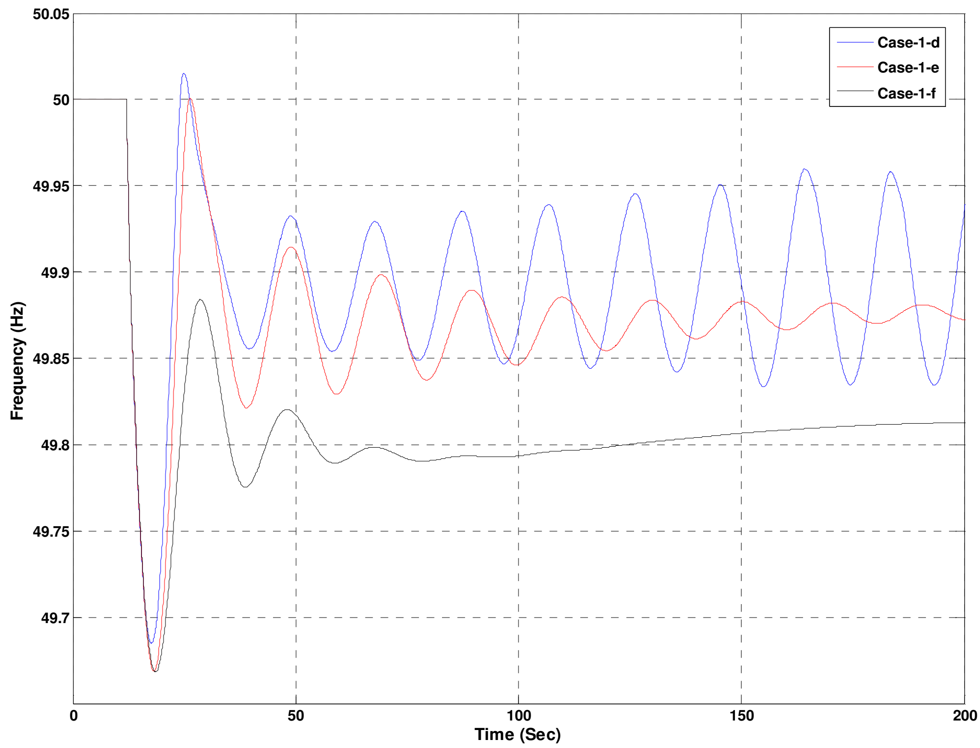

Fig. 4-25. Comparison of Case-1-d with Case-1-e and Case-1-f

As seen in Fig. 4-25, increasing speed droop of the system improves the damping but also increases the steady state frequency deviation. One other option is to reduce the PI parameters, thus the steady state value of the system frequency does not change. Two more simulations are performed taking Case-1-d as the base case. At first step some of HPPS are slowed down; case is referred as Case-1-g. Secondly all HPPs are slowed down in Case-1-h. The details on controller settings are presented in Appendix-F. The comparison of simulation results with Case-1-d are presented in Fig. 4-26.

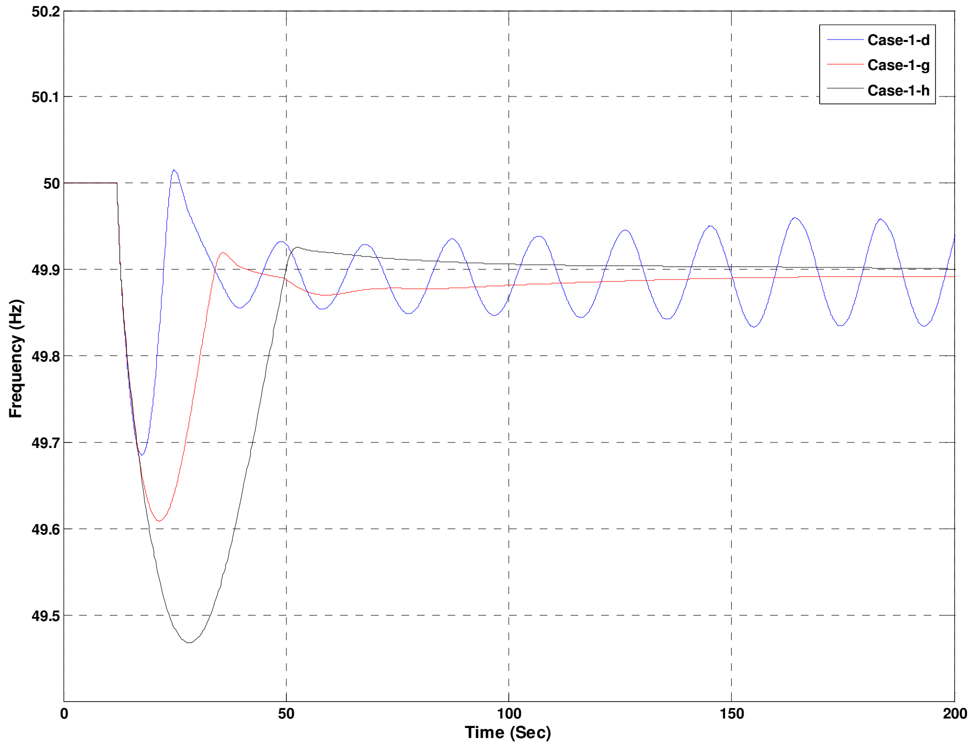

Fig. 4-26. Comparison of Case-1-d with Case-1-g and Case-1-h

As seen in Fig. 4-26, the steady state value remains constant however initial frequency deviation increases drastically.

4.4.1.3. Effects of Derivative Input in Hydro Power Plant Controller

The final study is performed to observe the effect of derivative input. It is previously stated that derivative input increases the stability margin of HPPs. Starting from this statement the HPP controllers are modified by adding a derivative input. Some plants are modified as first step, case is referred as Case-1-i and all HPPs are modified as second step and case is referred as Case-1-j. The details on controller structures can be found on Appendix-F. The comparison of simulation results with Case-1-d is given in Fig. 4-27.

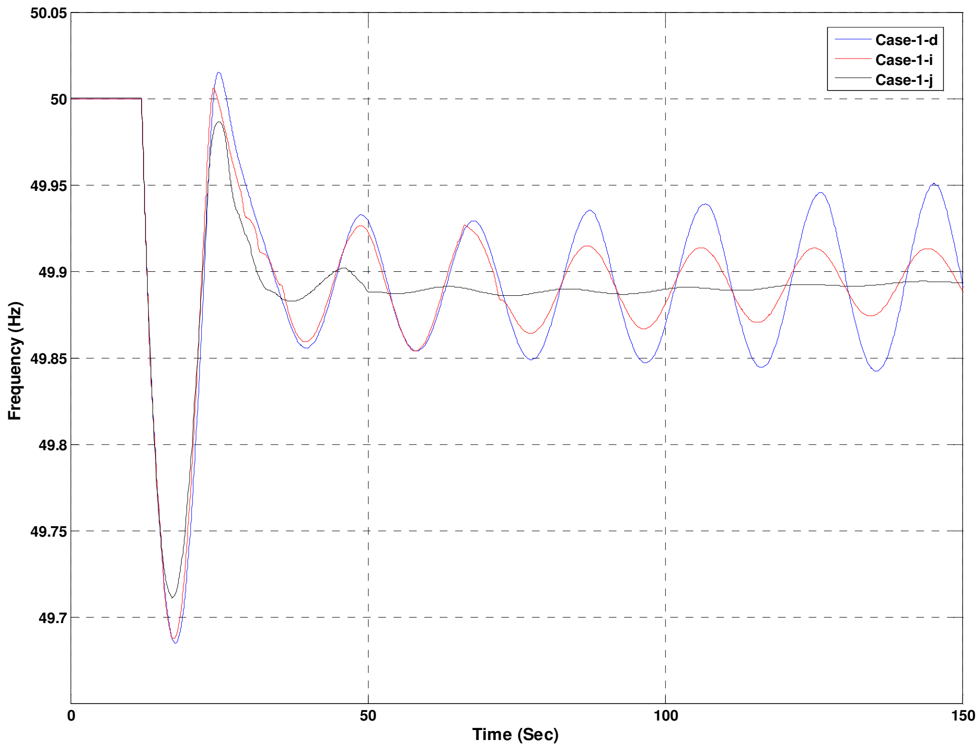

Fig. 4-27. Comparison of Case-1-d with Case-1-i and Case-1-j

As seen in Fig. 4-27, derivative input has a positive damping effect on oscillations with 20 – 30 seconds period.

As presented in figures 4-23 to 4-27, the study presents the negative effect of HPPs with current settings to power system frequency. Hence these effects and the effects of possible counter measures like changing controller and speed droop settings should be considered by TEİAŞ.

Although not in the scope of this study there are other factors affecting the power system frequency stability as presented in next section.

Further Factors Affecting System Frequency

As previously stated the load/frequency control is not performed singly with speed controllers. The power system is also equipped with a secondary control, and for effective secondary control there is also a power controller in plants as stated previously. This section discusses the effects of these controllers (power controller and secondary controller) on system frequency without going into much detail as the main subject of thesis work.

Power Controller

The power controller has different applications actively working in power plants. The main idea behind the controller is to change the reference power output of the unit according to the signals received from secondary control or plant operator. The applications can be grouped as;

- Power control driving speed control;

  In such a structure speed control performs primary control action and power control changes speed control set point (speed reference) by much slower settings in order not to interfere with the primary control action. The schematic is given in Fig. 4-28.

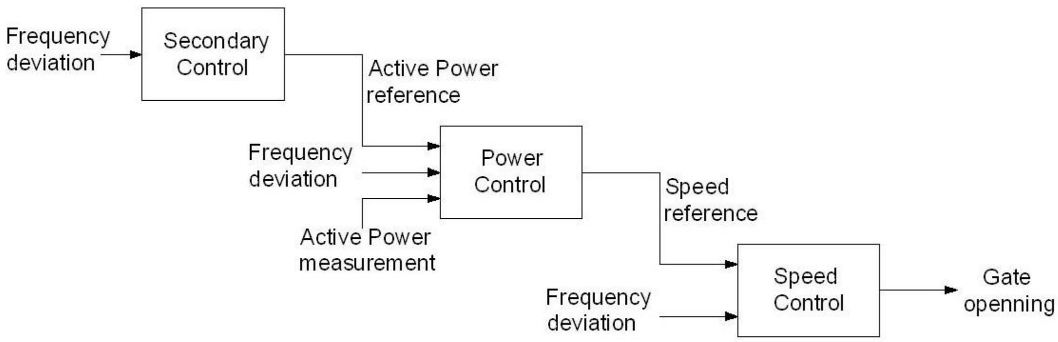

Fig. 4-28. The schematic of power control driving speed control

The change of speed reference effects unit output as shown in Fig. 4-29.

As seen in Fig. 4-29, changing the speed reference value changes the corresponding output power at 50 Hz for constant speed droop. Thus power control drives speed control by changing the reference speed value.

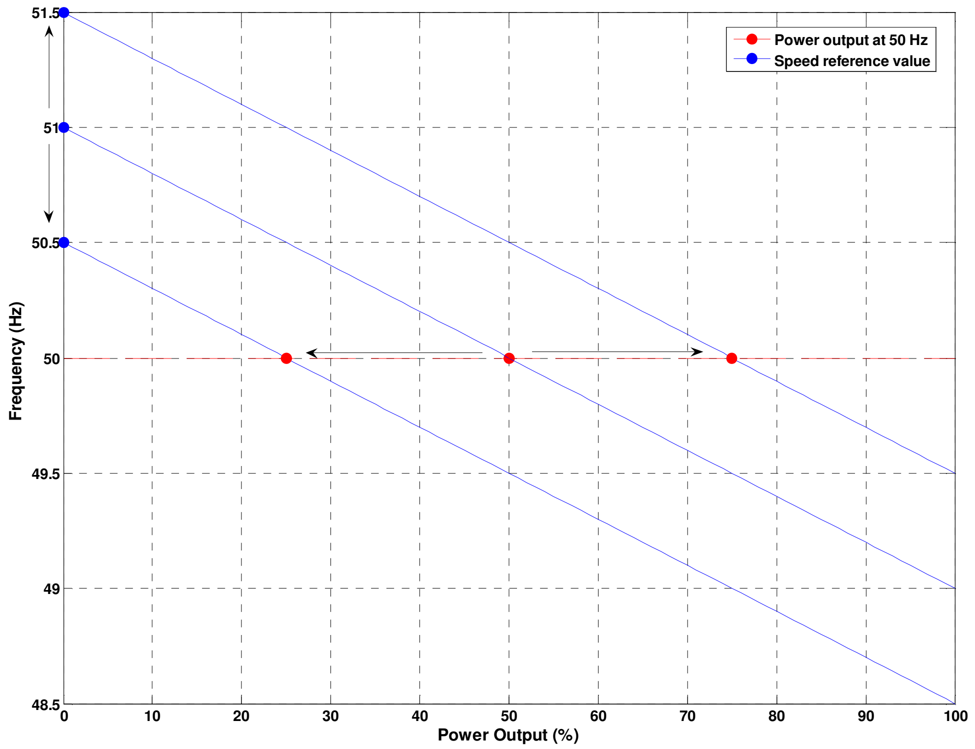

Fig. 4-29. Change of power output at 50 Hz by changing speed reference (4% speed droop)

- Power control in parallel with speed control;

Similar to previous case speed control performs the primary control. However in this case power control determines load reference value and directly drives guide vanes. In order not to interfere with primary control, power control is set to act much slower than speed controller. The schematic is given in Fig. 30.

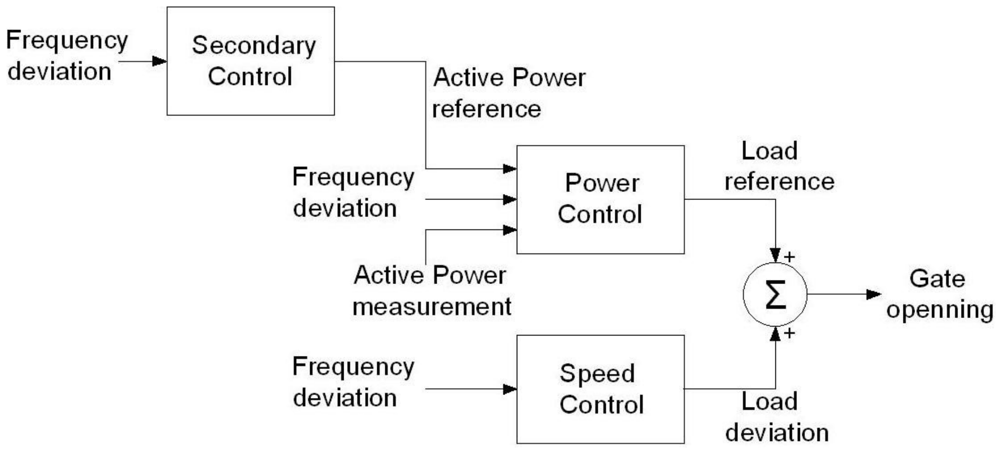

Fig. 4-30. The schematic of power control in parallel with speed control

As seen in Fig. 4-30, power control determines the load reference and speed control performs primary control action around this reference according to the frequency deviation and speed droop setting.

- Power control without speed control;

By eliminating speed control, power control may directly drive the guide vanes and perform primary control action. Although this approach has flaws, which is described in further sections, it is commonly used in Turkish power system. Since the speed control is deactivated, power control settings are tuned in order to perform satisfactory primary control action. The schematic of control is given in Fig. 4-31.

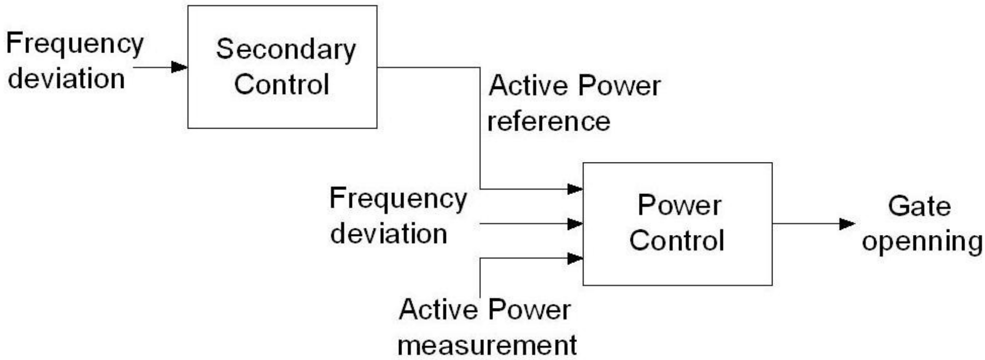

Fig. 4-31. The schematic of power control without speed control

4.5.1.1. Power Control Structure

The power controller structure is usually a PI controller as given in Fig. 4-32. The controller tries to diminish the error signal generated by three inputs; active power reference, measured output power (P_{gen}) and frequency bias.

As seen in Fig. 4-32, the active power reference is received from NLDC (AGC system). This signal may be received for each unit or for total generation in plant. The received reference signal is modified by frequency bias.

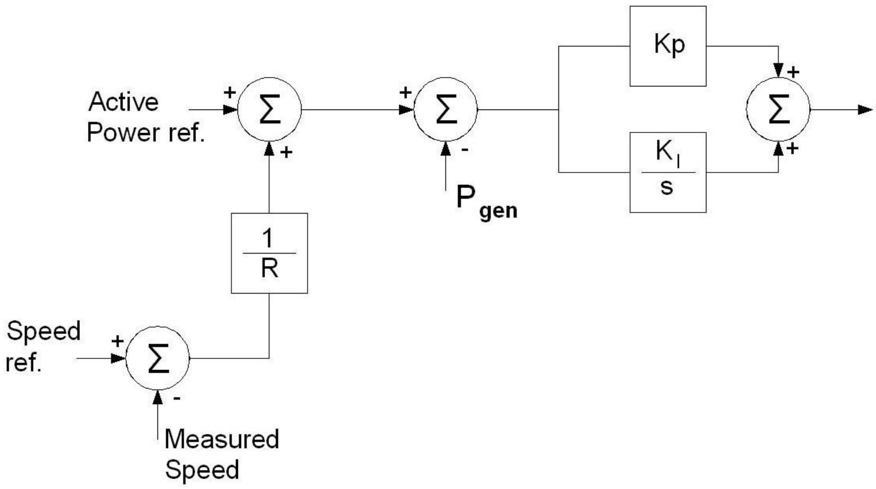

Fig. 4-32. Power controller structure

The frequency bias signal is calculated by multiplying the frequency deviation by 1/R (1/speed droop). The effect of frequency bias can be described as follows;

- Power control operating with speed control;

  For power control operating with speed control (driving speed control or in parallel with speed control), the frequency bias avoids the overrun of primary control action of speed control.

For a frequency deviation speed control changes the gate opening according to the speed droop. By changing the gate opening the output power of the unit also changes and unit performs primary action. However this change in power output is also detected by power controller and an error signal is created as a response. The frequency bias eliminates this error signal, which is formed due to primary control action, by changing the active power reference of the unit. Without the frequency bias the primary response of the unit will be eliminated by power control.

Further, as seen in Fig. 4-32, droop setting of power control can be set different than droop setting of speed control. In this case, the steady state response of the unit is determined by droop setting of power control.

In order to better understand these effects a simulation is performed. The structure given in Fig. 4-30 is used. A sample unit is considered to be connected to a very large system and a step -50 mHz change in frequency is applied. The observed outputs for power control with and without frequency bias is given in Fig. 4-33.

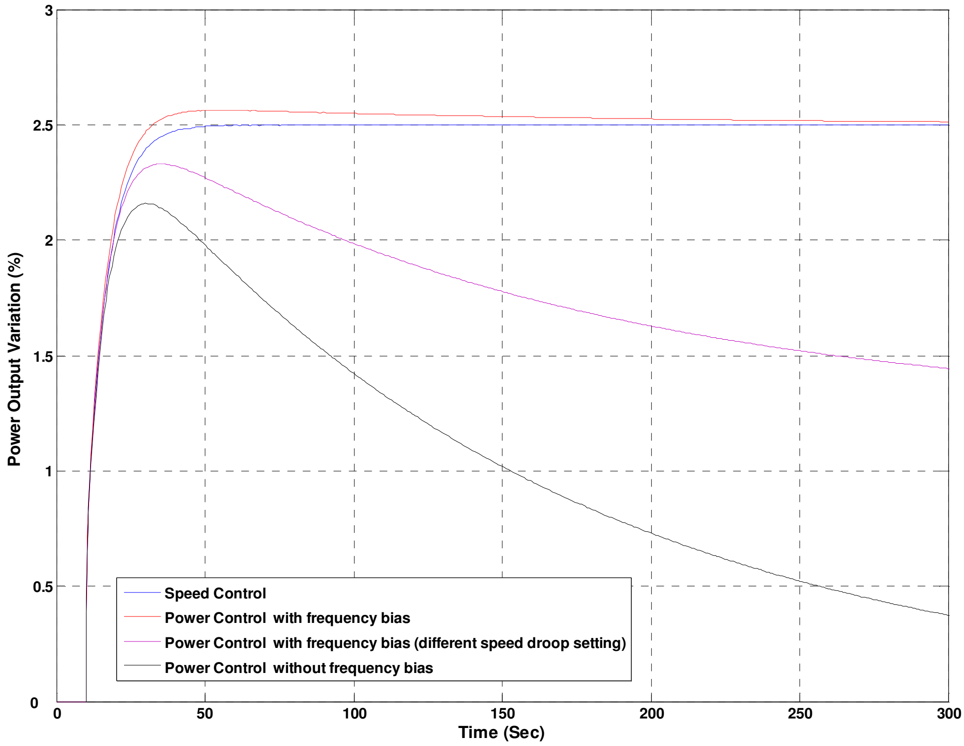

Fig. 4-33. Effect of frequency bias on power control in operation with speed control

As seen in Fig. 4-33, primary response of speed control is overrun by power control according to droop setting. If droop of power control is set to infinity (without frequency bias) the unit returns to initial conditions, and if droop of power control is set different than speed control, initial response of the unit is given according to droop setting of speed control and steady state response is determined by droop setting of power control.

- Power control operating without speed control;

For power control operating without speed control, the frequency bias is required for primary control action with speed droop. The primary control action is performed according to the equation 2-1;

$$\Delta P(p.u.) = \frac{\Delta f\,(p.u.)}{R}$$

The frequency deviation determines the power output variation according to the speed droop setting.

4.5.1.2. Field Test on Power Control without Speed Control

In order to determine the power control PI parameters a field test in Atatürk HPP is performed similar to the test described in section 4.2.2. The speed measurement signal of the controller is disabled and an artificial speed signal is supplied to the speed measuring system by utilizing a signal generator. Applying 50 Hz to the speed measurement system, the steady state operation is reached. Then step changes of ±200 mHz are applied and the response of the unit is recorded.

The exact controller structure is determined via plant documentation. As seen in Fig. 4-34 the PI power controller is followed by a PID position controller, where K_P', K_I' and K_d' are the PID gains of the position controller and T_g represents the time delay between position controller output and actual position of gate.

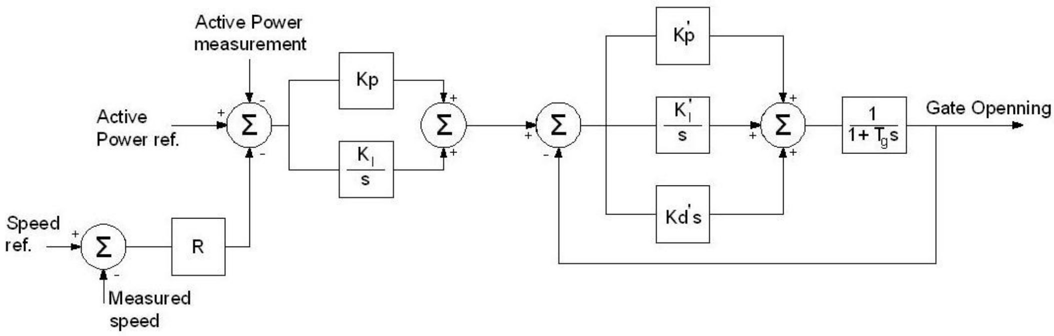

Fig. 4-34. The power controller block diagram of Atatürk HPP

The records are compared with simulation results. The settings of the controller are determined and results are compared with measurements in Fig. 4-35.

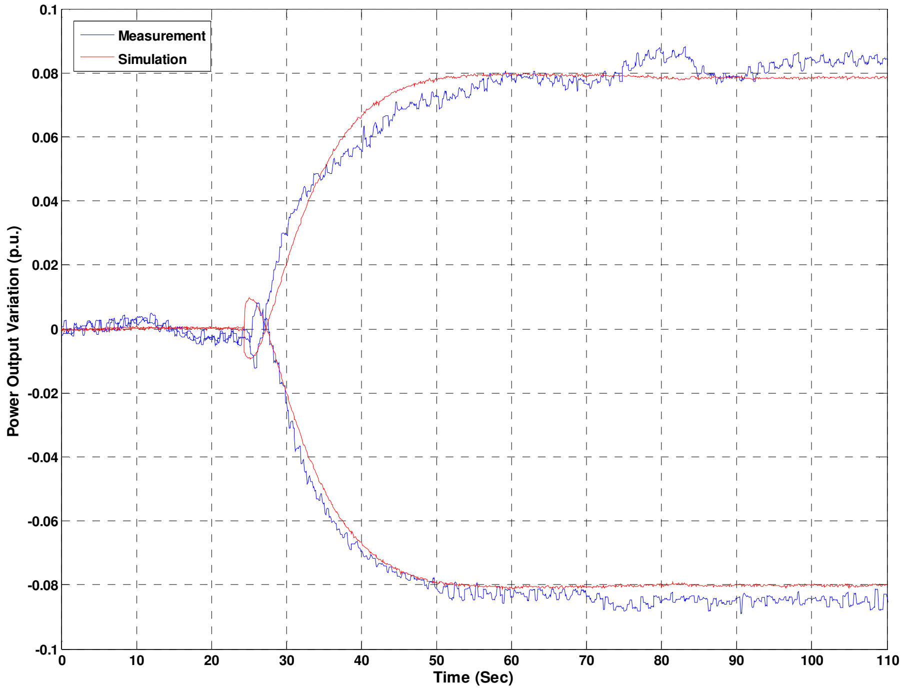

Fig. 4-35. The ±200 mHz step response of Unit 8 in Atatürk HPP

After reaching satisfactory results, the controller parameters are determined.

4.5.1.3. Stability Limits of Atatürk HPP Power Control Loop

The stability limits for Atatürk HPP power controller, are determined by the same method used in section 4.2.4. However the controller structure is slightly changed as given in Fig 4-36.

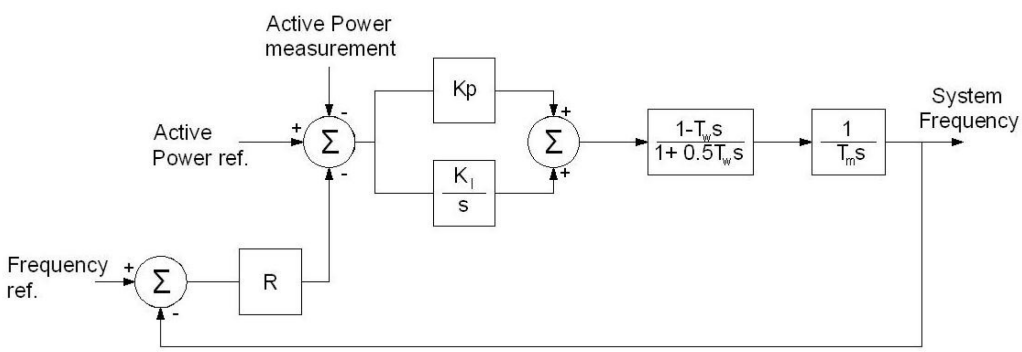

Fig. 4-36. The block diagram of HPP with power control

As the structure changes the transfer function is also changed to;

$$G(s) = \frac{(K_P s + K_I)(1 - T_w s)}{Rs(1 + 0.5T_w s)T_m s} \tag{4-18}$$

For the transfer function (4-18), the characteristic equation is in the form of equation 4-19. The derivation of the equation can be found in Appendix-E;

$$s^3(0.5X_1) + s^2(X_1 - X_2) + s(X_2 - X_2X_3) + X_2X_3 = 0 \tag{4-19}$$

where,

$$X_1 = R$$

$$X_2 = \frac{T_w K_P}{T_m}$$

$$X_3 = \frac{T_w K_I}{K_P}$$

As in previous cases, applying the criterion to the characteristic equation (4-19) gives;

- For $A_3 > 0 \rightarrow 0.5X_1 > 0$ (Droop should be larger than zero)
- For $A_2 > 0 \rightarrow X_1 > X_2$
- For $A_1 > 0 \rightarrow X_2 > X_2X_3$
- For $A_0 > 0 \rightarrow X_2X_3 > 0$
- For $B_1 > 0 \rightarrow A_1A_2 - A_3A_0 > 0$
- For $C_1 > 0 \rightarrow A_0 > 0$

If all conditions are satisfied, the stability boundaries can be found by equating $A_1A_2 - A_3A_0$ to zero, which gives;

$$X_2^2(X_3-1) + X_2(X_1-1.5X_1X_3) = 0 \tag{4-7}$$

The calculated stability boundaries for Atatürk HPP power control and determined operational settings are given in Fig. 4-37.

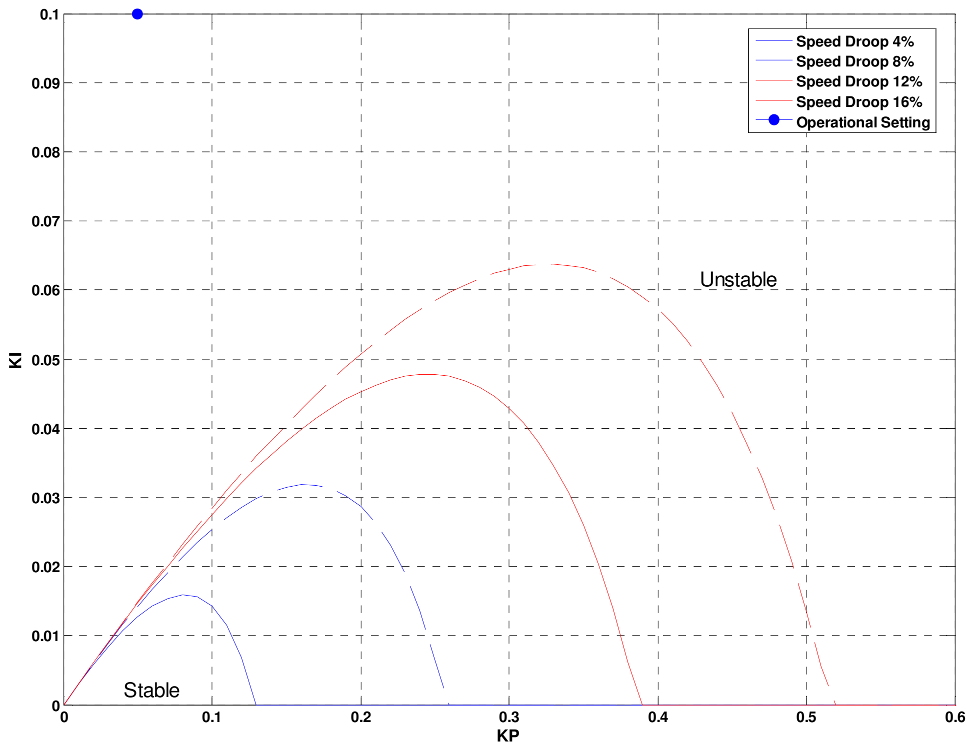

Fig. 4-37. Stability limit for Atatürk HPP power control settings

4.5.1.4. Structural Problems of Power Control without Speed Control

As seen in Fig. 4-35, the power controller of Atatürk HPP gives a very fast response to step frequency deviation. However, system frequency never changes in steps and always continuous. On the other hand, output power of a unit may change as a step function due to a fault or generation loss. This instantaneous change of output power and relatively slow change of frequency creates a false initial control action in power controllers, which is explained by following example.

Consider a case where a generator is feeding a load in island condition with power control structure. The settings of the controller are stable. Assume that the demand is increased by 1% with closing of a circuit breaker and load is independent of frequency. Since the system is in island conditions, the new demand will be supplied by the generator and generator output will increase. This increase in measured power output also affects the error signal before the controller block. Note that for the calculation of error signal, measured power is subtracted from reference power and frequency bias is added to this difference. However at the switching instant the frequency bias will be zero. Thus the error signal is composed of the difference between reference power and measured power, which is -1% (as much as the amount of demand increase). At this instant the controller will act due to the proportional part (P) and close the vanes. Even though demand is increased, controller initially acts to reduce the output power. Fig. 4-38 presents a sample vane opening, following to a step load increase of 1%.

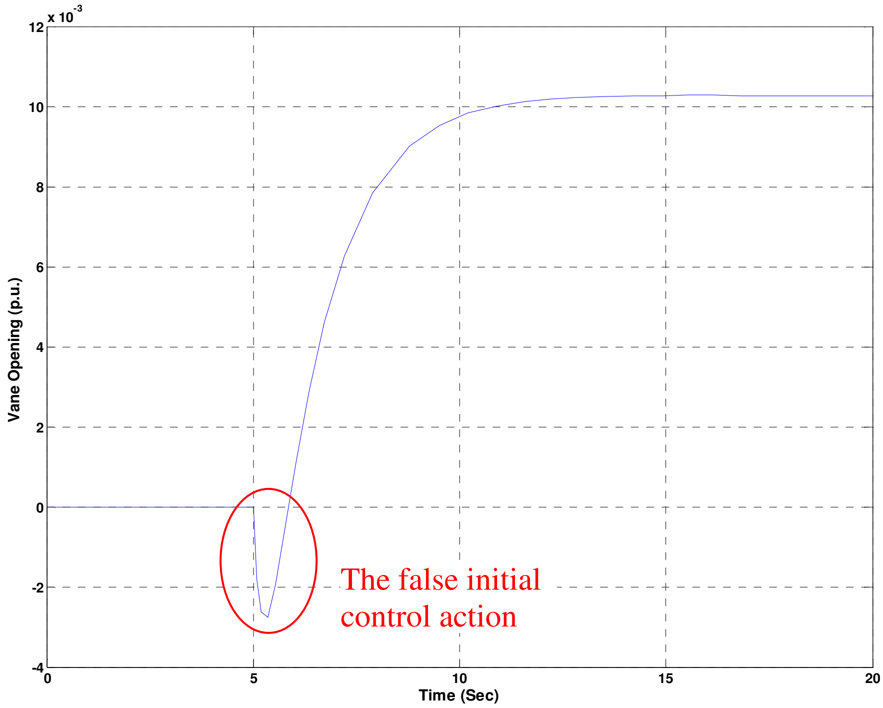

Fig. 4-38. Vane opening after a 1% demand increase (Power Control)

As seen in Fig. 4-38, the vanes are closed initially and then with increase in frequency deviation, frequency bias becomes more effective and corrected the initial inverse action.

As previously stated, the controller error has two components; one is the difference between measured and reference power and other is the frequency bias. Fig. 4-39 presents these signals for better understanding. As seen in Fig. 4-39, electrical power deviation is in the form of a step signal since the demand of the island and power reference of the controller are constants. At the instant of breaker closing the electrical power deviation introduces a negative step signal to controller input as seen in Fig. 4-39. Due to this drop, the controller error becomes negative and gates are closed. Following to this inverse action, with the effect of frequency bias, the error signal increases and becomes positive and gates are opened in order to supply increased demand.

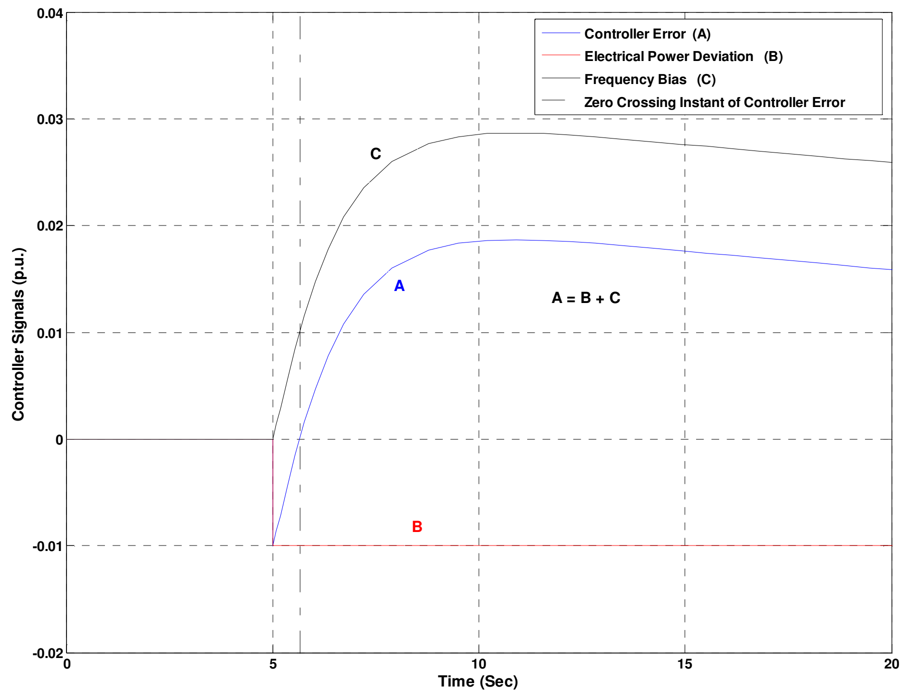

Fig. 4-39. Controller signal deviations after a 1% demand increase (Power Control)

It should be noted that this false initial control action is directly proportional with the P value of PI controller. Setting P as zero would immediately solve this problem. However as seen in Fig. 4-37, setting P to zero makes the unit unstable. Hence power control without speed control has also a conflict; either the unit will be unstable or the controller will have a false initial response to power deviations. It should also be noted that this problem is not only related with HPPs as in the case of speed controller. This controller structure will create similar problems in other power plants also.

In order to observe the effect of power control without speed control, a system wide simulation is performed with the model described previously. Utilizing the power control settings determined from field test, controllers of some power plants are converted to power control without speed control, case is referred Case-1-k. The detailed information about the controller structures is given in Appendix-F. Case-1 is used as base case for comparison. The simulation results are presented in Fig. 4-40.

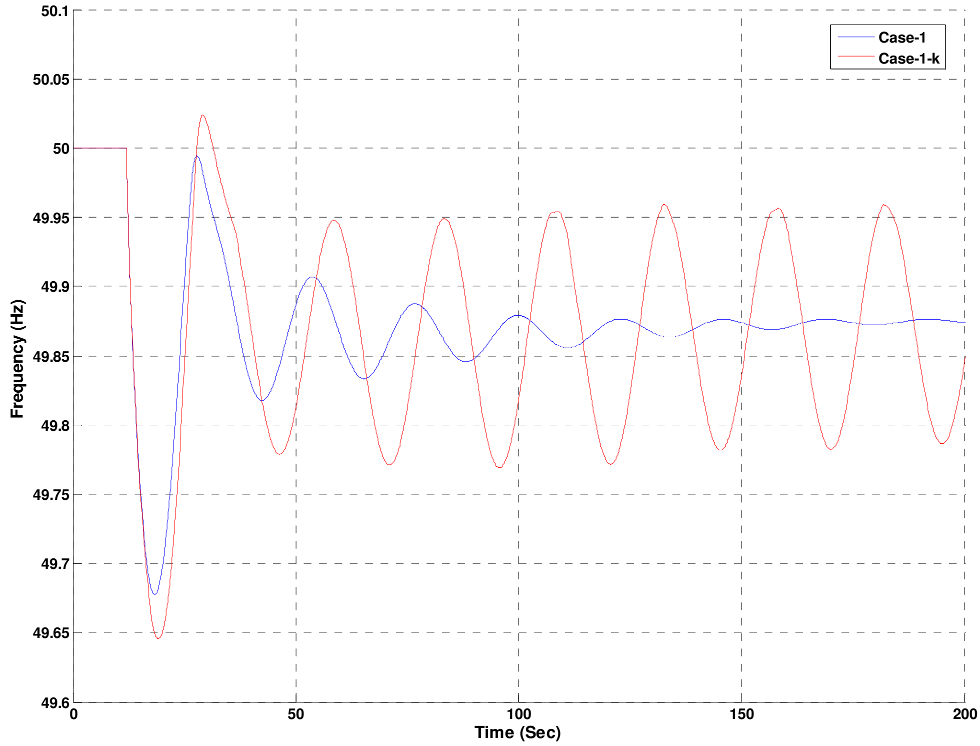

Fig. 4-40. Comparison of Case-1 with Case-1-k

As seen in Fig. 4-40, the power control without speed control has a negative effect on damping of oscillations with 20 – 30 seconds period. This effect should also be investigated in future studies.

Secondary Controller

As previously described, secondary control action is performed by AGC system. The installed system is SINAUT by SIEMENS. Although AGC system has many features like economic dispatch, power interchange control between two different areas …etc, most of them are not currently active. The main function of AGC, which is in service, is the load/frequency control function that performs the previously stated secondary control action. The structure of AGC is based on a PI controller and controller is driven by the frequency deviation signal.

In order to observe possible effects of such a PI controller on oscillations with 20 – 30 seconds period, a sample secondary controller is installed on the power system model. The new power system model is given in Fig. 4-41.

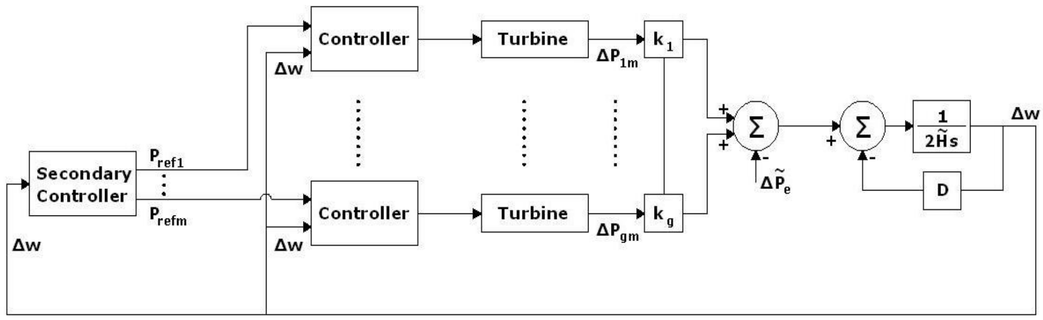

Fig. 4-41. The power system model including Secondary Control

The parameters of AGC are determined from NLDC and Case-1 is simulated again with the AGC system active. The case is referred as Case-1-m, simulation results are compared in Fig. 4-42.

As seen in Fig. 4-42, secondary control has a slightly negative effect on damping of oscillations with 20 – 30 seconds period. This effect should also be investigated in future studies by a more sophisticated model.

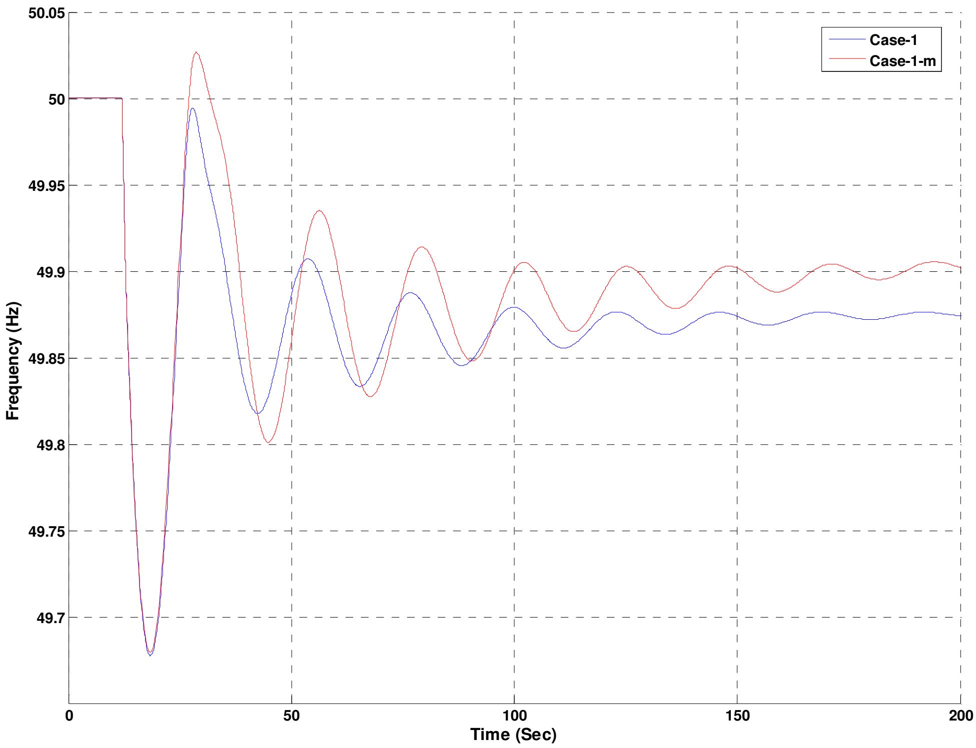

Fig. 4-42. Comparison of Case-1 with Case-1-m

CHAPTER 5

CONCLUSION AND FUTURE WORK

This study investigates the effects of hydro power plants' (HPP) governor settings on the Turkish power system frequency. For this purpose, the load/frequency controller accurate mathematical models are developed for two major power plants which provide considerable primary reserve for frequency regulation in Turkey. These controller models and parameters are validated by field tests. The unit controllers of other HPPs are developed based on the manufacturer documentation provided by the power plant staff. All assumptions made during the modeling are described in the study. After modeling the unit controllers, a representative power system model is developed for simulation studies.

The following are the main results determined from the computer simulation studies;

- The increase in contribution of HPPs with fast speed control settings (unstable in island operation) to primary frequency control has a negative effect on damping of frequency oscillations in Turkey. This phenomenon can be explained as follows; essentially if all controllers in a power system are stable in island operation, then the interconnected system will be stable. Even effects of small percentages of unstable controllers can be compensated by stable controllers. However in case of Turkish power system, reserve of HPPs, which have unstable controllers, corresponds to approximately 75 % of the overall reserve. The negative effects of these unstable controllers are eliminated by other plants to some extend depending on their reserve but essentially the increase in contribution of unstable controllers, negatively effects the damping of frequency oscillations.

● The increase in speed droop setting (i.e., decreasing the gain) of the HPP speed controllers has a positive effect on damping of frequency oscillations. However, this decreases the primary reserve contribution from the HPPs and increases the system overall speed droop, and therefore, the steady state frequency deviation will be larger after an event. Although this could be considered as a trade-off between frequency oscillation and deviation, frequency deviation is not a major problem. Since the AGC system is in operation, deviation in frequency will be eliminated by secondary control action. Hence the increasing speed droop reduces the primary control reserve and increases the secondary control reserve of HPPs. That is, most of the primary regulation will be performed by other plants and HPPs will be more effective in secondary control.

● Changing speed controller parameters (i.e., PI controller parameter) to make the unit stable in island operation has essentially a positive effect on damping of oscillations. However, the stable operation settings require less proportional gain (P) which corresponds to higher temporary droop (R_T). With the effect of higher temporary droop the wicket gates will have a reduced initial response which will limit the negative effect of the water column in the penstock. Also reducing the integration gain (I) corresponds to increasing of reset time constant (T_R) which results in slower elimination of temporary droop effect and hence slower opening of wicket gates. Thus the response of the overall system becomes sluggish and therefore, the initial frequency deviation and restoration time increases in case of a disturbance.

● Modification of the speed control structure with including a derivative of speed deviation input has a positive effect on damping of oscillations. Currently Birecik, Berke and Keban HPPs are equipped with controllers that have such an input signal. It is essentially not economical to modify every speed controller structure of HPPs lacking such configuration in Turkey. However, such modifications could be considered during rehabilitation of old plants and commissioning of new plants.

One of the main conclusions of the study is that the modification of HPPs' unit controller settings to improve response time conflicts with the stable operation of the units. That is, the controller settings required for stable operation are contradicting with settings required for a fast primary control response. The grid code of Turkish power system, which requires fast response (limit is maximum 30 seconds) from HPPs, should consider this conflict. The conclusion of this study proposes some modifications on the grid code. The load/frequency regulation performance of the HPPs should be individually evaluated taking into account the stability limits and characteristics of the individual power plants. In the study, the required parameter settings of the HPP unit controllers for stable load/frequency regulation are formulated based on the individual characteristics of the plant including the penstock, dam, and the generator inertia. These formulations can give idea to the TEİAŞ authorities in modifying the grid code.

Other factors, which might also have negative effects on frequency, such as controller structure type (e.g., power controller together with frequency bias) and AGC (i.e., secondary control), are also discussed in the study. However, only some preliminary studies are performed. After the preliminary studies it is observed that;

- Power controllers operating without speed controllers have a false initial response to instant changes in generator power output. That is, in case of an increase in generator power output the controller responds by closing regulating vanes initially or vice versa. Note that this effect is not due to inertia of water or any other property of the plant but a result of the controller structure. This effect can only be eliminated in the expense of controller stability. Hence it is concluded that the speed controller loop should always be active and power controller should be used only to regulate load or speed reference by the signals supplied from AGC system. Further power control should have relatively slower settings than speed control in order to eliminate the false initial response.

- The speed droop setting of power controller in operation with speed controller (i.e., in parallel or cascade) should be chosen carefully. In case of a different speed droop setting the final primary response of the unit will be determined by speed droop setting of power controller.

- Future studies could include the investigation of effects of power control and secondary control on Turkish power system frequency.

Given that the study focuses on the effect of HPP unit controllers, standard models (mostly IEEE standard models) are used to represent unit controllers of TPPs and NGCCPPs based on certain assumptions described in the thesis. The basic assumption is that those power plants' unit controller settings are set in a way such that the units are stable in providing frequency regulation. Future studies can deal with the negative effects (if any) of such power plants on the frequency.

REFERENCES

[1] IEEE/CIGRE Joint Task Force on Stability Terms and Definitions, "Definitions and Classification of Power System Stability", *IEEE Trans. Power Systems*, vol.19, pp. 1387–1399, May 2004.

[2] P. Kundur, *Power System Stability and Control*, New York: McGraw-Hill, 1994.

[3] "UCTE Operation Handbook", *Union for the Coordination of Transmission of Electricity*, June 2004.

[4] M. E. Cebeci, U. Karaagac, O. B. Tor and A. Ertaş , "The Effects of Hydro Power Plants' Governor Settings on the Stability of Turkish Power System Frequency " *ELECO Conf*, Bursa, Turkey, Dec. 2007.

[5] "Complementary Studies for the Synchronization of the Turkish Power System with the UCTE Power System", UCTE, May 2007.

[6] J. F. Douglas and R. D. Mathews, *Fluid Mechanics*, 2. Addison Wesley Longman Ltd.: 1996.

[7] S. Mansoor, "Behavior and Operation of Pumped Storage Hydro Plants", PhD Thesis, University of Wales.

[8] J. M. Undrill and J. L. Woodward, "Nonlinear Hydro Governing Model and Improved Calculation for Determining Temporary Droop", *IEEE Trans. Power Apparatus and Systems*, vol. Pas-86, pp. 443–453, Apr. 1967.

[9] F. R. Schleif AND A. B. Wilbor, "The Coordination of Hydraulic Turbine Governors for Power System Operation", *IEEE Trans. Power Apparatus and Systems*, vol. Pas-85, pp. 750–758, July 1966.

[10] IEEE Working Group on Prime Mover and Energy Supply Models for System Dynamic Performance Studies, "Hydraulic Turbine and Turbine Control Models for System Dynamic Studies" *IEEE Trans. Power Systems*, vol. 7, pp. 167–179, Feb. 1992.

[11] IEEE Committee Report, "Dynamic Models for Hydro Turbines in Power System Studies", *IEEE Trans. Power Apparatus and Systems*, 1973.

[12] C.D.Vournas and A.Zaharakis, "Hydro Turbine Transfer Functions with Hydraulic Coupling", *IEEE Trans. Energy Conversion*, vol. 8, pp. 527–532, Sept. 1993.

[13] C. C. Warnick, *Hydropower Engineering,* Prentice-Hall Ltd., 1984

[14] W. D. Stevenson, *Elements of Power System Analysis*, New York: McGraw-Hill, 1986.

[15] Energy Market Regulatory Authority of Turkey, http://www.epdk.org.tr/mevzuat/yonetmelik/elektrik/sebeke/sebeke.pdf, Jan. 2008.

[16] O. Yılmaz, "Participation of Combined Cycle Power Plants to Power System Frequency Control: Modeling and Application", Ms Thesis, Middle East Technical University, Apr. 2006.

[17] L. N. Hannett and B.Fardanesh, “Field Tests to Validate Hydro Turbine Governor Model Structure and Parameters”, *IEEE Trans.Power System*, Vol. 9, pp. 1744–1751, Nov. 1994.

[18] Mathworks Company, www.mathwork.com, Jan. 2008.

[19] Siemens Company, www.pti-us.com, Jan. 2008.

APPENDIX - A

LINEARISED TURBINE/PENSTOCK MODEL

The first order linear model of turbine-penstock used in Section 3.2.1.4 is derived by linearising equations (3-4) and (3-9), which is achieved by substituting x = $x_0+\Delta x$ for each variable, dropping the initial conditions and any terms higher than Δx. For equation (3-4)

$$\left(\bar{q}_0 + \Delta\bar{q}\right) = \left(\bar{G}_0 + \Delta\bar{G}\right)\sqrt{\bar{h}_0 + \Delta\bar{h}} \tag{A-1}$$

The terms under square root can be linearised using Taylor expansion of a polynomial raised to the ½ power as,

$$\left(x_0 + \Delta x\right)^{1/2} = \sqrt{x_0}\left(1 + \frac{\Delta x}{2x_0}\right) \tag{A-2}$$

Replacing the linearization in equation A-1

$$\bar{q}_0 + \Delta\bar{q} = \left(\bar{G}_0 + \Delta\bar{G}\right)\sqrt{\bar{h}_0}\left(1 + \frac{\Delta\bar{h}}{2\bar{h}_0}\right) \tag{A-3}$$

Eliminating the initial conditions

$$\Delta\bar{q} = \Delta\bar{G}\sqrt{\bar{h}_0} + \bar{G}_0\frac{\Delta\bar{h}\sqrt{\bar{h}_0}}{2\bar{h}_0} \tag{A-4}$$

From equation 3-9

$$\Delta\bar{h} = -\Delta\bar{q}T_w s \tag{A-5}$$

Substituting equation A-5 in equation A-4 gives

$$\Delta\bar{q} = \Delta\bar{G}\sqrt{\bar{h}_0} - \frac{\bar{G}_0\sqrt{\bar{h}_0}}{2\bar{h}_0}T_w s\Delta\bar{q} \tag{A-6}$$

Solving for $\Delta\bar{q}$ gives

$$\Delta\bar{q} = \Delta\bar{G}\frac{\sqrt{\bar{h}_0}}{1+\frac{\bar{G}_0\sqrt{\bar{h}_0}}{2\bar{h}_0}T_w s} \tag{A-7}$$

The equation for mechanical power developed in the turbine is

$$\bar{P}_m = A_t\bar{q}\bar{h} \tag{A-8}$$

Linearising equation A-8

$$\Delta\bar{P}_m = A_t\bar{q}_0\Delta\bar{h} + A_t\Delta\bar{q}\bar{h}_0 \tag{A-9}$$

Substituting equation A-5 into A-9

$$\Delta\bar{P}_m(s) = A_t\left(\bar{h}_0 - \bar{q}_0T_w s\right)\Delta\bar{q} \tag{A-10}$$

Substituting A-7 in A-10

$$\frac{\Delta\overline{P}_m(s)}{\Delta\overline{G}(s)} = \frac{A_t\left(\overline{h}_0 - \overline{q}_0 T_w s\right)\sqrt{\overline{h}_0}}{1 + \dfrac{\overline{G}_0\sqrt{\overline{h}_0}}{2\overline{h}_0} T_w s} \tag{A-11}$$

Note that $\overline{G}_0 = \dfrac{\overline{q}_0}{\sqrt{\overline{h}_0}}$

$$\frac{\Delta\overline{P}_m(s)}{\Delta\overline{G}(s)} = \frac{A_t\overline{h}_0\sqrt{\overline{h}_0}\left(1 - \dfrac{\overline{q}_0}{\overline{h}_0} T_w s\right)}{1 + \dfrac{\overline{q}_0}{2\overline{h}_0} T_w s} = A_t\overline{h}_0\sqrt{\overline{h}_0}\left(\frac{1 - T_{w0}s}{1 + 0.5T_{w0}s}\right) \tag{A-12}$$

Note that in calculation of T_w base values are utilized for flow and head. However the T_{w0} parameter corresponds to operating condition. Hence while utilizing linearised model in stability studies water time constant should be adjusted according to loading condition of HPP [7].

APPENDIX - B

LOAD FLOW SIMULATIONS OF INITIAL CONDITIONS PRIOR TO ISLAND TESTS IN ATATÜRK AND BIRECIK HYDRO POWER PLANTS

In order to confirm the model generated in Matlab – SIMULINK software, another simulation study is performed in PSS/E software. PSS/E software requires a load flow simulation of initial conditions before the dynamic simulations. Hence network models for islanded regions are prepared for conditions prior to islanding of Atatürk and Birecik power plants. The required data is supplied by TEİAŞ and the model is constructed. The results of the load flow study for both tests are given in Fig. B-1 and Fig. B-2. Utilizing these load flow simulations the Matlab models of Atatürk and Birecik HPPs are validated by dynamic simulations. The results of modeling studies are presented in section 4.2.

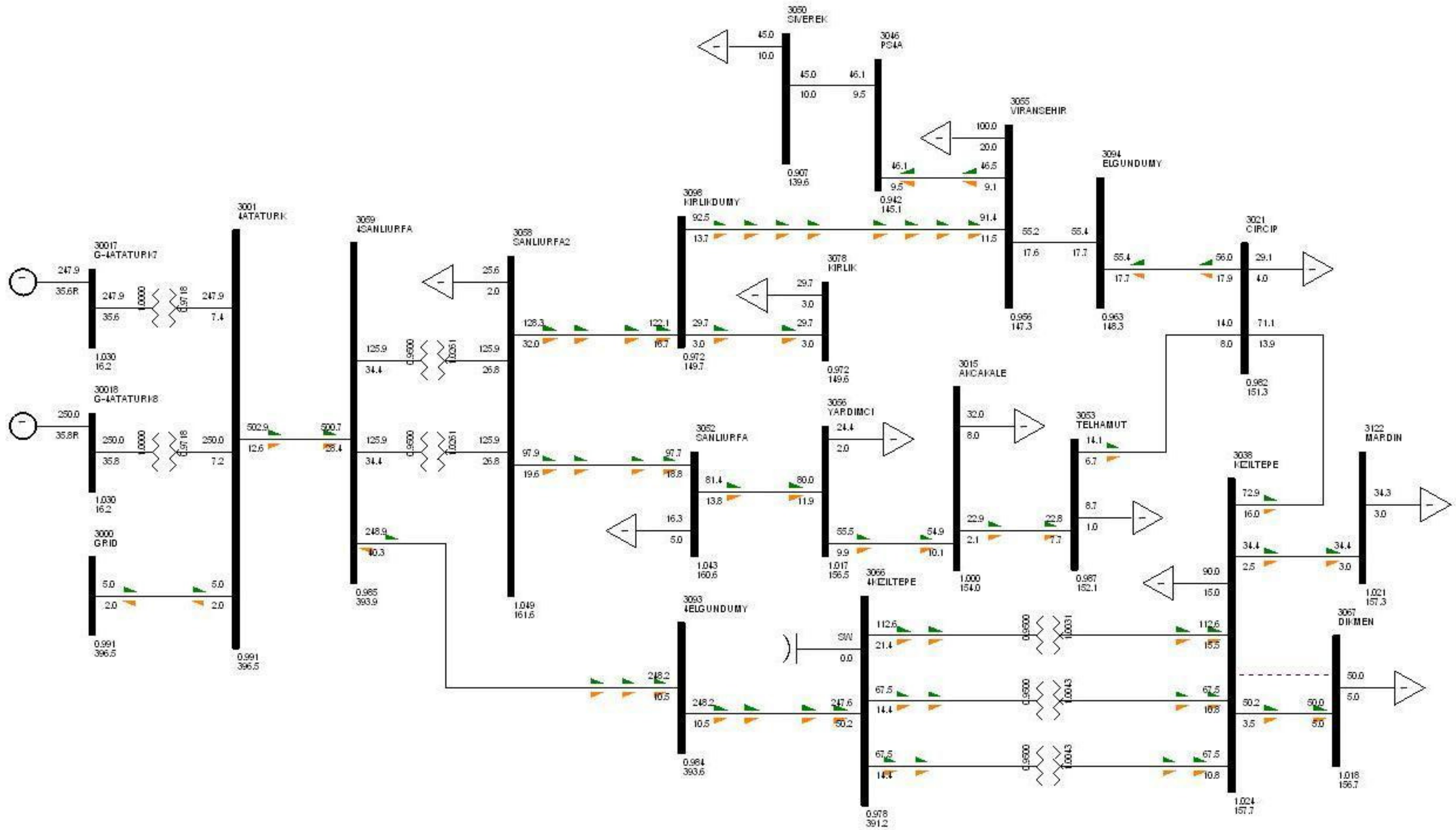

Fig. B-1. Pre-island load flow simulation results for island test in Atatürk HPP

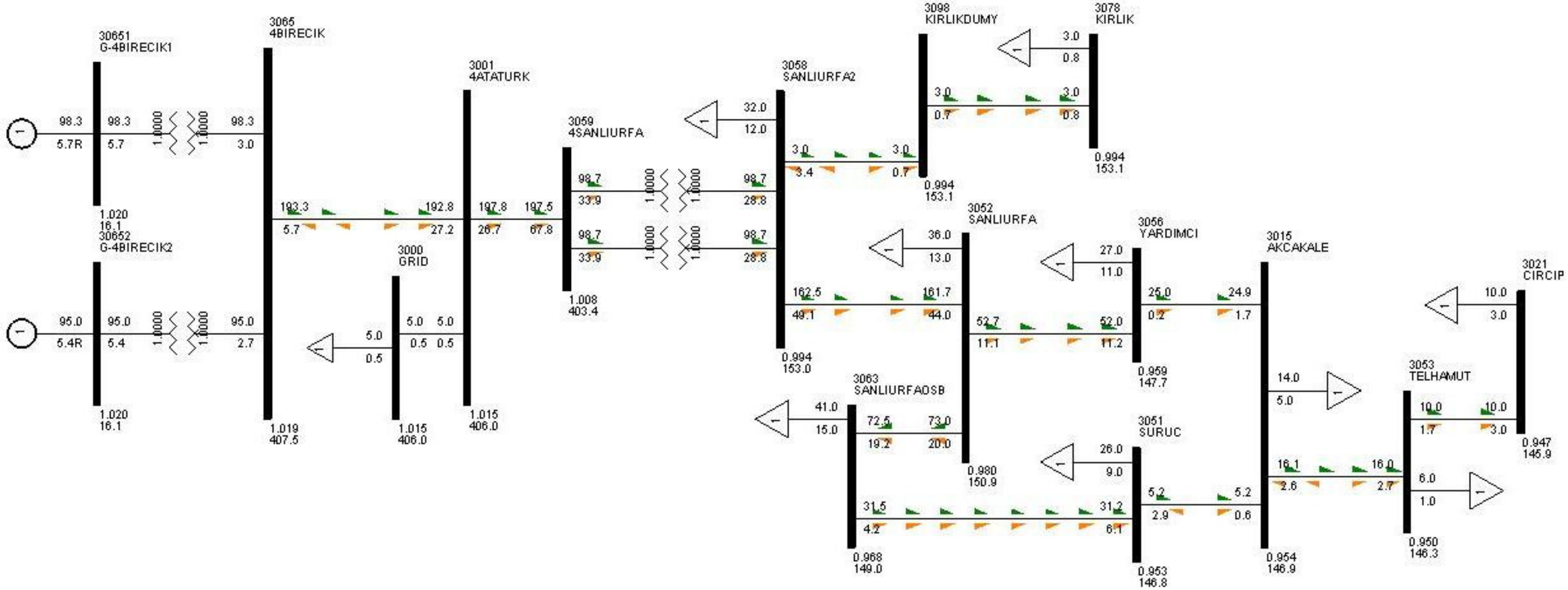

Fig. B-2. Pre-island load flow simulation results for island test in Birecik HPP

APPENDIX - C

SYSTEM CHARACTERISTIC EQUATION FOR ATATÜRK HYDRO POWER PLANT

The system characteristic equation used in Routh's test to determine the stability margins in Section 4.2.4 is derived from equation (4-1) which can be written as,

$$\frac{(K_P s + K_I)(1 - T_w s)}{[R(K_P s + K_I) + s](1 + 0.5T_w s)T_m s} + 1 = 0 \qquad \text{(C-1)}$$

Solving equation C-1 yields

$$s^3[0.5RK_pT_mT_w + 0.5T_mT_w] + s^2[RK_pT_m + T_m + 0.5RK_IT_mT_w - K_pT_w]$$
$$+ s[RK_IT_m + K_p - K_IT_w] + K_I = 0 \qquad \text{(C-2)}$$

Dividing equation C-2 by $T_w^2T_m$

$$\frac{s^3}{T_w}\left[0.5 + 0.5RK_p\right] + \frac{s^2}{T_w^{\,2}}\left[RK_p + 1 + 0.5RK_IT_w - \frac{K_pT_w}{T_m}\right] + \frac{s}{T_w^{\,3}}\left[RK_IT_w + \frac{K_pT_w}{T_m} - \frac{K_IT_w^{\,2}}{T_m}\right]$$
$$+ \frac{1}{T_w^{\,4}}\left[\frac{K_IT_w^{\,2}}{T_m}\right] = 0 \qquad \text{(C-3)}$$

Set $X_1 = RK_P$

$X_2 = RK_IT_w$

$X_3 = \dfrac{T_wK_P}{T_m}$

$X_4 = \dfrac{K_IT_w}{K_P}$

Multiply both sides by T_w^4 and scale $s_{new} = s\,T_w$

$$s^3 0.5(1+X_1)+s^2(X_1+0.5X_2-X_3+1)+s(X_2+X_3-X_3X_4)+X_3X_4=0 \quad \text{(C-4)}$$

Equation C-4 is used for Routh Hurwitz method.

APPENDIX - D

SYSTEM CHARACTERISTIC EQUATION FOR BIRECIK HYDRO POWER PLANT

The system characteristic equation used in Routh's test to determine the stability margins in Section 4.3.3 is derived from equation (4-10) which can be written as,

$$\frac{(s+1)(K_P s + K_I)(1-T_w s)}{[R(K_P s + K_I) + s](1+0.5T_w s)T_m s} + 1 = 0 \qquad \text{(D-1)}$$

Solving equation D-1 yields

$$s^3[0.5RK_pT_mT_w+0.5T_mT_w - K_pT_w]+s^2[RK_pT_m+T_m+0.5RK_IT_mT_w +K_p - K_pT_w - K_IT_w]$$
$$+s[RK_IT_m+K_p+K_I - K_IT_w]+K_I = 0 \qquad \text{(D-2)}$$

Dividing equation D-2 by $T_w^2T_m$

$$\frac{s^3}{T_w}\left[0.5+0.5RK_p+\frac{K_p}{T_m}\right]+\frac{s^2}{T_w^{\,2}}\left[RK_p+1+0.5RK_IT_w+\frac{K_p}{T_m}-\frac{K_IT_w}{T_m}-\frac{K_pT_w}{T_m}\right]$$
$$+\frac{s}{T_w^{\,3}}\left[RK_IT_w+\frac{K_pT_w}{T_m}+\frac{K_IT_w}{T_m}-\frac{K_IT_w^{\,2}}{T_m}\right]+\frac{1}{T_w^{\,4}}\left[\frac{K_IT_w^{\,2}}{T_m}\right]=0 \qquad \text{(D-3)}$$

Set $X_1 = RK_P$

$X_2 = RK_IT_w$

$X_3 = \dfrac{T_wK_P}{T_m}$

$X_4 = \dfrac{K_IT_w}{K_P}$

$$X_5 = \frac{1}{T_w}$$

Multiply both sides by $T_w^{\ 4}$ and scale $s_{new} = s\ T_w$

$$\begin{aligned} &s^3[0.5(1+X_1)+X_3X_5]+s^2(X_1+0.5X_2-X_3+1+X_3X_5-X_3X_4X_5)+ \\ &s(X_2+X_3-X_3X_4+X_3X_4X_5)+X_3X_4=0 \end{aligned} \tag{D-4}$$

Equation D-4 is used for Routh Hurwitz method.

APPENDIX - E

SYSTEM CHARACTERISTIC EQUATION FOR POWER CONTROL LOOP OF ATATÜRK HYDRO POWER PLANT

The system characteristic equation used in Routh's test to determine the stability margins in Section 4.5.1 is derived from equation (4-10) which can be written as,

$$\frac{(K_P s + K_I)(1 - T_w s)}{Rs(1 + 0.5T_w s)T_m s} + 1 = 0 \qquad \text{(E-1)}$$

Solving equation E-1 yields

$$s^3[0.5RT_mT_w] + s^2[RT_m - K_pT_w] + s[K_p - K_IT_w] + K_I = 0 \qquad \text{(E-2)}$$

Dividing equation E-2 by $T_w^2 T_m$

$$\frac{s^3}{T_w}[0.5R] + \frac{s^2}{T_w^2}\left[R - \frac{K_pT_w}{T_m}\right] + \frac{s}{T_w^3}\left[\frac{K_pT_w}{T_m} - \frac{K_IT_w^2}{T_m}\right] + \frac{1}{T_w^4}\left[\frac{K_IT_w^2}{T_m}\right] = 0 \qquad \text{(E-3)}$$

Set $\quad X_1 = R\,,\ X_2 = \dfrac{T_wK_P}{T_m}\,,\ X_3 = \dfrac{T_wK_I}{K_P}$

Multiply both sides by T_w^4 and scale $s_{new} = s\ T_w$

$$s^3(0.5X_1) + s^2(X_1 - X_2) + s(X_2 - X_2X_3) + X_2X_3 = 0 \qquad \text{(E-4)}$$

Equation E-4 is used for Routh Hurwitz method.

APPENDIX - F

GENERATION AND CONTROLLER INFORMATION OF SIMULATION CASES

Table F-1. Generation profile of Case-1

Hydro Power Plants								
Plant	**Units**	**Rating (MW)**	**Generation (MW)**	**Reserve (MW)**	**% of System Reserve**	**Speed Droop**	**Controller Settings**	**Derivative Input**
ALTINKAYA		4 x 175	150	15	1.4%	4%	Unstable	-
ATATÜRK		8 x 300	700	140	13.3%	4%	Unstable	-
BERKE		3 x 175	271	54	5.2%	4%	Unstable	✓
BİRECİK		6 x 126	650	130	12.4%	4%	Unstable	✓
HASAN UĞR.		4 x 125	0	0	0.0%	4%	Unstable	-
KARAKAYA		6 x 300	920	184	17.5%	4%	Unstable	-
KEBAN	1-4	4 x 157	1111	222	21.1%	4%	Unstable	✓
	5-8	4 x 180			0.0%	4%	Unstable	✓
OYMAPINAR		4 x 135	110	22	2.1%	4%	Unstable	-
Total	**-**	**-**	**3912**	**767.4**	**72.9%**		**-**	
Other Power Plants								
Plant	**Units**	**Rating (MW)**	**Generation (MW)**	**Reserve (MW)**	**% of System Reserve**	**Speed Droop**	**Controller Settings**	-
TPP	-	8500	700*	35	3.3%	5%	Stable	-
NGCCPP	-	6000	5000*	250	23.8%	5%	Stable	-
Plants with constant gen.	-	-	8138	0	0.0%	-	-	-
Total	**-**	**-**	**13838**	**285**	**27.1%**	-	**-**	-
SYSTEM TOTAL			**17750**	**1052.4**	**-**	-	**-**	-

* Generation of units contributing to primary control

Table F-2. Generation profile of Case-1-a

Plant	Units	Rating (MW)	Generation (MW)	Reserve (MW)	% of System Reserve	Speed Droop	Controller Settings	Derivative Input
Hydro Power Plants								
ALTINKAYA		4 x 175	150	15	1.5%	4%	Unstable	-
ATATÜRK		8 x 300	200	40	4.0%	4%	Unstable	-
BERKE		3 x 175	271	54	5.5%	4%	Unstable	✓
BİRECİK		6 x 126	650	130	13.1%	4%	Unstable	✓
HASAN UĞR.		4 x 125	200	40	4.0%	4%	Unstable	-
KARAKAYA		6 x 300	920	184	18.5%	4%	Unstable	-
KEBAN	1-4	4 x 157	1111	222	22.4%	4%	Unstable	✓
	5-8	4 x 180			0.0%	4%	Unstable	✓
OYMAPINAR		4 x 135	110	22	2.2%	4%	Unstable	-
Total	**-**	**-**	**3612**	**707.4**	**71.3%**		**-**	
Other Power Plants								
Plant	**Units**	**Rating (MW)**	**Generation (MW)**	**Reserve (MW)**	**% of System Reserve**	**Speed Droop**	**Controller Settings**	-
TPP	-	8500	700*	35	3.5%	5%	Stable	-
NGCCPP	-	6000	5000*	250	25.2%	5%	Stable	-
Plants with constant gen.	-	-	8438	0	0.0%	-	-	-
Total	**-**	**-**	**14138**	**285**	**28.7%**	-	**-**	-
SYSTEM TOTAL			**17750**	**992.4**	**-**	-	**-**	-

* Generation of units contributing to primary control

Table F-3. Generation profile of Case-1-b

Hydro Power Plants								
Plant	**Units**	**Rating (MW)**	**Generation (MW)**	**Reserve (MW)**	**% of System Reserve**	**Speed Droop**	**Controller Settings**	**Derivative Input**
ALTINKAYA		4 x 175	150	15	1.9%	4%	Unstable	-
ATATÜRK		8 x 300	200	40	5.0%	4%	Unstable	-
BERKE		3 x 175	271	54	6.8%	4%	Unstable	✓
BİRECİK		6 x 126	650	130	16.4%	4%	Unstable	✓
HASAN UĞR.		4 x 125	200	40	5.0%	4%	Unstable	-
KARAKAYA		6 x 300	920	184	23.2%	4%	Unstable	-
KEBAN	1-4	4 x 157	111	22	2.8%	4%	Unstable	✓
	5-8	4 x 180			0.0%	4%	Unstable	✓
OYMAPINAR		4 x 135	110	22	2.8%	4%	Unstable	-
Total	**-**	**-**	**2612**	**507.4**	**64.0%**		**-**	
Other Power Plants								
Plant	**Units**	**Rating (MW)**	**Generation (MW)**	**Reserve (MW)**	**% of System Reserve**	**Speed Droop**	**Controller Settings**	-
TPP	-	8500	700*	35	4.4%	5%	Stable	-
NGCCPP	-	6000	5000*	250	31.5%	5%	Stable	-
Plants with constant gen.	-	-	9438	0	0.0%	-	-	-
Total	**-**	**-**	**15138**	**285**	**36.0%**	-	**-**	-
SYSTEM TOTAL			**17750**	**792.4**	**-**	-	**-**	-

* Generation of units contributing to primary control

Table F-4. Generation profile of Case-1-c

Hydro Power Plants								
Plant	**Units**	**Rating (MW)**	**Generation (MW)**	**Reserve (MW)**	**% of System Reserve**	**Speed Droop**	**Controller Settings**	**Derivative Input**
ALTINKAYA		4 x 175	150	15	1.2%	4%	Unstable	-
ATATÜRK		8 x 300	1200	240	19.2%	4%	Unstable	-
BERKE		3 x 175	271	54	4.3%	4%	Unstable	✓
BİRECİK		6 x 126	650	130	10.4%	4%	Unstable	✓
HASAN UĞR.		4 x 125	0	0	0.0%	4%	Unstable	-
KARAKAYA		6 x 300	920	184	14.7%	4%	Unstable	-
KEBAN	1-4	4 x 157	1611	322	25.7%	4%	Unstable	✓
	5-8	4 x 180			0.0%	4%	Unstable	✓
OYMAPINAR		4 x 135	110	22	1.8%	4%	Unstable	-
Total	**-**	**-**	**4912**	**967.4**	**77.2%**		**-**	
Other Power Plants								
Plant	**Units**	**Rating (MW)**	**Generation (MW)**	**Reserve (MW)**	**% of System Reserve**	**Speed Droop**	**Controller Settings**	-
TPP	-	8500	700*	35	2.8%	5%	Stable	-
NGCCPP	-	6000	5000*	250	20.0%	5%	Stable	-
Plants with constant gen.	-	-	7138	0	0.0%	-	-	-
Total	**-**	**-**	**12838**	**285**	**22.8%**	-	**-**	-
SYSTEM TOTAL			**17750**	**1252.4**	**-**	-	**-**	-

* Generation of units contributing to primary control

Table F-5. Generation profile of Case-1-d

Hydro Power Plants									
Plant	**Units**	**Rating (MW)**	**Generation (MW)**	**Reserve (MW)**	**% of System Reserve**	**Speed Droop**	**Controller Settings**	**Derivative Input**
ALTINKAYA		4 x 175	150	15	1.0%	4%	Unstable	-
ATATÜRK		8 x 300	2000	400	27.5%	4%	Unstable	-
BERKE		3 x 175	271	54	3.7%	4%	Unstable	✓
BİRECİK		6 x 126	650	130	9.0%	4%	Unstable	✓
HASAN UĞR.		4 x 125	200	40	2.8%	4%	Unstable	-
KARAKAYA		6 x 300	920	184	12.7%	4%	Unstable	-
KEBAN	1-4	4 x 157	1611	322	22.2%	4%	Unstable	✓
	5-8	4 x 180			0.0%	4%	Unstable	✓
OYMAPINAR		4 x 135	110	22	1.5%	4%	Unstable	-
Total	**-**	**-**	**5912**	**1167.4**	**80.4%**		**-**	
Other Power Plants								
Plant	**Units**	**Rating (MW)**	**Generation (MW)**	**Reserve (MW)**	**% of System Reserve**	**Speed Droop**	**Controller Settings**	-
TPP	-	8500	700*	35	2.4%	5%	Stable	-
NGCCPP	-	6000	5000*	250	17.2%	5%	Stable	-
Plants with constant gen.	-	-	6138	0	0.0%	-	-	-
Total	**-**	**-**	**11838**	**285**	**19.6%**	-	**-**	-
SYSTEM TOTAL			**17750**	**1452.4**	**-**	-	**-**	-

* Generation of units contributing to primary control

Table F-6. Generation profile of Case-1-e

Hydro Power Plants								
Plant	**Units**	**Rating (MW)**	**Generation (MW)**	**Reserve (MW)**	**% of System Reserve**	**Speed Droop**	**Controller Settings**	**Derivative Input**
ALTINKAYA		4 x 175	150	15	1.0%	10%	Unstable	-
ATATÜRK		8 x 300	2000	400	27.5%	4%	Unstable	-
BERKE		3 x 175	271	54	3.7%	4%	Unstable	✓
BİRECİK		6 x 126	650	130	9.0%	4%	Unstable	✓
HASAN UĞR.		4 x 125	200	40	2.8%	10%	Unstable	-
KARAKAYA		6 x 300	920	184	12.7%	10%	Unstable	-
KEBAN	1-4	4 x 157	1611	322	22.2%	10%	Unstable	✓
	5-8	4 x 180			0.0%	10%	Unstable	✓
OYMAPINAR		4 x 135	110	22	1.5%	10%	Unstable	-
Total	**-**	**-**	**5912**	**1167.4**	**80.4%**		**-**	
Other Power Plants								
Plant	**Units**	**Rating (MW)**	**Generation (MW)**	**Reserve (MW)**	**% of System Reserve**	**Speed Droop**	**Controller Settings**	-
TPP	-	8500	700*	35	2.4%	5%	Stable	-
NGCCPP	-	6000	5000*	250	17.2%	5%	Stable	-
Plants with constant gen.	-	-	6138	0	0.0%	-	-	-
Total	**-**	**-**	**11838**	**285**	**19.6%**	-	**-**	-
SYSTEM TOTAL			**17750**	**1452.4**	**-**	-	**-**	-

* Generation of units contributing to primary control

Table F-7. Generation profile of Case-1-f

Plant	Units	Rating (MW)	Generation (MW)	Reserve (MW)	% of System Reserve	Speed Droop	Controller Settings	Derivative Input
Hydro Power Plants								
ALTINKAYA		4 x 175	150	15	1.0%	10%	Unstable	-
ATATÜRK		8 x 300	2000	400	27.5%	10%	Unstable	-
BERKE		3 x 175	271	54	3.7%	10%	Unstable	✓
BİRECİK		6 x 126	650	130	9.0%	10%	Unstable	✓
HASAN UĞR.		4 x 125	200	40	2.8%	10%	Unstable	-
KARAKAYA		6 x 300	920	184	12.7%	10%	Unstable	-
KEBAN	1-4	4 x 157	1611	322	22.2%	10%	Unstable	✓
	5-8	4 x 180			0.0%	10%	Unstable	✓
OYMAPINAR		4 x 135	110	22	1.5%	10%	Unstable	-
Total	**-**	**-**	**5912**	**1167.4**	**80.4%**		**-**	
Other Power Plants								
Plant	**Units**	**Rating (MW)**	**Generation (MW)**	**Reserve (MW)**	**% of System Reserve**	**Speed Droop**	**Controller Settings**	-
TPP	-	8500	700*	35	2.4%	5%	Stable	-
NGCCPP	-	6000	5000*	250	17.2%	5%	Stable	-
Plants with constant gen.	-	-	6138	0	0.0%	-	-	-
Total	**-**	**-**	**11838**	**285**	**19.6%**	-	**-**	-
SYSTEM TOTAL			**17750**	**1452.4**	**-**	-	**-**	-

* Generation of units contributing to primary control

Table F-8. Generation profile of Case-1-g

Hydro Power Plants								
Plant	**Units**	**Rating (MW)**	**Generation (MW)**	**Reserve (MW)**	**% of System Reserve**	**Speed Droop**	**Controller Settings**	**Derivative Input**
ALTINKAYA		4 x 175	150	15	1.0%	4%	Unstable	-
ATATÜRK		8 x 300	2000	400	27.5%	4%	Stable	-
BERKE		3 x 175	271	54	3.7%	4%	Stable	✓
BİRECİK		6 x 126	650	130	9.0%	4%	Stable	✓
HASAN UĞR.		4 x 125	200	40	2.8%	4%	Unstable	-
KARAKAYA		6 x 300	920	184	12.7%	4%	Unstable	-
KEBAN	1-4	4 x 157	1611	322	22.2%	4%	Unstable	✓
	5-8	4 x 180			0.0%	4%	Unstable	✓
OYMAPINAR		4 x 135	110	22	1.5%	4%	Unstable	-
Total	**-**	**-**	**5912**	**1167.4**	**80.4%**		**-**	
Other Power Plants								
Plant	**Units**	**Rating (MW)**	**Generation (MW)**	**Reserve (MW)**	**% of System Reserve**	**Speed Droop**	**Controller Settings**	-
TPP	-	8500	700*	35	2.4%	5%	Stable	-
NGCCPP	-	6000	5000*	250	17.2%	5%	Stable	-
Plants with constant gen.	-	-	6138	0	0.0%	-	-	-
Total	**-**	**-**	**11838**	**285**	**19.6%**	-	**-**	-
SYSTEM TOTAL			**17750**	**1452.4**	**-**	-	**-**	-

* Generation of units contributing to primary control

Table F-9. Generation profile of Case-1-h

Hydro Power Plants								
Plant	**Units**	**Rating (MW)**	**Generation (MW)**	**Reserve (MW)**	**% of System Reserve**	**Speed Droop**	**Controller Settings**	**Derivative Input**
ALTINKAYA		4 x 175	150	15	1.0%	4%	Stable	-
ATATÜRK		8 x 300	2000	400	27.5%	4%	Stable	-
BERKE		3 x 175	271	54	3.7%	4%	Stable	✓
BİRECİK		6 x 126	650	130	9.0%	4%	Stable	✓
HASAN UĞR.		4 x 125	200	40	2.8%	4%	Stable	-
KARAKAYA		6 x 300	920	184	12.7%	4%	Stable	-
KEBAN	1-4	4 x 157	1611	322	22.2%	4%	Stable	✓
	5-8	4 x 180			0.0%	4%	Stable	✓
OYMAPINAR		4 x 135	110	22	1.5%	4%	Stable	-
Total	**-**	**-**	**5912**	**1167.4**	**80.4%**		**-**	
Other Power Plants								
Plant	**Units**	**Rating (MW)**	**Generation (MW)**	**Reserve (MW)**	**% of System Reserve**	**Speed Droop**	**Controller Settings**	-
TPP	-	8500	700*	35	2.4%	5%	Stable	-
NGCCPP	-	6000	5000*	250	17.2%	5%	Stable	-
Plants with constant gen.	-	-	6138	0	0.0%	-	-	-
Total	**-**	**-**	**11838**	**285**	**19.6%**	-	**-**	-
SYSTEM TOTAL			**17750**	**1452.4**	**-**	-	**-**	-

* Generation of units contributing to primary control

Table F-10. Generation profile of Case-1-i

Hydro Power Plants								
Plant	**Units**	**Rating (MW)**	**Generation (MW)**	**Reserve (MW)**	**% of System Reserve**	**Speed Droop**	**Controller Settings**	**Derivative Input**
ALTINKAYA		4 x 175	150	15	1.0%	4%	Unstable	-
ATATÜRK		8 x 300	2000	400	27.5%	4%	Unstable	✓
BERKE		3 x 175	271	54	3.7%	4%	Unstable	✓
BİRECİK		6 x 126	650	130	9.0%	4%	Unstable	✓
HASAN UĞR.		4 x 125	200	40	2.8%	4%	Unstable	-
KARAKAYA		6 x 300	920	184	12.7%	4%	Unstable	-
KEBAN	1-4	4 x 157	1611	322	22.2%	4%	Unstable	✓
	5-8	4 x 180			0.0%	4%	Unstable	✓
OYMAPINAR		4 x 135	110	22	1.5%	4%	Unstable	-
Total	**-**	**-**	**5912**	**1167.4**	**80.4%**		**-**	
Other Power Plants								
Plant	**Units**	**Rating (MW)**	**Generation (MW)**	**Reserve (MW)**	**% of System Reserve**	**Speed Droop**	**Controller Settings**	-
TPP	-	8500	700*	35	2.4%	5%	Stable	-
NGCCPP	-	6000	5000*	250	17.2%	5%	Stable	-
Plants with constant gen.	-	-	6138	0	0.0%	-	-	-
Total	**-**	**-**	**11838**	**285**	**19.6%**	-	**-**	-
SYSTEM TOTAL			**17750**	**1452.4**	**-**	-	**-**	-

* Generation of units contributing to primary control

Table F-11. Generation profile of Case-1-j

Hydro Power Plants								
Plant	**Units**	**Rating (MW)**	**Generation (MW)**	**Reserve (MW)**	**% of System Reserve**	**Speed Droop**	**Controller Settings**	**Derivative Input**
ALTINKAYA		4 x 175	150	15	1.0%	4%	Unstable	✓
ATATÜRK		8 x 300	2000	400	27.5%	4%	Unstable	✓
BERKE		3 x 175	271	54	3.7%	4%	Unstable	✓
BİRECİK		6 x 126	650	130	9.0%	4%	Unstable	✓
HASAN UĞR.		4 x 125	200	40	2.8%	4%	Unstable	✓
KARAKAYA		6 x 300	920	184	12.7%	4%	Unstable	✓
KEBAN	1-4	4 x 157	1611	322	22.2%	4%	Unstable	✓
	5-8	4 x 180			0.0%	4%	Unstable	✓
OYMAPINAR		4 x 135	110	22	1.5%	4%	Unstable	✓
Total	**-**	**-**	**5912**	**1167.4**	**80.4%**		**-**	
Other Power Plants								
Plant	**Units**	**Rating (MW)**	**Generation (MW)**	**Reserve (MW)**	**% of System Reserve**	**Speed Droop**	**Controller Settings**	-
TPP	-	8500	700*	35	2.4%	5%	Stable	-
NGCCPP	-	6000	5000*	250	17.2%	5%	Stable	-
Plants with constant gen.	-	-	6138	0	0.0%	-	-	-
Total	**-**	**-**	**11838**	**285**	**19.6%**	-	**-**	-
SYSTEM TOTAL			**17750**	**1452.4**	**-**	-	**-**	-

* Generation of units contributing to primary control

Table F-12. Generation profile of Case-1-k

Hydro Power Plants								
Plant	**Units**	**Rating (MW)**	**Generation (MW)**	**Reserve (MW)**	**% of System Reserve**	**Speed Droop**	**Controller Settings**	**Active Controller**
ALTINKAYA		4 x 175	150	15	1.4%	4%	Unstable	Power
ATATÜRK		8 x 300	700	140	13.3%	4%	Unstable	Speed
BERKE		3 x 175	271	54	5.2%	4%	Unstable	Power
BİRECİK		6 x 126	650	130	12.4%	4%	Unstable	Power
HASAN UĞR.		4 x 125	0	0	0.0%	4%	Unstable	Power
KARAKAYA		6 x 300	920	184	17.5%	4%	Unstable	Speed
KEBAN	1-4	4 x 157	1111	222	21.1%	4%	Unstable	Power // Speed
	5-8	4 x 180			0.0%	4%	Unstable	
OYMAPINAR		4 x 135	110	22	2.1%	4%	Unstable	Speed
Total	**-**	**-**	**3912**	**767.4**	**72.9%**		**-**	
Other Power Plants								
Plant	**Units**	**Rating (MW)**	**Generation (MW)**	**Reserve (MW)**	**% of System Reserve**	**Speed Droop**	**Controller Settings**	-
TPP	-	8500	700*	35	3.3%	5%	Stable	-
NGCCPP	-	6000	5000*	250	23.8%	5%	Stable	-
Plants with constant gen.	-	-	8138	0	0.0%	-	-	-
Total	**-**	**-**	**13838**	**285**	**27.1%**	-	**-**	-
SYSTEM TOTAL			**17750**	**1052.4**	**-**	-	**-**	-

* Generation of units contributing to primary control

Table F-13. Generation profile of Case-2

Hydro Power Plants								
Plant	**Units**	**Rating (MW)**	**Generation (MW)**	**Reserve (MW)**	**% of System Reserve**	**Speed Droop**	**Controller Settings**	**Derivative Input**
ALTINKAYA		4 x 175	300	50	5.4%	4%	Unstable	-
ATATÜRK		8 x 300	1000	200	21.6%	4%	Unstable	-
BERKE		3 x 175	300	50	5.4%	4%	Unstable	✓
BİRECİK		6 x 126	300	78	8.4%	4%	Unstable	✓
HASAN UĞR.		4 x 125	100	25	2.7%	4%	Unstable	-
KARAKAYA		6 x 300	550	50	5.4%	4%	Unstable	-
KEBAN	1-4	4 x 157	360	100	10.8%	4%	Unstable	✓
	5-8	4 x 180	600	120	12.9%	4%	Unstable	✓
OYMAPINAR		4 x 135	0	0	0.0%	4%	Unstable	-
Total	**-**	**-**	**3510**	**673**	**72.5%**		**-**	
Other Power Plants								
Plant	**Units**	**Rating (MW)**	**Generation (MW)**	**Reserve (MW)**	**% of System Reserve**	**Speed Droop**	**Controller Settings**	-
TPP	-	8500	600*	30	3.2%	5%	Stable	-
NGCCPP	-	6000	4500*	225	24.2%	5%	Stable	-
Plants with constant gen.	-	-	11390	0	0.0%	-	-	-
Total	**-**	**-**	**16490**	**255**	**27.5%**	-	**-**	-
SYSTEM TOTAL			**20000**	**928**	**-**	-	**-**	-

* Generation of units contributing to primary control

Table F-14. Generation profile of Case-3

Hydro Power Plants								
Plant	**Units**	**Rating (MW)**	**Generation (MW)**	**Reserve (MW)**	**% of System Reserve**	**Speed Droop**	**Controller Settings**	**Derivative Input**
ALTINKAYA		4 x 175	300	50	3.9%	4%	Unstable	-
ATATÜRK		8 x 300	1550	250	19.5%	4%	Unstable	-
BERKE		3 x 175	475	50	3.9%	4%	Unstable	✓
BİRECİK		6 x 126	650	100	7.8%	4%	Unstable	✓
HASAN UĞR.		4 x 125	100	25	2.0%	4%	Unstable	-
KARAKAYA		6 x 300	1375	125	9.8%	4%	Unstable	-
KEBAN	1-4	4 x 157	360	100	7.8%	4%	Unstable	✓
	5-8	4 x 180	600	120	9.4%	4%	Unstable	✓
OYMAPINAR		4 x 135	355	50	3.9%	4%	Unstable	-
Total	**-**	**-**	**5765**	**870**	**68.0%**		**-**	
Other Power Plants								
Plant	**Units**	**Rating (MW)**	**Generation (MW)**	**Reserve (MW)**	**% of System Reserve**	**Speed Droop**	**Controller Settings**	-
TPP	-	8500	700*	35	2.7%	5%	Stable	-
NGCCPP	-	6000	5000*	250	19.5%	5%	Stable	-
Plants with constant gen.	-	-	8735	0	0.0%	-	-	-
Total	**-**	**-**	**14435**	**285**	**22.3%**	-	**-**	-
SYSTEM TOTAL			**21500**	**1280**	**-**	-	**-**	-

* Generation of units contributing to primary control